University of Southern Queensland

Faculty of Health, Engineering and Sciences

UNIVERSITY
OF SOUTHERN
QUEENSLAND

Particle and Particle-Like Solitary Wave Dynamics in

Fluid Media

A thesis submitted in fulfillment of the requirements of

Doctor of Philosophy

Nawin Raj

2015

ABSTRACT

This research deals with the study of various nonlinear wave processes in dispersive media by means of asymptotic methods developed upon existing exact methods in application to non-integrable systems. The aim of the research is to analyse wave models possessing solitary solutions and establish common features in the description of such solutions and classical particles. The new model equations have been derived for the description of long transverse waves propagating in the generalized atomic chain. The mathematical analogy between the model equations describing internal waves in stratified fluid (the Korteweg–de Vries and Gardner–Ostrovsky equations) and waves in discrete chain models (the generalized sine-Gordon–Toda model or Frenkel–Kontorova model) have been established. Chain models are described by sets of ODEs which can be readily solved with a high accuracy by existing well-developed solvers in mathematical software. The research includes solutions to important wave problems by means of approximate asymptotic and numerical methods. Results obtained provide an insight in understanding of details of nonlinear wave propagation in continuous and discrete media. An effective numerical code has been developed for the modeling of nonlinear phenomena both in continuous media and in the discrete models of interacting oscillators.

LIST OF PUBLICATIONS

The following publications were produced during the period of study:

1. Obregon M., Raj N., Stepanyants Y. Numerical study of nonlinear wave processes by means of discrete chain models. 4-th International Conference on Computational Methods (ICCM2012), 25–27 November 2012, Gold Coast, Australia (www.ICCM-2012.org). Full paper was submitted to the journal Chaos, 2015.

2. Nikitenkova S.P., Ostrovsky L.A., Raj N., Stepanyants Y. A. Nonlinear vector waves in the atomic chain model. VII International Conference "Solitons, Collapses and Turbulence: Achievements, Developments and Perspectives" (SCT-14), Abstracts, 4–8 August, 2014.

3. Nikitenkova S.P., Raj N., Stepanyants Y.A. Nonlinear vector waves of a flexural mode in a chain model of atomic particles. Communications in Nonlinear Science and Numerical Simulation, 2015, v. 20, n. 3, 731–742.

4. Raj N., Stepanyants Y.A. Interactions of vector solitons within the framework of vector mKdV equation. Communications in Nonlinear Science and Numerical Simulation, 2015 (submitted).

CERTIFICATION OF DISSERTATION

The work contained in this thesis has not been previously submitted to meet the requirements for an award at this or any other higher educational institution. To the best of my knowledge and belief, the thesis contains no material previously published or written by another person except where due reference is made.

Candidate: Nawin Raj

Signed:

_____

Date:

_____

ENDORSEMENT

Principal Supervisor: Professor Yury Stepanyants

Signed:

_____

Date:

_____

ACKNOWLEDGMENTS

I would like to express my sincere gratitude and thankfulness to my principle supervisor, Professor Yury Stepanyants for his continuous inspiration, support, patience, and individual feedback throughout the course of my PhD study. It has been a great privilege and blessing to work under his guidance and share the tremendous knowledge and experience he has in the area of our study. He has always been very approachable providing continuous motivation to obtain new and efficient results.

I would also like to express my sincere gratitude and appreciation to my associate supervisor Associate Professor Dmitry Strunin, for his continuous encouragement, support, valuable advice, and suggestions.

I gratefully acknowledge the University of Southern Queensland (USQ) for offering me the USQ Postgraduate Research Scholarship to perform this research successfully, without which this work would not have been possible.

I am also very thankful to all of the staff in the Department of Mathematics and Computing for their cooperation. I extend my gratitude and appreciation to my postgraduate colleagues for their discussions, comments, and advice, especially during our group seminars.

Finally, I wish to thank my wife, children and parents for their patience and support at all times during the course of my study.

LIST OF FIGURES

CONTENTS

Chapter 1   Introduction and Literature Review

Nonlinearity is a fascinating element of nature and its importance has been appreciated for many years when considering large-amplitude wave motions observed in various fields ranging from fluids and plasmas to solid-state, chemical, biological, and geological systems (Remoissenet, 2002). Fermi *et al.* (1955) carried out simulations on one-dimensional nonlinear lattice and obtained the results contradicting to their expectations. The unexpected results generated a lot of interest in the area of nonlinear science. This also gave rise to a wide array of fields such as soliton theory, discrete lattice dynamics and Kolmogorov–Arnold–Moser theory, all of which remain active research fields to date. Among the main examples, one can classify the Toda lattice, the Ablowitz–Ladik equation and the Calogero–Moser *N*-body problem (see the works of Calegero (1971) and Moser (1975)) (Kevrekidis, 2011).

This research extends the theory of transverse nonlinear waves in a chain of masses with elastic couplings. The approach was first used by Gorbacheva and Ostrovsky (1983) in their investigation of transverse nonlinear waves. However, this research considers next two neighboring atoms in relation to the investigation in this problem. Furthermore, the presence of different types of solitons is investigated. The features of nonlinear behavior and the chain model can provide valuable information for study of molecules in biology and chemistry. The theory also has many applications in theoretical physics. The model of "strings", "chains" and "lattices" could be

successfully used to model difficult problems of nonlinear theory (Gorbacheva &
Ostrovsky, 1983).

The next part of the research uses chain models described by sets of ordinary
differential equations to numerically study nonlinear wave processes in dispersive
media. The one dimensional chain model is used to simulate internal waves in a rotating
ocean. This equation is well known as the Gardner–Ostrovsky equation. The electric
version of sine-Gordon-Toda chain and Ostrovsky equation are derived from the ladder
type transmission line with the nonlinear capacitor and inductance.

An experimental study of ship waves have many constraints such as using large wave
trough, the relative weak nonlinearity at far distances from the source and the
complexity of recording equipment (Stepanyants, 1983). Stepanyants (1983)
demonstrated the use of two dimensional electric networks for experiments. Hirota and
Suzuki (1973) also used a nonlinear lumped *LC* (Capacitor and Inductor) network to
observe the fundamental properties of solitons indicated by Zabusky and Kruskal
(1965). The use of the chain model derived in this study extends the method to provide
better understanding of important nonlinear wave processes.

1.1   Solitons and Solitary Wave dynamics

Solitary waves or solitons demonstrate particle-like behavior as keeping its shape while
moving at constant speed and upon interaction; the solitons remain unchanged in the
course of interaction with each other apart from a phase shift. Solitary waves arise in

both continuous systems, such as water in the shallow basin, and discrete systems such as the Toda lattice (mechanical or electrical) (Toda, 1989a). Morikazu Toda was the first who discovered solitons in a discrete, integrable system. This system is currently well known as Toda lattice (see (1.1)):

$$\frac{d^2}{dt^2} \ln\left(1+u_n\right) = u_{n+1} - 2u_n + u_{n-1}. \tag{1.1}$$

The stable nature of solitons and its experimental observation in various physical systems like biophysics, solid state physics, non-linear optics, atomic physics, granular crystals, plasma physics, nonlinear meta-materials, water waves and among others have made it a central aspect of research. Since there are so many force sources in nature (torsion, gravity, electron-electron interactions, electron-phonon, spin exchange etc.) that lead to an apparently inexhaustible store of solitons in condensed matter physics (Bishop *et al.,* 1980). An important factor in the decay of water waves is the viscosity of the medium which is a manifestation of friction.

Waves and particles have been intimately related in physical theory since the formulation of quantum mechanics in the 1920s (Rebbi, 1979). These special waves are described as a quantity of energy that is permanently confined to a definite region and while in motion, they retain their shape after collision and without dissipation. Such remarkable behavior is familiar in particle dynamics. If two solitary waves with different speeds interacting through the collision are considered, they recover their initial form and propagate like independent particles. Solitons were also found as solutions for other non-linear wave equations and it became clear that they are the

motion most characteristic of many nonlinear waves (Toda, 1989a). Since the soliton is a nonlinear dispersive wave packet equivalent of the linear dispersive, the analogy with particle behavior is quite strong. This important development made particle physicists realise that many field theoretical model for particle interactions possessed soliton solutions and that the solitons could to be interpreted as additional particle-like structures in the theory. In these investigations it was established at the quantum level that solitons are associated with a variety of remarkable phenomena.

1.2   Historical Developments

The concept "solitary wave" was coined by J. Scott-Russell who presented the first documented observation of this unusual occurrence in Scottish canal. J. Scott-Russell left a very clear and picturesque description of his observation of a solitary wave on a water surface in one of his subsequent report of 1844 (Ablowitz & Segur, 1981).

The term soliton was coined by Zabusky and Kruskal (1965) to reflect both the solitary-wave-like character and the particle-like interaction properties (Scott, 2005). It is also interesting to note that, prior to the investigations of Zabusky and Kruskal, analytical expressions describing collision events between solitary waves within the framework of the equation describing dislocations in solids were found by Seeger *et al.* (1953). This equation is called the sine-Gordon equation (1.2):

$$\frac{\partial^2 u}{\partial t^2} - \frac{\partial^2 u}{\partial x^2} + \alpha^2 \sin u = 0 \; . \tag{1.2}$$

The complete integrability of the sine-Gordon equation (1.2) was established by Ablowitz *et al.* (1973) and they found a family of multisoliton solutions, which represent in this particular cases kinks and anti-kinks – the specific kind of dissipation less shock waves. The sine-Gordon equation is a particular case of the nonlinear Klein–Gordon equation.

Frenkel and Kontorova (1939) introduced the equation as a model for the dislocation in a crystal. It was shown that the displacement of atoms connected by linear springs may propagate as a kink in the periodic crystal field. The discovery of the inverse scattering transform (IST) for the solution of nonlinear partial differential equations (PDEs) is the most important development in the theory of solitons as the solitons can be defined in a rigorous manner. As has been shown in the numerous publications, the IST method can be treated as the extension of the Fourier transformation onto nonlinear dynamics. It is a unique method of solving the nonlinear initial value problem.

Zakharov (1968) showed that the time evolution of the envelope of a weakly nonlinear deep-water wave train is described by the nonlinear Schrödinger equation (NLS) (see equation (1.3) below) which was later exactly solved by Zakharov and Shabat (1972) by the IST method:

$$i\left(\frac{\partial u}{\partial t} + V_g\,\frac{\partial u}{\partial x}\right) + \alpha\,|u|^2\,u \;+\; \beta\,\frac{\partial^2 u}{\partial x^2} = 0\,. \tag{1.3}$$

This was an important discovery as it has been shown that the exact solutions are deep water wave envelope solitons. The initial wave packet in this case evolves into a number of envelope solitons and a dispersive tail. More importantly, these solutions

5

were verified experimentally by Yuen and Lake (1975). The Klein–Gordon equation is considered to be the relativistic version of the NLS equation. Various forms of the nonlinear Klein–Gordon equation are seen to have exact, soliton-like solutions when separation of variables is postulated and the family for which these exact solutions are found includes the sine-Gordon equation as a special case (Grundland & Infeld, 1992).

Parallel to these investigations, the instability of electromagnetic waves propagating in nonlinear dispersive media was predicted (Ostrovskii, 1963), (Bespalov & Talanov, 1966), (Karpman, 1967) and in another important development it was shown theoretically by Hasegawa and Tappert (1973) that the envelope of a light wave propagating in an optical fiber can also be described by the NLS equation which led to the existence of bright solitons being predicted. This prediction was later verified by Mollenauer *et al.* (1980) observed bright-soliton propagation in a single fiber and from the standpoint of technological applications, such optical–fiber solitons are very important. The stability of solitons can make long distance transmission possible with twice the capacity without the use of repeaters thereby providing a major break-through in information transfer. Magnetic envelope solitons were also an important area of study and envelope solitons of the NLS type were predicted theoretically by Zvezdin and Popkov (1983) for magnetostatic waves in magnetic films and later observed experimentally by Kalinikos *et al.* (1983).

Korteweg–de Vries (KdV) equation (1.4) is an important mathematical model of waves in shallow water. The equation is named after Diederik Korteweg and Gustav de Vries (1895), although the similar equation was first formulated by Boussinesq (1871):

$$\frac{\partial u}{\partial t} + \alpha u \frac{\partial u}{\partial x} + \beta \frac{\partial^3 u}{\partial x^3} = 0. \qquad\qquad \textbf{(1.4)}$$

Korteweg and de Vries analytically derived a nonlinear partial differential equation with the delicate balance between the non-linearity and dispersion which describes the propagation of long waves of small amplitude in dispersive media. The KdV equation has a long history as the prototype of nonlinear wave equations, and from its study current nonlinear theory has emerged, including such concepts as the soliton, recurrence phenomena, conserved quantities, integrable systems, initial value problems (the inverse scattering transform), and so forth. It is used to describe other physical phenomena such as acoustic waves in crystals and ion acoustic waves in plasmas.

The paper by Gardner *et al*. (1967) made an important contribution to the development of the theory as they showed that the analytical solution of the KdV equation can be obtained if the initial shape of the wave is sufficiently localized. They introduced a linear problem (the eigenvalue problem) where the potential represents the solution of the KdV equation. Their theoretical results were in remarkable agreement with the many of experimental results obtained by John Scott Russell (1844) more than one hundred and fifty years ago (Remoissenet, 2002).

The stability of solitons results from the balance in the effects of dispersion and non-linearity. It is now widely appreciated that the classic solitons have their genesis in the balancing of competing tendencies, typically dispersive effects tending to spread a wave-packet are balanced (or nearly so) by nonlinear terms favoring self-steepening or

shock front formation, because of the different velocities of 'Fourier' components (Bishop *et al.,* 1980).

1.3 Nonlinear *LC* circuit and nonlinear lattice

Toda (1989b) showed that the equations of motion of one dimensional lattice of particles with exponential interactions are integrable and admit exact solution. Analytical solutions of equations of motion in an anharmonic one dimensional lattice were obtained and existence of solitons in a nonlinear lattice was found. This system is shown to be equivalent to an *LC* circuit with certain nonlinear capacitance. The figure 1.1 shows the arrangement of the circuit.
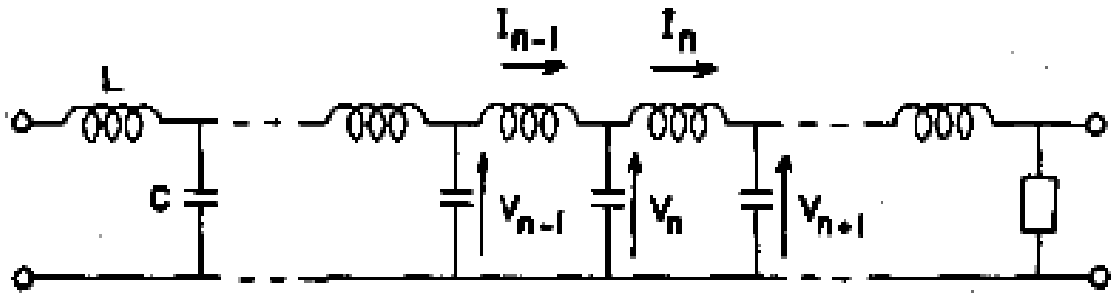
Figure 1.1: Nonlinear *LC* circuit equivalent to a nonlinear lattice (Toda, 1989b).

Similar nonlinear lumped *LC* circuit was used by Hirota and Suzuki (1973) to conduct theoretical and experimental study of lattice solitons. Stepanyants (1983) used electrical simulation of ship waves with the use of *LC* networks. It was demonstrated that a complete analogy can be established between the equations of hydrodynamics and the network equations in a linear approximation.

8

1.4 Ostrovsky and Gardner-Ostrovsky Equation

Many important extensions have been considered for the Korteweg-de Vries (KdV) which consider factors such as stratification, friction, higher-order linearity and rotation. One such interesting extension was considered by Ostrovsky (1978). The Ostrovsky equation is a modification of the Korteweg-de Vries equation which presents a model for gravity waves under the influence of Coriolis force. The equation is given as (Apel *et al.,* (2007)):

$$\frac{\partial}{\partial x}\left(\frac{\partial \eta}{\partial t} + c\frac{\partial \eta}{\partial x} + \alpha\eta\frac{\partial \eta}{\partial x} + \beta\frac{\partial^3 \eta}{\partial x^3}\right) = \frac{f^2}{2c}\eta. \tag{1.5}$$

This equation is an important model for the propagation of small-amplitude internal waves in a rotating fluid. However, the equation is not integrable and it is an important problem to consider in fluid dynamics to find the numerical solution for this equation.

An extra term with cubic nonlinearity in Korteweg–de Vries (KdV) equation is called the Gardner equation (Apel *et al*., 2007):

$$\frac{\partial \eta}{\partial t} + \left(c + \alpha\eta + \alpha_1\eta^2\right)\frac{\partial \eta}{\partial x} + \beta\frac{\partial^3 \eta}{\partial x^3} = 0. \tag{1.6}$$

This equation is valid for small nonlinearity and specific stratification and describes strongly nonlinear internal solitons (Stepanyants, 1991). The Gardner-Ostrovsky equation describes long internal waves of large amplitude. It takes into account the dispersion effects due to nonhydrostaticity caused by the finiteness of depth and earth's

rotation (Obregon & Stepanyants, 2012). The equation is given as (Obregon & Stepanyants, 2012):

$$\frac{\partial}{\partial x}\left(\frac{\partial \eta}{\partial t}+c\frac{\partial \eta}{\partial x}+\alpha\eta\frac{\partial \eta}{\partial x}+\alpha_1\eta^2\frac{\partial \eta}{\partial x}+\beta\frac{\partial^3 \eta}{\partial x^3}\right)=\gamma\,\eta\,. \qquad (1.7)$$

1.5 Techniques

1.5.1 Chain Model of Nonlinear Vector Waves of Flexural Modes

A chain model for the description of flexural transverse waves in the nonlinear chain of atoms is considered to formulate a nonlinear vector equation for the phonon modes. One of the pioneering work in this area was published by Gorbacheva and Ostrovsky (1983), who considered the interaction between only the nearest particles and derived in the long-wave approximation, the non-integrable vector modified Korteweg–de Vries (mKdV) equation. The simplest stationary solutions to that equation were also found. This work can be extended to a more general model taking into account the interaction not only between the nearest atoms, but also between the next neighbours of these two atoms. Such generalization allows one to model quadratic spectra of phonons which is observed experimentally. In the long-wave approximation, several new model equations can be derived, and some of them are important due to their applicability to the real crystals and, perhaps, to energy transport in alpha-spiral molecules (Davydov, 1985). Both periodic and solitary stationary solutions can be obtained within the framework of

this model equation. This work is extended to helical soliton and their interaction with plane and other helical solitons (Nikitenkova *et al.,* 2015).

1.5.2   One Dimensional Chain Model

Chain models have been used in many works both in the experimental and numerical embodiments. One of the examples of the mechanical chain model is described, e.g., in the book by (Dodd *et al*., 1982), where it is shown that the sine-Gordon partial differential equation (PDE) can be modeled by a chain of coupled pendulums. Another well-known example is the remarkable Toda chain model (1989a), which has not been yet realized experimentally in the mechanical embodiment, but has been practically incarnated in the electric version and used in many theoretical and numerical studies. Other examples relate to the chains of coupled nonlinear oscillators representing electromagnetic transmission lines capable to model the sine-Gordon equation (Parmentier, 1978), (Rabinovich & Trubetskov, 1989), Korteweg–de Vries (KdV), (Lonngren, 1978), (Rabinovich & Trubetskov, 1989), and even more complicated wave equations describing, e.g., the interaction of Langmuir and ion-acoustic waves in plasma (Rabinovich & Trubetskov, 1989).

There are also two-dimensional generalizations of chain models representing square or hexagonal lattices which can be used for the modeling of PDEs in two spatial variables and time [see e.g., (Stepanyants, 1981); (Zolotaryuk *et al.,* 1988) and references therein]. The discrete models in many cases can be realized experimentally which can represent an analogous computer designed to the solution of a particular PDE. The main

task is to get the approximation of the PDE by means of the chain model. This could be solved with existing higher-quality ordinary differential equations (ODE) solvers. This approach to solving the PDE will be free from the problem of numerical instability. This is a major problem when solutions of partial differential equations are investigated. The numerical stability determines the accuracy of finding the solution to these PDEs.

1.6   Research Objectives

The aim of the research is to derive new nonlinear vector equations for the phonon modes by considering flexural transverse waves in a nonlinear chain of particles. The study will consider particular cases of the derived equation which are 'vector mKdV', 'second order cubic Benjamin-Ono (socBO), 'nonlinear pseudo-diffusion', and in the scaler case, the Kolmogorov-Petrovsky-Piskunov equation. The equations will be used to find stationary solutions and numerically study non stationary interactions of solitary waves of different polarisations. Furthermore, the non stationary dynamics of plane and helical solitons moving in the same direction along the x-axis, having the same and different polarisations will also be investigated. An efficient numerical code for integrable and non integrable forms of the vector mKdV equation will be developed and used to investigate interactions between different types of plane and helical solitary waves.

Secondly, one dimensional chain will be developed to model complex nonlinear physical phenomena. The model will effectively show that these nonlinear wave processes in dispersive media can be numerically studied by means of proposed discrete

chain model described by sets of ODEs. This idea will be applied to the modeling of solitary wave propagation in a rotating ocean described by the Gardner–Ostrovsky PDE. An efficient numerical code will be used to investigate the terminal decay of KdV and Gardner solitons within the framework of the adiabatic approximation.

1.7   Content of this Research

The techniques and numerical simulations formulated in this research are original. They extend and build upon previously developed methods and techniques of work acknowledged accordingly. In application to problem studied in this project the used techniques are adequate and very efficient. The numerical FORTRAN code used for simulation of nonlinear wave phenomena with the help of discrete chain models provided significant advantage in computations and very efficient and accurate results. The research extends many important areas of nonlinear wave dynamics which are new and provide valuable breakthrough in the soliton theory. The outline of the research is as follows:

- Chapter 2 – Flexural transverse waves in a nonlinear chain of particles have been considered and a nonlinear vector equation for the phonon modes is derived. In the long-wave approximation, various new nonlinear equations can be obtained depending on the parameters between the chain particles. Among them there are equations possessing both the linear dispersion relation, $\omega \sqcup \kappa$ and quadratic dispersion in the limiting case when the wavenumber goes

to zero $\omega \square \kappa^2$. The former case is typical for isotropic crystals, whereas the latter case is typical for strongly anisotropic crystals with the strong coupling between first next two neighboring particles from each side (Lifshitz, 1952). The chain equation when each particle of number n is linked with two next neighboring atoms from both sides is formulated. Similar equation has been derived in Gorbacheva and Ostrovsky (1983) where the coupling with only the nearest neighboring particle was taken into consideration. The derived equation is new and its properties were not studied before. Among the solutions of this equation are plane and helical nonlinear waves, both periodic and solitary. The structures of such waves have been found analytically.

- Chapter 3 – Nonlinear non stationary wave evolution and interactions were considered in this chapter. The vector mKdV equation derived in chapter 2 is studied numerically. Different graphical results of the plane and helical soliton interactions are presented. The integrable and non integrable cases are compared.

- Chapter 4 – Many nonlinear wave processes in dispersive media are numerically studied by means of chain models described by sets of ordinary differential equations (ODEs). Accurate and efficient results are obtained by using the standard ODE solvers within the framework of the developed approach based on the physical analogy between the wave processes in different media. The concept is demonstrated in application to the modeling of solitary wave propagation in a rotating ocean described by the Gardner–Ostrovsky PDE using a modified Toda chain model. The results are compared with approximate

14

theoretical findings and earlier published data obtained from the direct numerical modeling of the Gardner–Ostrovsky PDE.

- Chapter 5 – contains conclusion and discussions of results obtained in the research. It also highlights further avenues of the research in this field.

Chapter 2 Non-Linear Stationary Waves in a Vector Model of a String

2.1 Introduction

The research work and results of this chapter has been successfully published in the journal Communications in Nonlinear Science and Numerical Simulation, 2014.

The work on nonlinear vector waves in the atomic chain model has been presented in VII International Conference:

"Solitons, Collapses and Turbulence: Achievements, Developments and Perspectives" (SCT-14), 4-8 August, 2014.

Due to its various important applications, there has been an intensive study of anharmonic chains and lattices in past decades. Some notable studies include Maugin (1999), Potapov *et al.* (2001), Brandt & Kulbachinsky (2007), Syrkin *et al.* (2009), Kevrekidis (2011), Rudenko & Solodov (2011). The theory of such discrete structures remains very topical due to their numerous applications in theoretical physics. Some of the examples are, the theory of crystal heat transport, thermalization in a set of coupled oscillators by Fermi *et al.* (1955), Toda (1989b), molecular physics involving transport of excitations in long spiral molecules by Davydov (1985), Christiansen *et al.* (1997), X-ray spectroscopy by Belenkii *et al.* (1988), and dusty plasma by Fortov *et al.* (2004), Farokhi *et al.* (2006).

Anharmonic chains and lattices are also studied in application to electric transmission lines (Scott, 1970), (Toda, 1989b). In the majority of cases either longitudinal modes or mixed longitudinal and transverse modes were studied this far. In the one-dimensional case in application to a chain of atoms the equation of motion for longitudinal modes is scalar describing atom vibrations in the direction of wave propagation [see, e.g., (Fermi *et al.,* 1955), (Toda, 1989a)]. However, when the transverse modes are considered (see figure 2.1), the equation of motion becomes vector (Gorbacheva & Ostrovsky, 1983), (Destrade & Saccomandi, 2008). The particle displacements are described in two perpendicular directions transverse to the direction of wave propagation. In both these cases of longitudinal and transverse vibrations the dispersion law of phonon (acoustic) modes in the long-wave approximation is linear, $\omega \sim k$, where ω is the wave frequency and k is the wave number of infinitesimal amplitude perturbations.
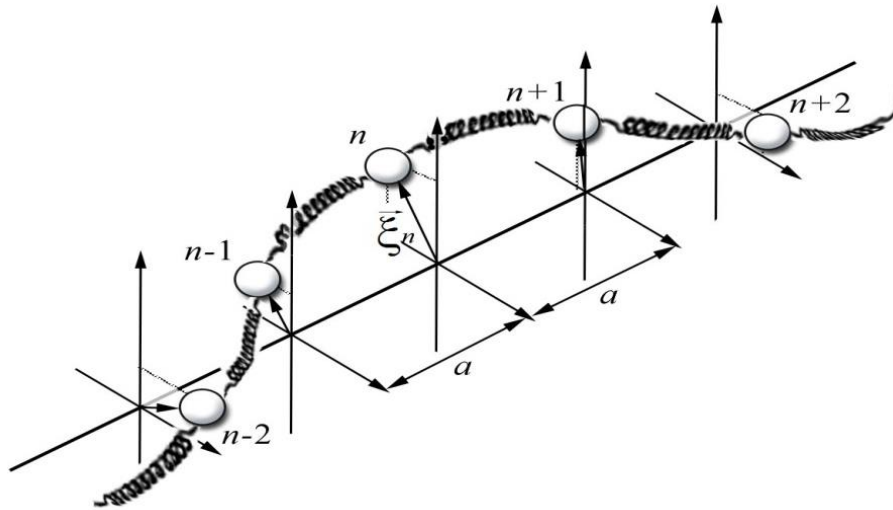
Figure 2.1: Longitudinal and transverse oscillations of equal mass particles in an atomic chain (Gorbacheva & Ostrovsky, 1983).

17

It is an experimental fact that in many cases the transverse flexural modes in crystals demonstrate the quadratic dispersion law in the long-wave approximation, $\omega \sim k^2$. The quadratic dispersion law is typical for anisotropic crystals with strong difference between the inlayer and interlayer forces; for example, for the graphite (C). Figure 2.2 from Nicklow *et al.* (1972) shows the dispersion laws in the anisotropic crystals. I.M. Lifshitz (1952) in his pioneering work pointed out at the importance of the quadratic dispersion law for strongly anisotropic crystals and suggested a simplified model for the description of flexural modes in crystal layers by analogy with the vibrations of elastic thin plate. Similar model is applicable for the flexural modes in the chain of atoms when particles interact not only with the nearest neighbours but also with the next two in the chain (Belenkii *et al.*, 1988), (Syrkin *et al.*, 2009).
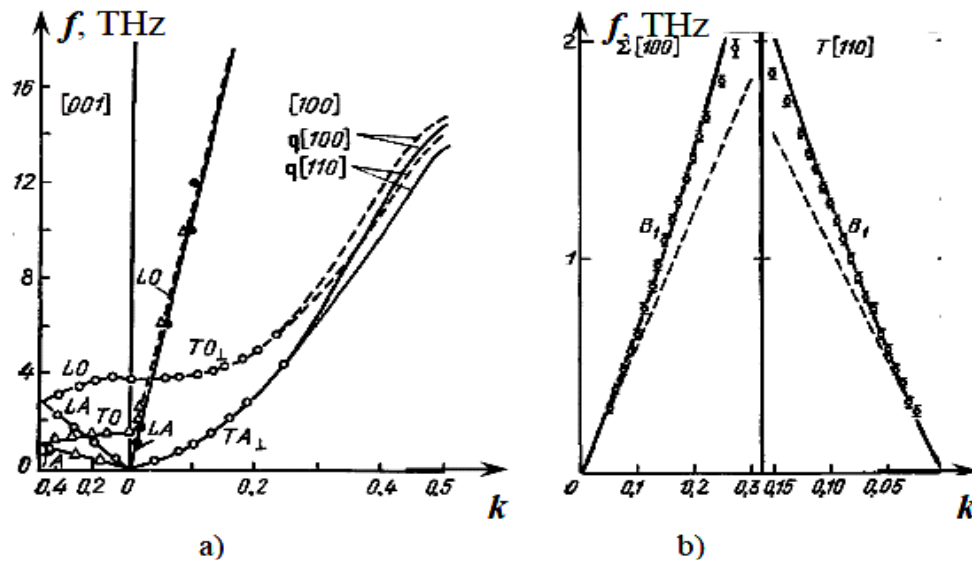
Figure 2.2: Quadratic phonon dispersion in Graphite (a) and linear phonon dispersion in GaS (b). The wavenumber is given in relative units (Nicklow *et al.*, 1972).

In what follows, flexural transverse waves in an anharmonic chain of atoms are used to derive the nonlinear vector equation for phonon modes in the long-wave approximation taking into account weak dispersion.

2.2 Derivation of the Vector Equation

Consider the chain of equal mass atoms shown in figure 2.1. The equation of motion for the atom with number n can be written as:

$$m\frac{d^2\xi_n}{dt^2} = \mathbf{F}_{n-2} + \mathbf{F}_{n-1} + \mathbf{F}_{n+1} + \mathbf{F}_{n+2},$$ (2.1)

where m is the mass of each atom, $\xi_n = (y_n, z_n)$ is the two-component transverse displacement vector with the y and z-components orthogonal to the axis x, the axis along which perturbations propagate, and $\mathbf{F}_n$ are transverse forces exerting on the nth atom of the chain from its nearest and next neighbours.

Following the approach used in the paper by Gorbacheva and Ostrovsky (1983), the transverse force exerting on the atom is in the form:

$$F_{n\pm j} = \pm\beta_j\left[T + jaK\left(\frac{1}{\cos\alpha_{n\pm j}} - 1\right)\right]\sin\alpha_{n\pm j},$$ (2.2)

where β_j are some coefficients which characterise the strength of the corresponding force (without loss of generality, we can put $\beta_1 = 1$ which is presumed in what follows), T is the uniform tension of the chain, K is the analogue of Hook's constant, α_n is the

19

local angle between the chain and axis x, $j = 1$ for the nearest two neighbouring atoms and $j = 2$ for the next two atoms.

In the case of a plane polarisation when the displacement ξ has only one y component, the angle $\alpha_{n \pm j}$ can be expressed in terms of displacements:

$$\tan \alpha_{n \pm j} = \pm (y_{n \pm j} - y_n) / (ja).$$

The displacement expressions can be manipulated to find the following:

$$\sin \alpha_{n \pm j} = \frac{\tan \alpha_{n \pm j}}{\sqrt{1 + \tan^2 \alpha_{n \pm j}}} = \pm \frac{y_{n \pm j} - y_n}{\sqrt{(ja)^2 + (y_{n \pm j} - y_n)^2}}, \qquad (2.3)$$

$$\cos \alpha_{n + j} = \frac{1}{\sqrt{1 + \tan^2 \alpha_{n \pm j}}} = \frac{ja}{\sqrt{(ja)^2 + (y_{n \pm j} - y_n)^2}}. \qquad (2.4)$$

For relatively small angles, $\alpha_{n \pm j} \ll 1$, these expressions can be presented in the approximate form:

$$\sin \alpha_{n \pm j} \approx \pm \frac{y_{n \pm j} - y_n}{ja} \left[1 - \frac{(y_{n \pm j} - y_n)^2}{2(ja)^2} \right]; \qquad \cos \alpha_{n + j} \approx 1 - \frac{(y_{n \pm j} - y_n)^2}{2(ja)^2}. \qquad (2.5)$$

Hence, the y-component of the force exerting on the nth atom is:

$$Y_{n \pm j} \approx \pm \frac{y_{n \pm j} - y_n}{ja} \left[T + \frac{jaK - T}{2(ja)^2} (y_{n \pm j} - y_n)^2 \right]. \qquad (2.6)$$

Similarly, the z-component of the force exerting on the nth atom is:

20

$$Z_{n \pm j} \approx \pm \frac{z_{n \pm j} - z_n}{ja} \left[T + \frac{jaK - T}{2(ja)^2} \left(z_{n \pm j} - z_n \right)^2 \right] \tag{2.7}$$

and the total force $F = (Y, Z)$ is:

$$\mathbf{F}_{n \pm j} \approx \pm \frac{\xi_{n \pm j} - \xi_n}{ja} \left[T + \frac{jaK - T}{2(ja)^2} \left| \xi_{n \pm j} - \xi_n \right|^2 \right]. \tag{2.8}$$

The Newtonian equation of motion for the nth atom in the chain can be written as:

$$
\begin{aligned}
m \frac{d^2 \xi_n}{dt^2} = & \frac{\xi_{n+1} - \xi_n}{a} \left[T + \frac{aK - T}{2a^2} \left| \xi_{n+1} - \xi_n \right|^2 \right] - \frac{\xi_n - \xi_{n-1}}{a} \left[T + \frac{aK - T}{2a^2} \left| \xi_n - \xi_{n-1} \right|^2 \right] + \\
& \beta_2 \left\{ \frac{\xi_{n+2} - \xi_n}{2a} \left[T + \frac{2aK - T}{8a^2} \left| \xi_{n+2} - \xi_n \right|^2 \right] - \frac{\xi_n - \xi_{n-2}}{2a} \left[T + \frac{2aK - T}{8a^2} \left| \xi_n - \xi_{n-2} \right|^2 \right] \right\}
\end{aligned} \tag{2.9}
$$

This equation can be further simplified and reduced to the following:

$$
\begin{aligned}
\frac{d^2 \overline{\xi}_n}{d\tau^2} = & \overline{\xi}_{n+1} - 2\overline{\xi}_n + \overline{\xi}_{n-1} + \frac{1}{2}(\mu - 1) \left[\left| \overline{\xi}_{n+1} - \overline{\xi}_n \right|^2 \left(\overline{\xi}_{n+1} - \overline{\xi}_n \right) - \left| \overline{\xi}_n - \overline{\xi}_{n-1} \right|^2 \left(\overline{\xi}_n - \overline{\xi}_{n-1} \right) \right] + \\
& \frac{\beta_2}{2} \left\{ \overline{\xi}_{n+2} - 2\overline{\xi}_n + \overline{\xi}_{n-2} + \frac{1}{8}(2\mu - 1) \left[\left| \overline{\xi}_{n+2} - \overline{\xi}_n \right|^2 \left(\overline{\xi}_{n+2} - \overline{\xi}_n \right) - \left| \overline{\xi}_n - \overline{\xi}_{n-2} \right|^2 \left(\overline{\xi}_n - \overline{\xi}_{n-2} \right) \right] \right\}
\end{aligned} \tag{2.10}
$$

where $\tau = (T/am)^{1/2} t$, $\overline{\xi}_n = \xi_n / a$ and $\mu = aK/T$.

In the linear approximation one can derive the dispersion relation for waves of infinitesimal amplitude of the form $\overline{\xi}_n \sim \exp[i(\omega t - \kappa n)]$:

$$\omega^2 = 4 \sin^2 \frac{\kappa}{2} \left(1 + 2\beta_2 \cos^2 \frac{\kappa}{2} \right). \tag{2.11}$$

21

The same equation has been derived by Brandt and Kulbachinsky (2007). As follows from this equation, β_2 cannot be less than $-1/2$, otherwise the dispersion relation becomes complex which is physically inconsistent.

In the limiting case $\beta_2 = -1/2$, the dispersion relation reduces to:

$$\omega^2 = 4\sin^4\frac{\kappa}{2}. \qquad\qquad\qquad (2.12)$$

The graph of the dispersion relation (2.11) is shown in figure 2.3 as a function of phase constant κ and three values of the parameter β_2.
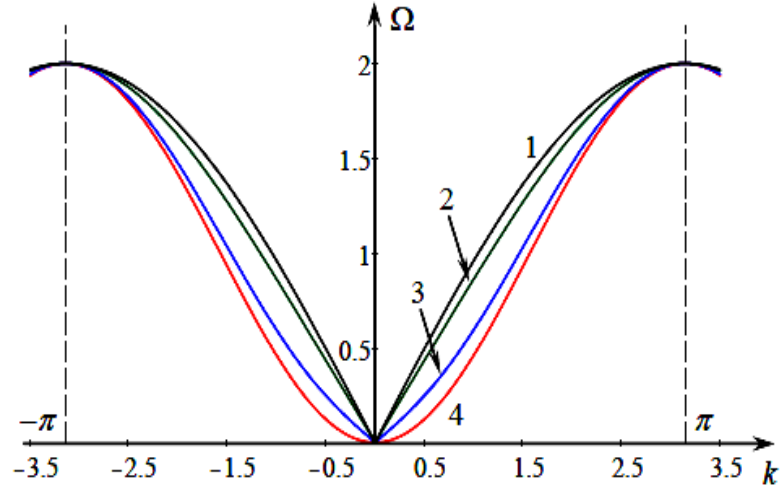
Figure 2.3: Dispersion relation (2.11) for the first Brillouin zone, $-\pi \leq \kappa \leq \pi$, at different values of the coupling constant: line 1 – $\beta_2 = 0$, line 2 – $\beta_2 = -1/8$, line 3 – $\beta_2 = -0.4$, and line 4 – $\beta_2 = -0.5$. Brillouin zone is the fundamental period closest to the origin for the periodic dispersion relation.

The parameter β_2 can be varied in the long wave approximation ($\kappa \to 0$) to obtain different dispersion dependences observable in experiments: the linear dispersion law,

$\omega \sim \kappa$, shown in figure 2.2 (a) by solid line with black dots (cf. line 1 in figure 2.3 obtained for $\beta_2 = 0$), the weak linear dependence with a comparable positive quadratic correction shown in figure 2.2 (b) by solid lines with open circles (cf. line 2 in figure 2.3 obtained for $\beta_2 = -0.4$), and the pure quadratic dispersion law $\omega \sim \kappa^2$ shown in figure 2.2 (a) by solid line with open circles (cf. line 3 in figure 2.3 obtained for $\beta_2 = -0.5$).

When the linear dispersion predominates in the long wave approximation, $\kappa \ll 1$, the Taylor series expansion of equation (2.11) yields:

$$\omega \approx \sqrt{1+2\beta_2}\,\kappa - \frac{1+8\beta_2}{24\sqrt{1+2\beta_2}}\kappa^3 + \frac{1+64\beta_2\left(1+\beta_2\right)}{1920\left(1+2\beta_2\right)^{3/2}}\kappa^5 - \ldots \ . \tag{2.13}$$

This series is valid if $1 + 2\beta_2 \neq 0$. When $\beta_2 = -1/2$, equation (2.14) is obtained from equation (2.12):

$$\omega \approx \frac{\kappa^2}{2} - \frac{\kappa^4}{24} + \ldots \ . \tag{2.14}$$

Another interesting case occurs when $\beta_2 = -1/8$, in this boundary case, the dispersion relation (2.13) in the long wave approximation is:

$$\omega \approx \frac{\sqrt{3}}{2}\kappa - \frac{\sqrt{3}}{360}\kappa^5 + \ldots \ , \tag{2.15}$$

and the dispersion correction $\sim\kappa^5$ is negative and weakest.

In the cases when $\beta_2 > -1/8$, the dispersion correction to the first term is negative, whereas in the cases when $\beta_2 < -1/8$, the dispersion correction becomes positive.

In the long-wave approximation equation (2.10) can be reduced to the partial differential equation (PDE). The main focus is in the case when coefficient $(1 + 2\beta_2)^{1/2}$ in the dispersion relation (2.13) is close to or equal to zero, i.e. when $\beta_2 \approx -1/2$ and almost quadratic dispersion law occurs, $\omega \sim \kappa^2$.

Another limiting case is when the linear dispersion law occurs, $\omega \sim \kappa$ with $\beta_2 = 0$. This has been considered in the work by Gorbacheva and Ostrovsky (1983) and Destrade and Saccomandi (2008). To derive the PDE, functions $\overline{\xi}_{n \pm j}$ ($j = 1, 2$) is expanded into the Taylor series around the point $x = n\,a$, where a is the interatomic distance in the chain (see figure 2.1):

$$\overline{\xi}_{n \pm j} = \overline{\xi}(x) \pm \overline{\xi}'(x)\,j + \overline{\xi}''(x)\frac{j^2}{2} \pm \overline{\xi}'''(x)\frac{j^3}{3!} + \overline{\xi}^{(IV)}(x)\frac{j^4}{4!} \pm \ldots, \qquad \textbf{(2.16)}$$

where x is a continuous variable with the unit length equaled to the size of one cell a in the atomic chain shown in figure 2.1. Substituting this into equation (2.10) and after simple manipulation the following PDE is obtained:

$$\frac{\partial^2 \overline{\xi}}{\partial \tau^2} = \left(1 + 2\beta_2\right)\frac{\partial^2 \overline{\xi}}{\partial x^2} + \frac{1 + 8\beta_2}{12}\frac{\partial^4 \overline{\xi}}{\partial x^4} + \frac{1 + 32\beta_2}{360}\frac{\partial^6 \overline{\xi}}{\partial x^6} + \frac{\mu\left(1 + 4\beta_2\right) - \left(1 + 2\beta_2\right)}{2}\frac{\partial}{\partial x}\left(\left|\frac{\partial \overline{\xi}}{\partial x}\right|^2 \frac{\partial \overline{\xi}}{\partial x}\right). \qquad \textbf{(2.17)}$$

Equation (2.18) is obtained after differentiating equation (2.17) with respect to x and introducing a new variable, $\mathbf{u} = \partial\overline{\xi}_n / \partial x$,

24

$$\frac{\partial^2 \mathbf{u}}{\partial \tau^2} - \left(1 + 2\beta_2\right)\frac{\partial^2 \mathbf{u}}{\partial x^2} - \frac{1 + 8\beta_2}{12}\frac{\partial^4 \mathbf{u}}{\partial x^4} - \frac{1 + 32\beta_2}{360}\frac{\partial^6 \mathbf{u}}{\partial x^6} - \frac{\mu\left(1 + 4\beta_2\right) - \left(1 + 2\beta_2\right)}{2}\frac{\partial^2}{\partial x^2}\left(\left|\mathbf{u}\right|^2 \mathbf{u}\right) = 0. \quad \textbf{(2.18)}$$

The fourth term in this equation proportional to the sixth derivative of u should be taken into account only in the case when the first dispersive term proportional to the fourth derivative is anomalously small, i.e. when $\beta_2 \approx -1/8$, otherwise it can be omitted.

Note that the nonlinear term can also turn to zero if $\mu = (1 + 2\beta_2)/(1 + 4\beta_2)$. Then, higher order nonlinear terms needs to be taken into account. Such cases will not be considered in this study.

If $\beta_2 \neq -1/2$, then for the unidirectional wave propagation, equation (2.18) can be reduced to:

$$\frac{\partial \mathbf{u}}{\partial \tau} + \sqrt{1 + 2\beta_2}\frac{\partial \mathbf{u}}{\partial x} + \frac{1 + 8\beta_2}{24\sqrt{1 + 2\beta_2}}\frac{\partial^3 \mathbf{u}}{\partial x^3} + \frac{1 + 32\beta_2}{720\sqrt{1 + 2\beta_2}}\frac{\partial^5 \mathbf{u}}{\partial x^5} + \frac{\mu\left(1 + 4\beta_2\right) - \left(1 + 2\beta_2\right)}{4\sqrt{1 + 2\beta_2}}\frac{\partial}{\partial x}\left(\left|\mathbf{u}\right|^2 \mathbf{u}\right) = 0. \quad \textbf{(2.19)}$$

As has been aforementioned, the derived equations (2.18) and (2.19) for transverse oscillations can be considered as the generalisations of the vector string equation earlier derived by Gorbacheva and Ostrovsky (1983) and Destrade and Saccomandi (2008).

In the case of $\beta_2 = 0$, i.e. when the interaction with only the nearest two particles is taken into account, and the interaction with the second neighbour atoms is neglected, equation (2.19) reduces exactly to:

$$\frac{\partial \mathbf{u}}{\partial \tau} + \frac{\partial \mathbf{u}}{\partial x} + \frac{1}{24}\frac{\partial^3 \mathbf{u}}{\partial x^3} + \frac{\mu - 1}{4}\frac{\partial}{\partial x}\left(\left|\mathbf{u}\right|^2 \mathbf{u}\right) = 0. \quad \textbf{(2.20)}$$

The higher order dispersive terms with the sixth derivative in equation (2.18) or with the fifth-derivative in equation (2.19) can be kept only if the coefficient β_2 is very close or exactly equal to $-1/8$. In the particular case when $\beta_2 = -1/8$ equation (2.18) reduces to:

$$\frac{\partial^2 \mathbf{u}}{\partial \tau^2} - \frac{3}{4}\frac{\partial^2 \mathbf{u}}{\partial x^2} + \frac{1}{120}\frac{\partial^6 \mathbf{u}}{\partial x^6} - \frac{2\mu-3}{8}\frac{\partial^2}{\partial x^2}\left(|\mathbf{u}|^2 \mathbf{u}\right) = 0, \tag{2.21}$$

and its one-directional counterpart (2.19) is given as:

$$\frac{\partial \mathbf{u}}{\partial \tau} + \frac{\sqrt{3}}{2}\frac{\partial \mathbf{u}}{\partial x} - \frac{\sqrt{3}}{360}\frac{\partial^5 \mathbf{u}}{\partial x^5} + \frac{\sqrt{3}}{24}(2\mu-3)\frac{\partial}{\partial x}\left(|\mathbf{u}|^2 \mathbf{u}\right) = 0. \tag{2.22}$$

In another particular case when $\beta_2 = -1/2$ the second term in equation (2.18) vanishes and the quadratic dispersion dependence (2.14) in the long wave approximation is obtained.

In the near-critical case when $\beta_2 = -1/2 + \varepsilon$, $0 < \varepsilon \ll 1$ is a small parameter.

In this case, equation (2.18) reduces to:

$$\frac{\partial^2 \mathbf{u}}{\partial \tau^2} + \frac{1}{4}\frac{\partial^4 \mathbf{u}}{\partial x^4} = 2\varepsilon\frac{\partial^2 \mathbf{u}}{\partial x^2} - \frac{\mu}{2}\frac{\partial^2}{\partial x^2}\left(|\mathbf{u}|^2 \mathbf{u}\right). \tag{2.23}$$

In this equation it is assumed that both terms in the right-hand side ($\sim\varepsilon$ and $\sim\mu$) are very small and they can be neglected in the zero-order approximation. When $\beta_2 = -1/2$ so that $\varepsilon = 0$, equation (2.23) can be treated as the vector version of the 'second order cubic Benjamin–Ono (socBO) equation'. Similar (but scalar) equation with the

quadratic nonlinearity has been studied in Hereman *et al.* (1986), Taghizadeh *et al.* (2011), and Najafi (2012) where exact soliton solutions were constructed by different methods.

For waves propagating only in one direction, in this case, to the right, equation (2.23) can be further simplified. It can be presented in the factorised form:

$$\left(\frac{\partial}{\partial\tau}+\frac{1}{2}\hat{H}\frac{\partial^2}{\partial x^2}\right)\left(\frac{\partial}{\partial\tau}-\frac{1}{2}\hat{H}\frac{\partial^2}{\partial x^2}\right)\mathbf{u}=\frac{\partial^2}{\partial x^2}\left(2\varepsilon\mathbf{u}-\frac{\mu}{2}|\mathbf{u}|^2\mathbf{u}\right),\qquad\textbf{(2.24)}$$

where $\hat{H}$ is the operator of the Hilbert transform:

$$\hat{H}\{f\}=\frac{1}{\pi}\int\limits_{-\infty}^{+\infty}\frac{f(x')}{x'-x}\,dx';\quad\hat{H}^{-1}=-\hat{H},$$

and the principal value of the improper integral is assumed.

Neglecting the right-hand side of equation (2.24), the following equation in the leading order for linear waves propagating to the right is can be given as:

$$\left(\frac{\partial}{\partial\tau}+\frac{1}{2}\hat{H}\frac{\partial^2}{\partial x^2}\right)\mathbf{u}=0\,,\qquad\textbf{(2.25)}$$

which provides the dispersion relation (2.14). This equation in the scalar case (i.e. when u is a one-component vector) can be treated as the linearised version of the Benjamin–Ono (BO) equation which is very well known in the theory of internal waves in the deep oceans (Ablowitz & Segur, 1981), (Apel *et al.,* 2007).

After application of the Hilbert transform, this equation reduces to the equation of "imaginary diffusion" for the vector variable u:

$$\frac{\partial\left(\hat{H}\mathbf{u}\right)}{\partial\tau} = \frac{1}{2}\frac{\partial^2\mathbf{u}}{\partial x^2} \qquad\qquad (2.26)$$

In the next approximation taking into account small but finite terms in the right-hand side of equation (2.23), equation (2.26) can be rewritten in the form:

$$\frac{\partial^2}{\partial x^2}\left(\frac{\partial\left(\hat{H}\mathbf{u}\right)}{\partial\tau} - \frac{1}{2}\frac{\partial^2\mathbf{u}}{\partial x^2} + 2\varepsilon\mathbf{u} - \frac{\mu}{2}|\mathbf{u}|^2\,\mathbf{u}\right) = 0. \qquad\qquad (2.27)$$

Integrating this equation twice with the zero constants of integration, the following nonlinear 'pseudo-diffusion' vector equation is obtained:

$$\frac{\partial\left(\hat{H}\mathbf{u}\right)}{\partial\tau} = \frac{1}{2}\frac{\partial^2\mathbf{u}}{\partial x^2} - 2\varepsilon\mathbf{u} + \frac{\mu}{2}|\mathbf{u}|^2\,\mathbf{u}. \qquad\qquad (2.28)$$

This is a new equation which was not known before. In the scalar case the equation resembles the aforementioned BO equation, but does not coincide with it (the classical BO equation contains another nonlinear term $\sim uu_x$ which is typical for hydrodynamic problems).

It can be noticed that the BO equation is one of the completely integral models in the theory of nonlinear waves (Ablowitz & Segur, 1981). On the other hand, equation (2.28) resembles the equation of nonlinear diffusion, the Kolmogorov–Petrovsky–Piskunov (KPP) equation (1937) [see also the corresponding article in the Encyclopedia

of Nonlinear Science by A. Scott (2005)] (the KPP equation contains simply u_τ rather than $\left(\hat{H}u\right)_\tau$ in the left-hand side).

2.3 Stationary Waves

As the first step, a family of stationary waves within the framework of equation (2.18) could be considered. It can be assumed that $\beta_2 \neq -1/8$ and the term with the sixth-order derivative can be omitted.

Looking for solutions which depend on one variable $s = x - Vt$ only, where V is the velocity of a stationary wave, the following vector ODE is obtained:

$$\frac{d^2\mathbf{u}}{ds^2} + 12\frac{1+2\beta_2 - V^2}{1+8\beta_2}\mathbf{u} + 6\frac{\mu\left(1+4\beta_2\right)-\left(1+2\beta_2\right)}{1+8\beta_2}|\mathbf{u}|^2\mathbf{u} = 0. \qquad (2.29)$$

To exclude spatially growing solutions for $\overline{\xi}(x)$ ($\mathbf{u} = \partial\overline{\xi}/\partial x$), zeros are chosen for both the constants of integration.

Multiplying this equation by $d\mathbf{u}/ds$, the first integral is given as:

$$\frac{1}{2}\left|\frac{d\mathbf{u}}{ds}\right|^2 + 6\frac{1+2\beta_2 - V^2}{1+8\beta_2}|\mathbf{u}|^2 + \frac{3}{2}\frac{\mu\left(1+4\beta_2\right)-\left(1+2\beta_2\right)}{1+8\beta_2}|\mathbf{u}|^4 = E. \qquad (2.30)$$

This equation can be interpreted as the energy integral for the point particle of unit mass moving in the potential field:

$$P(\mathbf{u}) = 6\frac{1+2\beta_2 - V^2}{1+8\beta_2}|\mathbf{u}|^2 + \frac{3}{2}\frac{\mu(1+4\beta_2)-(1+2\beta_2)}{1+8\beta_2}|\mathbf{u}|^4. \qquad (2.31)$$

The character of stationary solutions depends on the coefficient of the potential function.

There are in general four options which are discussed.

2.3.1 Case 1: Both Coefficients in P(u) are Negative

In this case:

$$\frac{1+2\beta_2 - V^2}{1+8\beta_2} < 0 \quad \text{and} \quad \frac{\mu(1+4\beta_2)-(1+2\beta_2)}{1+8\beta_2} < 0, \qquad (2.32)$$

there is only one global maximum in the potential function (see figure 2.4), and there are no limited motions in the equivalent dynamical system (2.29) (i.e. the motion is unstable on both sides of the global maximum). Corresponding solutions of equation (2.29) are unlimited and not interesting.

The conditions (2.32) can be fulfilled either when:

- $-1/8 < \beta_2 < 0$, $V^2 > 1 + 2\beta_2$, $\mu < (1 + 2\beta_2)/(1 + 4\beta_2)$; or when

- $-1/2 < \beta_2 < -1/8$, $V^2 < 1 + 2\beta_2$, $\mu > (1 + 2\beta_2)/(1 + 4\beta_2)$

[As stated parameter $\mu > 0$, see its definition after equation (2.10)].
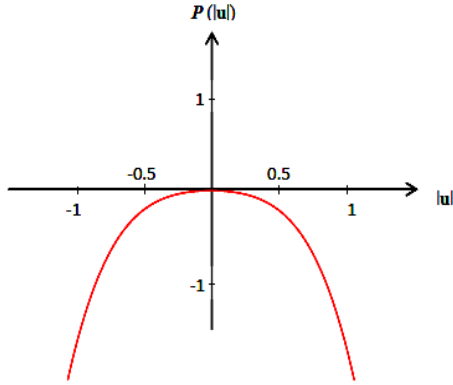
Figure 2.4: The above graph shows the qualitative shape of the cross-sections of 3D potential function (2.31) in equation (2.30) corresponding to case 1 above.

2.3.2 Case 2: The Quadratic Coefficient in P(u) is Negative and the Quartic Coefficient is Positive.

In this case:

$$\frac{1+2\beta_2-V^2}{1+8\beta_2} < 0 \text{ and } \frac{\mu(1+4\beta_2)-(1+2\beta_2)}{1+8\beta_2} > 0 . \tag{2.33}$$

There is one local maximum and two global minima in the potential function (see graph in figure 2.5).
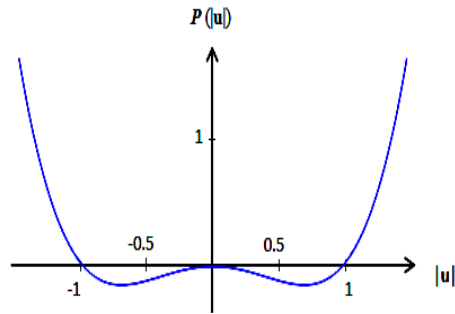
Figure 2.5: The above graph shows the qualitative shape of the cross-sections of 3D potential function (2.31) in equation (2.30) corresponding to case 2 above.

31

Such situation may occur when β_2 varies from $-1/4$ to 0, but the parameters should be such that either:

❖ $-1/4 < \beta_2 < -1/8$, $V^2 < 1 + 2\beta_2$, $\mu < (1 + 2\beta_2)/(1 + 4\beta_2)$; or

❖ $-1/8 < \beta_2 < 0$, $V^2 > 1 + 2\beta_2$, $\mu > (1 + 2\beta_2)/(1 + 4\beta_2)$.

In this case there are periodic motions with $E < 0$ in the dynamical system (2.29) around shifted centres $|u| = |u_0|$,

where

$$|\mathbf{u}_0| = \sqrt{\frac{V^2 - (1 + 2\beta_2)}{\mu(1 + 4\beta_2) - (1 + 2\beta_2)}}. \tag{2.34}$$

Periodic motions with shifted centres correspond to periodic stationary waves on a constant pedestal in terms of $|u|$, but in terms of atom displacement such solutions correspond to periodic waves on infinitely growing background. Such solutions are not interesting and not discussed in this study.

However, in the limiting case of waves with infinite periods and $E = 0$, such solutions reduce to solitary waves in terms of $|u|$ or kinks in terms of $|\xi|$. These solutions are limited and in the scalar case (when vector u has only one component u) are described by the following equations:

$$u(s) = \frac{A_s}{\cosh(s/\Delta_s)}, \quad \bar{y}(s) = 2A_s\Delta_s\left[\tan^{-1}\left(e^{-s/\Delta_s}\right) - C\right], \tag{2.35}$$

32

where characteristic solition width is:

$$\Delta_s = \frac{1}{|A_s|}\sqrt{\frac{1+8\beta_2}{3\left[\mu(1+4\beta_2)-(1+2\beta_2)\right]}} \, , \tag{2.36}$$

and velocity is:

$$V = \pm\sqrt{1+2\beta_2 + \frac{A_s^2}{4}\left[\mu(1+4\beta_2)-(1+2\beta_2)\right]} \, . \tag{2.37}$$

Both are linked with the soliton amplitude and C is an arbitrary constant. The soliton amplitude A_s may be both positive and negative and it can move both to the right and to the left; in terms of particle displacement $\bar{y}(s)$ the solution may be either kink or anti-kink.

If $C = 0$ then $\bar{y}(s)$ describes a kink propagating along the unperturbed atomic chain and displacing all atoms behind its front from zero to:

$$|\Delta\bar{y}| = \pi A_s \Delta_s = \frac{\pi}{\sqrt{3}}\sqrt{\frac{1+8\beta_2}{\mu(1+4\beta_2)-1-2\beta_2}} \, . \tag{2.38}$$

However if $C = \pi/4$ then the propagating kink $\bar{y}(s)$ transfers atoms from one level $-|\Delta\bar{y}|/2$ to another level $|\Delta\bar{y}|/2$ or vice versa.

When $-1/4 < \beta_2 < -1/8$, there is a solution representing the immovable kink with $V = 0$; in this case the corresponding standing soliton has maximal amplitude and minimal width is given as:

$$|A_s|_{\max} = \sqrt{\frac{-4(1+2\beta_2)}{\mu(1+4\beta_2)-1-2\beta_2}} \; ,$$

(2.39)

$$(\Delta_s)_{\min} = \sqrt{-\frac{1+8\beta_2}{12(1+2\beta_2)}} \; .$$

When soliton amplitude decreases from that maximal value, it becomes moving, and its speed increases on absolute value and approaches $(1 + 2\beta_2)^{1/2}$.

Such soliton can be dubbed the "slow soliton". The dependence of slow soliton's speed on its amplitude is shown in figure 2.6 by line 1.
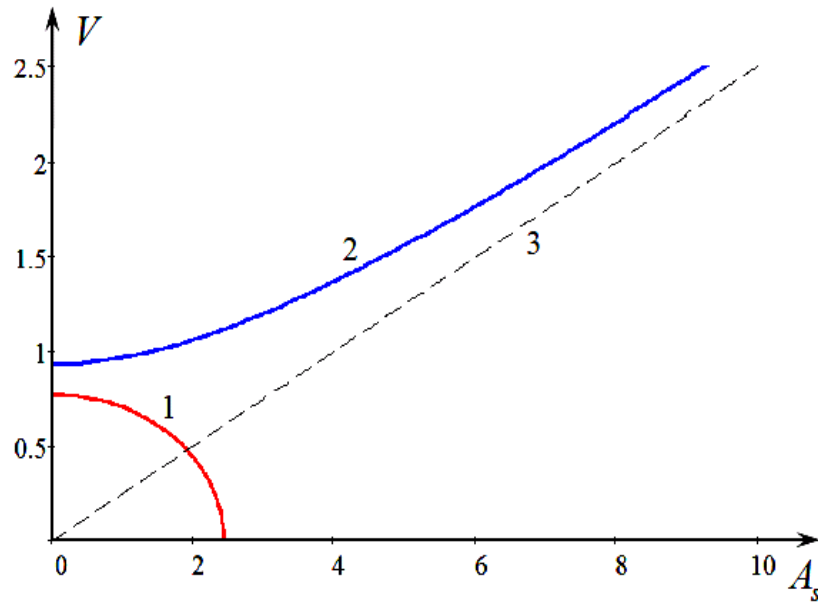
Figure 2.6: Dependence of soliton speed on amplitude for slow soliton (Line 1, generated for $\mu = 1$, $\beta_2 = -0.2$) and for fast soliton (line 2, generated for $\mu = 1.5$, $\beta_2 = -1/16$). Dashed line 3 shows asymptotic dependence of fast soliton speed on amplitude.

34
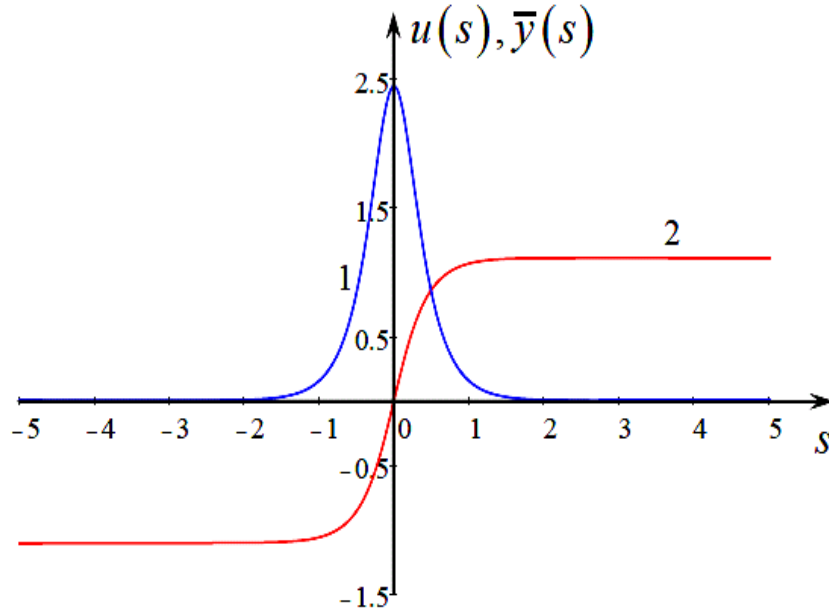
Figure 2.7: Standing soliton (line 1) and corresponding kink (line 2) as per equation (2.35). The plot was generated for $V = 0$, $\mu = 1$ and $\beta_2 = -0.2$.

When $-1/8 < \beta_2 < 0$, there is a family of fast solitons whose speed increases with amplitude from $V_{min} = (1 + 2\beta_2)^{1/2}$ to infinity when $A_s \to \infty$. The corresponding dependence of fast soliton speed on its amplitude is shown in figure 2.6 by line 2.

There is also a family of periodic waves with $E > 0$; these waves of large amplitude around the centre $|u| = 0$ are described by the following formula:

$$u(s) = u_0 \mathrm{sn}(ks, \gamma);$$

$$\xi(s) = -\frac{u_0}{\gamma k} \mathrm{arcosh} \sqrt{\frac{1 - \gamma^2 \mathrm{sn}^2(ks, \gamma)}{1 - \gamma^2}} \,, \tag{2.40}$$

where $\mathrm{arcosh}\, x \equiv \cosh^{-1} x$ is inverse function to $\cosh x$, sn is an elliptic function and:

35

$$k = \sqrt{2\frac{2\left[\mu\left(1+4\beta_2\right)-\left(1+2\beta_2\right)\right]u_0^2 + V^2 - 1 - 2\beta_2}{1+8\beta_2}}$$

$$\gamma^2 = \left\{2 + \frac{V^2 - 1 - 2\beta_2}{\left[\mu\left(1+4\beta_2\right)-\left(1+2\beta_2\right)\right]u_0^2}\right\}^{-1} \qquad (2.41)$$

2.3.3 Case 3: Quadratic Coefficient in the Potential P(u) is Positive and the Quartic Coefficient is Negative

In this case:

$$\frac{1+2\beta_2 - V^2}{1+8\beta_2} > 0 \text{ and } \frac{\mu\left(1+4\beta_2\right)-\left(1+2\beta_2\right)}{1+8\beta_2} < 0. \qquad (2.42)$$

There is one local minimum and two global maxima in the potential function (see figure 2.8).

Conditions (2.42) can be fulfilled either when:

❖ $-1/8 < \beta_2 < 0$, $V^2 < 1 + 2\beta_2$, $\mu < (1 + 2\beta_2)/(1 + 4\beta_2)$; or when

❖ $-1/2 < \beta_2 < -1/8$, $V^2 > 1 + 2\beta_2$, $\mu > (1 + 2\beta_2)/(1 + 4\beta_2)$ $(\mu > 0)$.

In this case there are periodic motions in the equivalent dynamical system (2.29) around the centre $|u| = 0$ with $0 < E < P_{max}(u)$. In the limit of infinite period these solutions reduce to the kink-type solutions for $|u|$. Such solutions asymptotically approach constants, but represent infinitely growing solutions at infinity in terms of particle displacement $|\xi| \sim x$.

36
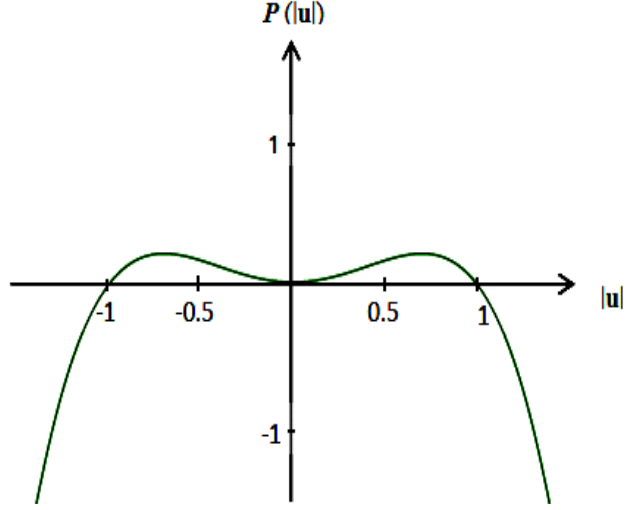
Figure 2.8: The above graph shows the qualitative shape of the cross-sections of 3D potential function (2.31) in equation (2.30) corresponding to case 3 above.

Such infinitely growing solutions are not interesting as well, whereas periodic solutions make sense and in the scalar case (when vector u has only one component u) they can be presented as:

$$u(s) = u_0 \text{sn}(ks, \gamma); \quad \xi(s) = -\frac{u_0}{\gamma k} \text{arcosh} \sqrt{\frac{1 - \gamma^2 \text{sn}^2(ks, \gamma)}{1 - \gamma^2}}, \quad \textbf{(2.43)}$$

where

$$k = \sqrt{\frac{2}{1 + 8\beta_2} \left\{ 1 + 2\beta_2 - V^2 + \left[(1 + 2\beta_2) - \mu(1 + 4\beta_2) \right] u_0^2 \right\}},$$

$$\gamma^2 = \left\{ \frac{1 + 2\beta_2 - V^2}{\left[\mu(1 + 4\beta_2) - (1 + 2\beta_2) \right] u_0^2} - 1 \right\}^{-1}.$$

2.3.4 Case 4: Both Coefficients in the Potential P(u) are Positive

In this case:

$$\frac{1+2\beta_2-V^2}{1+8\beta_2} > 0 \quad \text{and} \quad \frac{\mu\left(1+4\beta_2\right)-\left(1+2\beta_2\right)}{1+8\beta_2} > 0. \tag{2.44}$$

There is only one global minimum in the potential function (see figure 2.9). Conditions (2.44) can be fulfilled either when:

- ❖ $-1/8 < \beta_2 < 0$, $V^2 < 1 + 2\beta_2$, $\mu > (1 + 2\beta_2)/(1 + 4\beta_2)$; or when

- ❖ $-1/4 < \beta_2 < -1/8$, $V^2 > 1 + 2\beta_2$, $\mu < (1 + 2\beta_2)/(1 + 4\beta_2)$.
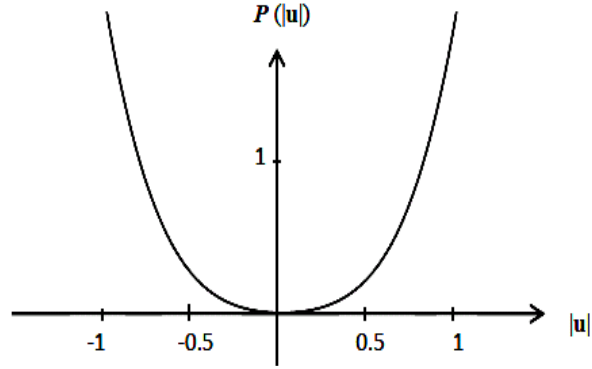
Figure 2.9: The above graph shows the qualitative shape of the cross-sections of 3D potential function (2.31) in equation (2.30) corresponding to case 4 above.

Then only periodic motions with $E > 0$ may occur in the equivalent dynamical system (2.29):

$$u(s)=u_0\text{sn}\left(ks,\gamma\right); \quad \xi(s)=-\frac{u_0}{\gamma k}\text{arcosh}\sqrt{\frac{1-\gamma^2\text{sn}^2\left(ks,\gamma\right)}{1-\gamma^2}}, \tag{2.45}$$

where

$$k = \sqrt{2\frac{1+2\beta_2 - V^2 + 2\left[\mu\left(1+4\beta_2\right) - \left(1+2\beta_2\right)\right]u_0^2}{1+8\beta_2}},$$

$$\gamma^2 = \left\{\frac{1+2\beta_2 - V^2}{\left[\mu\left(1+4\beta_2\right) - \left(1+2\beta_2\right)\right]u_0^2} + 2\right\}^{-1}.$$

2.4 Conclusion

It has been shown that flexural transverse waves in an anharmonic chain of atoms can be described by rather general vector differential-difference equation which can be reduced to the generalised "string equation" in the long-wave approximation. This equation possesses a rich spectrum of properties and can be reduced to many different equations in the particular cases. The basic differential-difference equation takes into account the interaction of each atom with two nearest neighbours from both sides. Such interaction in the linear approximation leads to the dispersion relation which depends on the strength of bonds between the nearest atoms and next neighbours. As the result, the dispersion relation in the long-wave approximation may be both linear and quadratic depending on the relationship between the bonds.

Experimental observations confirm that both these cases are realised in different crystals (Nicklow *et al.,* 1972). In one of the particular cases the equation derived can be reduced to the vector mKdV equation derived for the first time by Gorbacheva and Ostrovsky (1983) [see also (Destrade & Saccomandi, 2008)]. In another particular case our equation (2.18) can be reduced to the new model equation dubbed here the 'second order cubic Benjamin–Ono (socBO) equation'. Its further reduction leads to one wave

'pseudo-diffusion equation', which resembles the Kolmogorov–Petrovsky–Piskunov equation.

Chapter 3 Non-Linear Non Stationary Waves in a Vector Model of a String

3.1 Introduction

The previous chapter showed the existence of the stationary solitary waves. In addition to the stationary solitary waves, non stationary solitary waves also exist within the framework of the vector mKdV equation. The two typical cases are breathers and helical solitons. These solutions represent solitary waves propagating with the constant speeds and having non stationary internal structures – in the simplest embodiments they represent stationary propagating wave trains whose envelope and carrier waves move with different speeds.

There are many studies in which the problem of interaction of vector solitary waves within the framework of coupled sets of mKdV equations has been studied using different methods of numerical solution (Erbay, 1998), (Muslu & Erbay, 2003), (Ismail, 2008), (Ismail, 2009), (Uddin *et al.,* 2009), (Triki & Ismail, 2010), (Uddin & Jan, 2013).

Erbay (1998), by using asymptotic expansion technique based on the Lagrangian density formulation demonstrated that the nonlinear interaction between two transverse waves propagating in a generalized elastic solid is described asymptotically by the complex modified Korteweg–de Vries (cmKdV) equation. The derivation is for ion acoustic waves in unmagnetised plasma. It was claimed that for any non-integrable equation, solitons can interact and can gain or lose energy in collisions with each other and in particular the direct consequence of the non-integrability of the cmKdV equation

is that the collision of two solitary waves is possibly inelastic, with some residual radiation. However, the interaction of solitary waves under different polarization was just briefly discussed in that paper, but not investigated.

In the study by Erbay and Muslu, (2003), cmKdV equation was solved numerically by three different split-step Fourier schemes. The importance of interactions of solitary waves under different polarization was emphasized, but not investigated in detail. Numerical study of a complex integrable mKdV (civmKdV) equation similar to (2.47) with zero right-hand side was undertaken by Karney *et al.* (1979). They found the existence of two types of solitary waves, constant phase pulses and helical solitary waves.

The civmKdV equation and its relation to the non-integrable mKdV equation (2.47) have been examined numerically. The results obtained are presented in this chapter. It was confirmed that plane solitons and the corresponding kinks exist in the chain model in agreement with equations (2.33) and (2.34). Then, we investigated the non stationary dynamics of plane and helical solitons moving in the same direction along the *x*-axis, having the same and different polarisations.

The integrable and non integrable forms of the vector mKdV equation were numerically solved by the developed FORTRAN code (see Appendix B for full code). Exact solutions of the completely integrable mKdV equation were used as the test cases to validate the accuracy of the numerical code. The interactions between different types of solitary waves in integrable and non integrable cases are compared.

42

3.2 Breather Solutions

As has been mentioned, in the case of plane polarization, equation (2.20) reduces to the well-known and completely integrable scalar mKdV equation. This equation has breather solutions when the nonlinear coefficient is positive [see, e.g., (Lamb, 1980), (Ablowitz & Segur, 1981)]. The breather solutions may exist when the parameters of equation (2.20) correspond to case 2 in chapter 2. In the particular case of equation (2.20) the *plane polarised breather* is a two-parametric solution (Lamb, 1980):

$$u(x,\tau) = -\frac{8\beta}{3^{1/6}\sqrt{\mu-1}} \frac{\cos\Phi - (\beta/\alpha)\sin\Phi\tanh\Psi}{1+(\beta/\alpha)^2 \sin^2\Phi\,\mathrm{sech}^2\Psi}\,\mathrm{sech}\Psi \tag{3.1}$$

where

$$\Phi = 4\cdot 3^{1/3}\alpha x + \delta\tau + \varphi_0, \quad \Psi = 4\cdot 3^{1/3}\beta x + \gamma\tau + \psi_0, \quad \delta = 8\alpha(\alpha^2 - 3\beta^2),$$

$$\gamma = 8\beta(3\alpha^2 - \beta^2),$$

and φ_0 and ψ_0 are arbitrary constants.

Here, α and β are independent parameters which determine breather amplitude, width, as well as its group and phase speeds. The breather moves with the group speed $V_g = \gamma/2\beta$, whereas its phase speed is $V_{ph} = \delta/2\alpha$. The breather shape may be very different, depending on the parameters, α and β.

It may represent a pair of coupled solitons of opposite polarity moving jointly and oscillating around each other in one limiting case, or an envelope soliton similar to the

43

soliton of the NLS equation in another limiting case (Lamb, 1980), (Ablowitz & Segur, 1981). The *plane breather* solitary waves can propagate along the atomic chain at any angle, i.e. they may have any polarization in the plane perpendicular to the chain line. It can be speculated that *vector breathers* also can exist within the framework of the vector mKdV equation, but they were not found yet.

For the sake of illustration, two different kinds of plane-polarized breathers are shown in figure 3.1 (Malomed & Stepanyants, 2010). Similar solutions were found within the Gardner equation which is related to the mKdV equation (Grimshaw *et al.,* 2010).
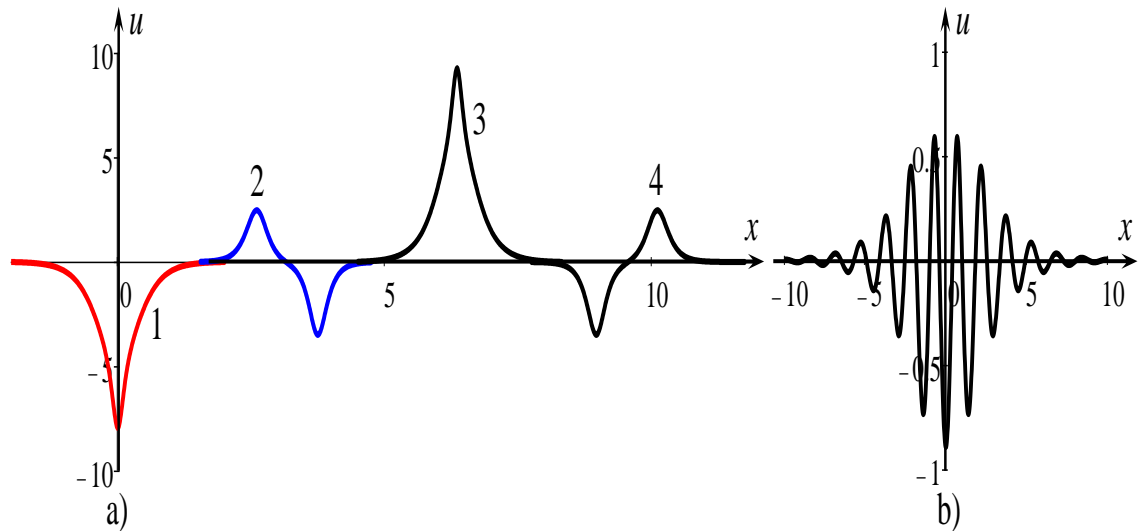
Figure 3.1: Typical breathers at different times: (a) two periodically interacting solitons in the consecutive time steps with the quarter of period interval; (b) a wave packet (Malomed and Stepanyants, 2010).

3.3 Helical Solutions

The mKdV equation (2.20) can be presented in the equivalent form as:

$$\frac{\partial \mathbf{u}}{\partial \tau} + \frac{\partial \mathbf{u}}{\partial x} + \frac{1}{24}\frac{\partial^3 \mathbf{u}}{\partial x^3} + \frac{\mu-1}{4}|\mathbf{u}|^2 \frac{\partial \mathbf{u}}{\partial x} = -\frac{\mu-1}{4}\mathbf{u}\frac{\partial |\mathbf{u}|^2}{\partial x} \qquad (3.2)$$

If the right-hand side of this equation equals zero, this equation is completely integrable (Karney *et al.,* 1979), but no physical application was found to this equation so far. If, however, the right-hand side of this equation is non-zero, but relatively small, then equation (3.2) can be treated as the perturbed completely integrable vector mKdV equation (civmKdV).

One of the options when the right-hand side is small is when the *x*-derivative of $|u|^2$ is small. This case is realised when the career wavelength is much less than the characteristic width of the envelope. Taking any exact solution of the civmKdV equation as the initial condition, its evolution can be studied numerically within the non-integrable vmKdV equation (3.2) under the influence of small right-hand side. Using this approach with the exact solution for the helical soliton of civmKdV equation, helical solitons exist within the non-integrable equation (3.2). Figure 3.3 and 3.4 show the helical solitons of different amplitudes and helicities obtained in numerical calculations. Helical solitons resemble envelope solitons of NLS equation, the helical career wave travels with different speed than its envelope.
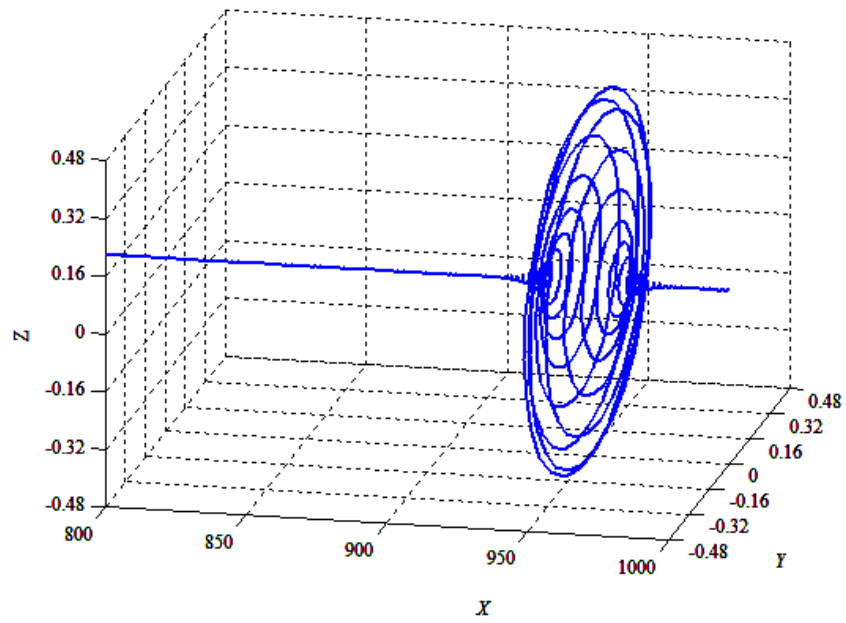
Figure 3.2: The bigger helical soliton obtained showing the envelope and the carrier wave inside.
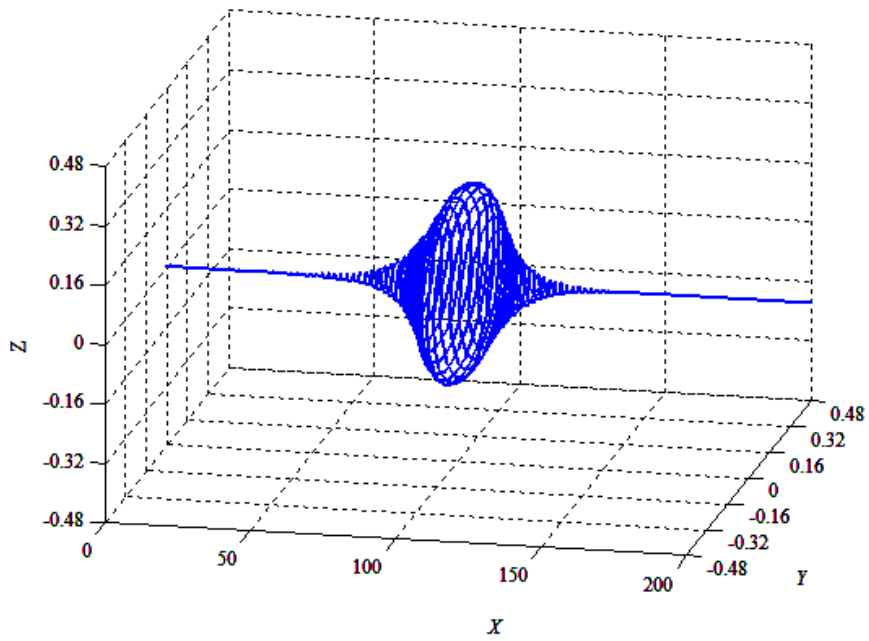
Figure 3.3 The smaller helical soliton obtained showing the envelope and the carrier wave inside.

46

3.4   Interaction of Solitary Waves – Numerical Results

A numerical modeling of chain vibrations was undertaken on the basis of fourth order Runga-Kutta method. The numerical codes have been developed in GFORTRAN and graphical results are obtained using MATLAB. The numerical code computes the interaction of plane solitons at different angles (see appendix).

3.5   Interaction of Plane Solitons

The interactions of plane solitons of the same and perpendicular polarizations were investigated both for the integrable and non-integrable cases. The graphs in both these cases show the nature of solitons before and after the interaction. Note that in the case of plane polarization when solitons are of the same or opposite polarity the vector mKdV equation reduces to the completely integrable scalar mKdV equation.

Soliton interaction in this case is elastic [see, e.g., (Lamb, 1980), (Ablowitz & Segur, 1981)]. Soliton interaction remains elastic even in the vector case of the integrable mKdV equation. But it is not the case when the vmKdV equation is non-integrable. The next st of graphs present the examples of interaction of solitons under different angles for the non-integrable case. Soliton interaction have been studied both numerically within the framework of vector mKdV equation (2.20) and within the discrete chain of particles (2.10). No difference was found in both of these cases.

It has been confirmed that the interaction of plane solitons in the integrable case is elastic for all angles between solitons. The two solitons of the same or opposite

47

polarities is found to interact elastically similar to the scalar mKdV solitons. The situation drastically changes when two plane solitons enter into the interaction being initially in the different planes in non-integrable case. The interesting feature during the interaction is the transfer of energy from the smaller soliton to the larger soliton (see figures 3.4 – 3.20). The figures 3.11, 3.16 and 3.20 show the larger soliton with an increase in amplitude after interaction. The interactions of solitons lying initially in other planes when the angle between the planes was 30° and 150° were also investigated to confirm the results obtained. A dispersive wave train was generated in the process of soliton interaction. The intensity of the wave train depended on the initial angle between these solitons.

However, interaction of two solitons lying initially in the nonparallel planes is essentially inelastic. In the former case, the solitons appear again after the collision with the same parameters as they had initially. In the latter case, the larger soliton is destroyed and transfers its energy to the smaller soliton and dispersive wave train.

The figures 3.4 – 3.20 show the interaction process between the plane solitons under different angles.

3.5.1 Interaction of Plane Solitons Initially at 45 degrees in the Non Integrable Case
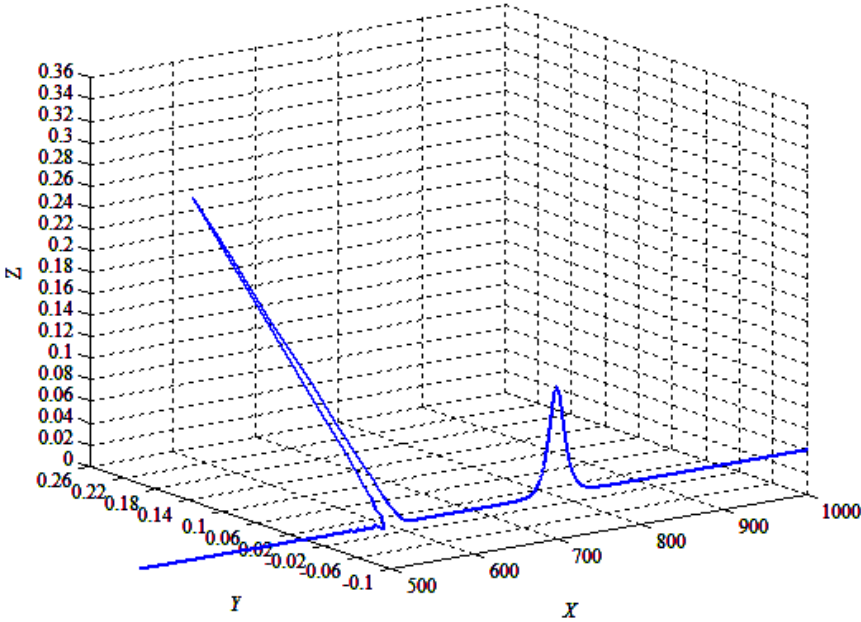
Figure 3.4: Two plane solitons initially at 45 degrees before interaction.
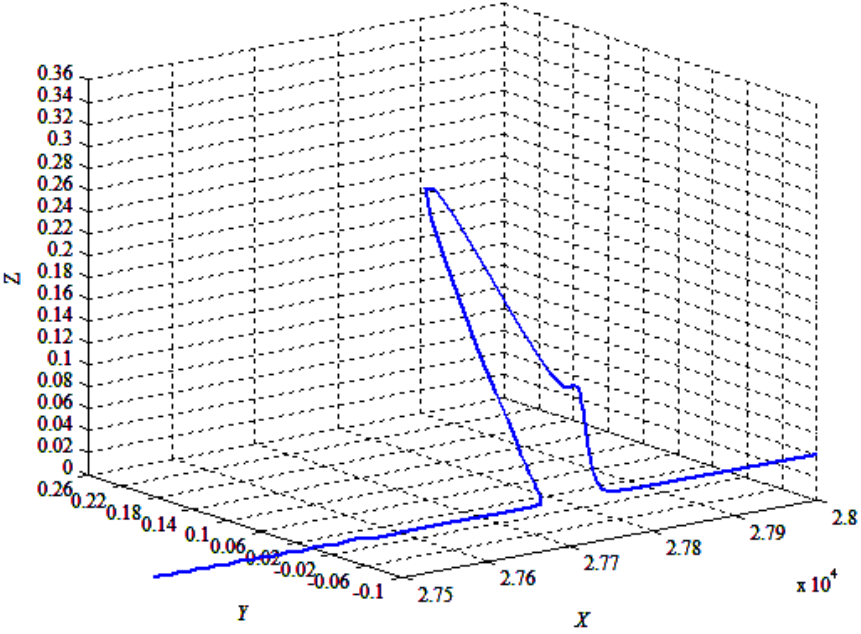
Figure 3.5: Two plane solitons initially at 45 degrees during interaction.
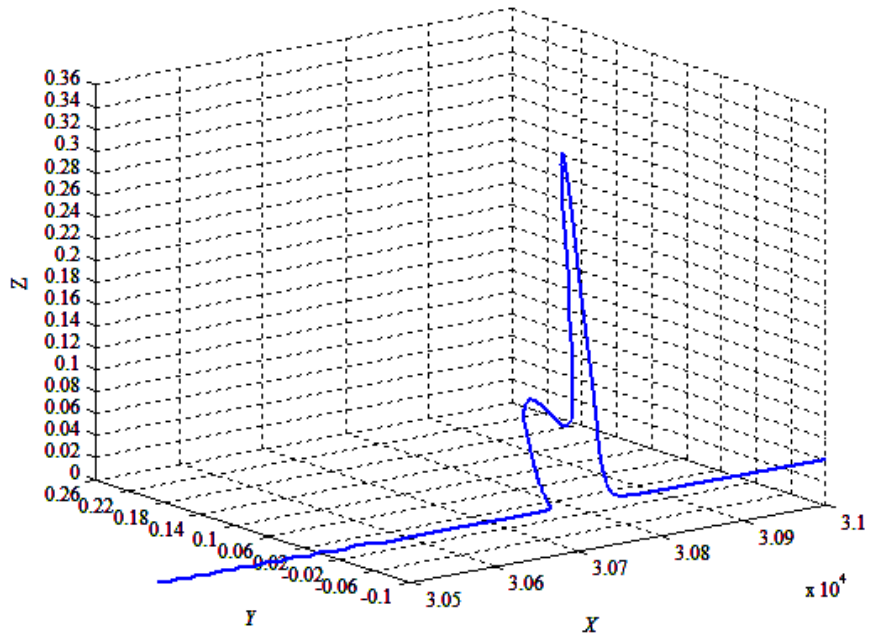
Figure 3.6: Two plane solitons initially at 45 degrees during interaction.
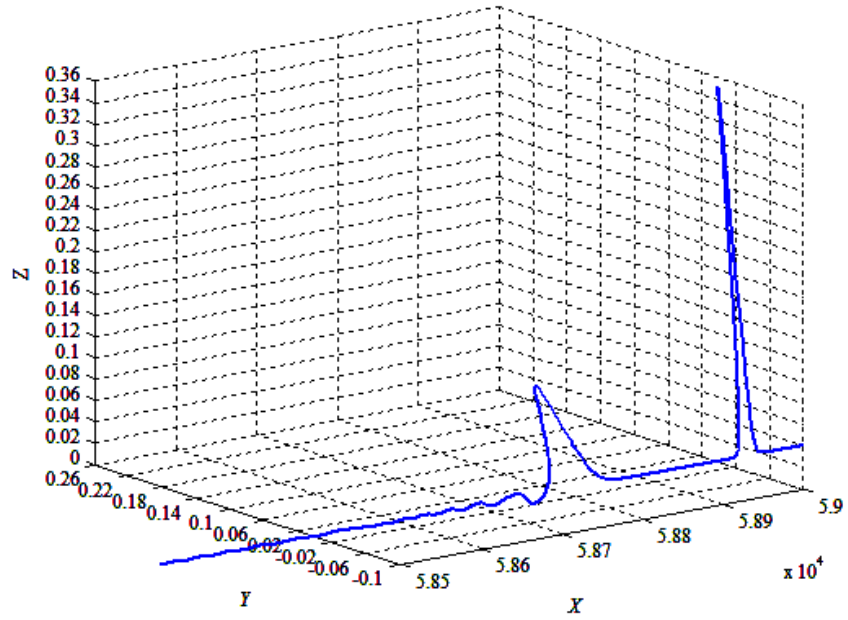
Figure 3.7: Two plane solitons initially at 45 degrees after interaction.

3.5.2 Interaction of Plane Solitons Initially at 60 degrees in the Non Integrable Case
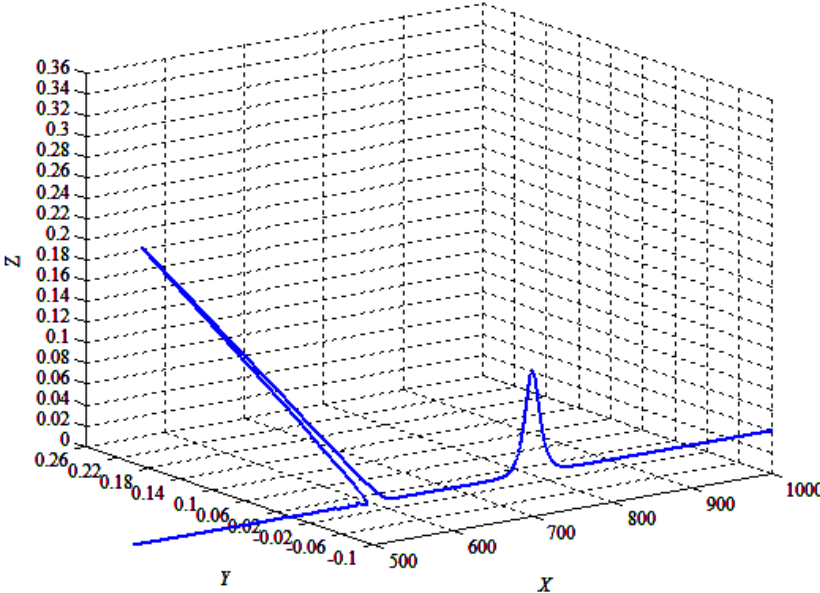
Figure 3.8: Two plane solitons initially at 60 degrees before interaction.
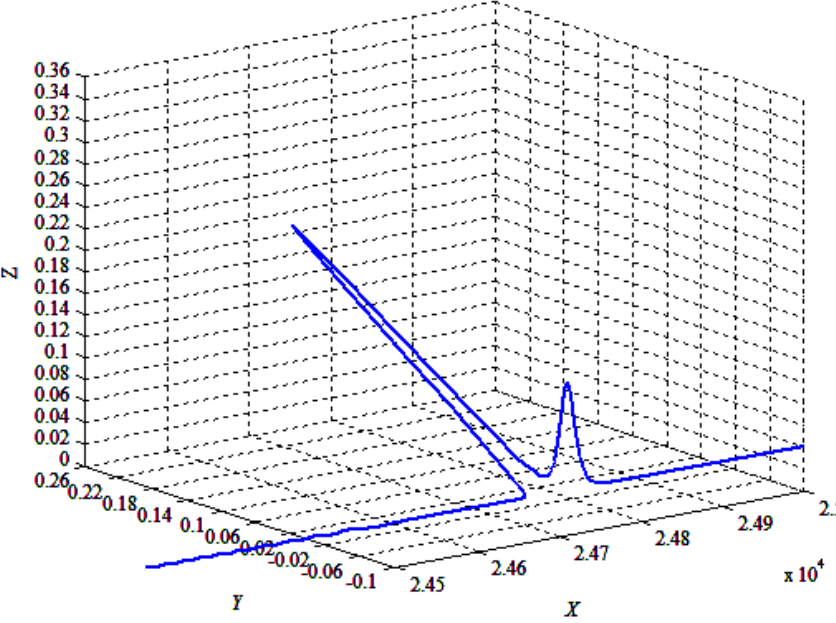
Figure 3.9: Two plane solitons initially at 60 degrees during interaction.
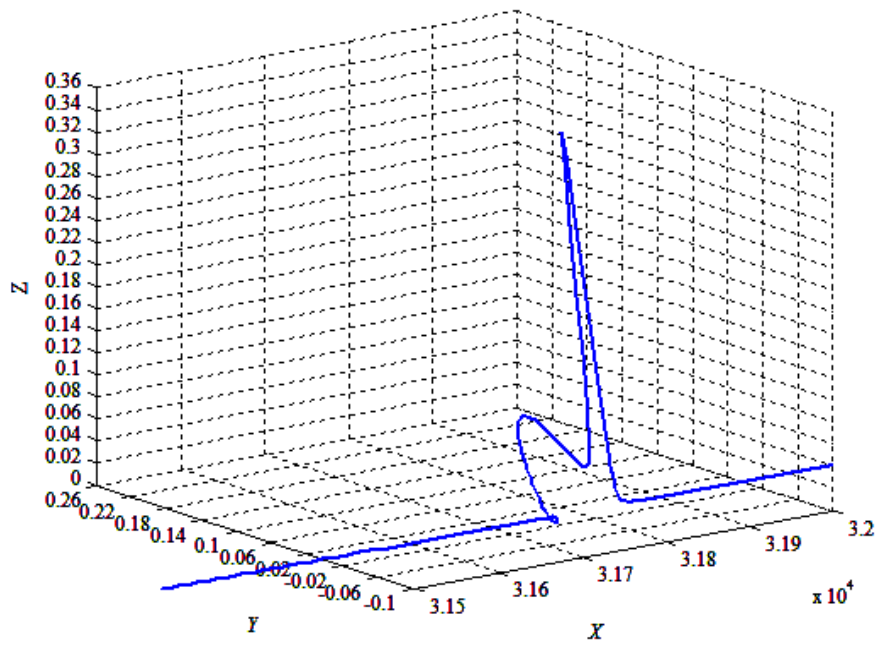
Figure 3.10: Two plane solitons initially at 60 degrees during interaction.
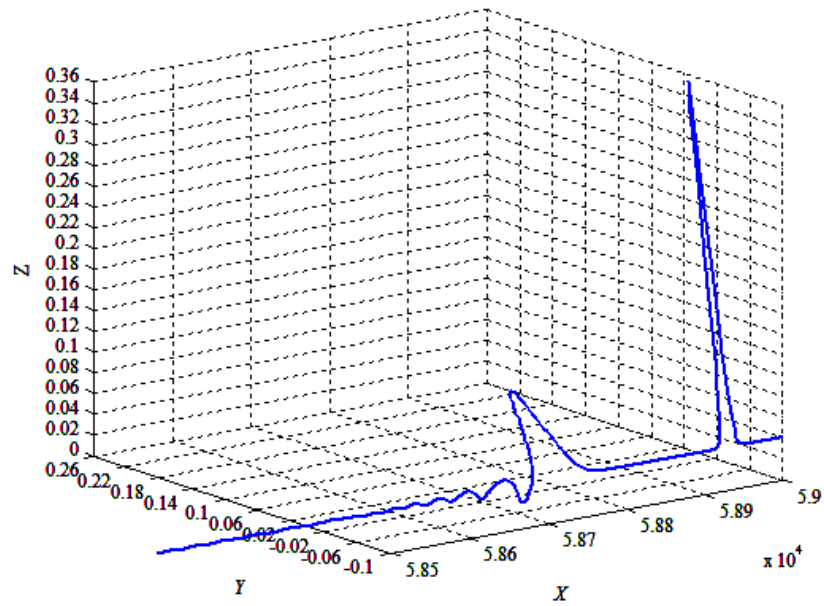
Figure 3.11: Two plane solitons initially at 60 degrees after interaction.

3.5.3 Interaction of Solitons Initially in Perpendicular Planes in Non Integrable Case
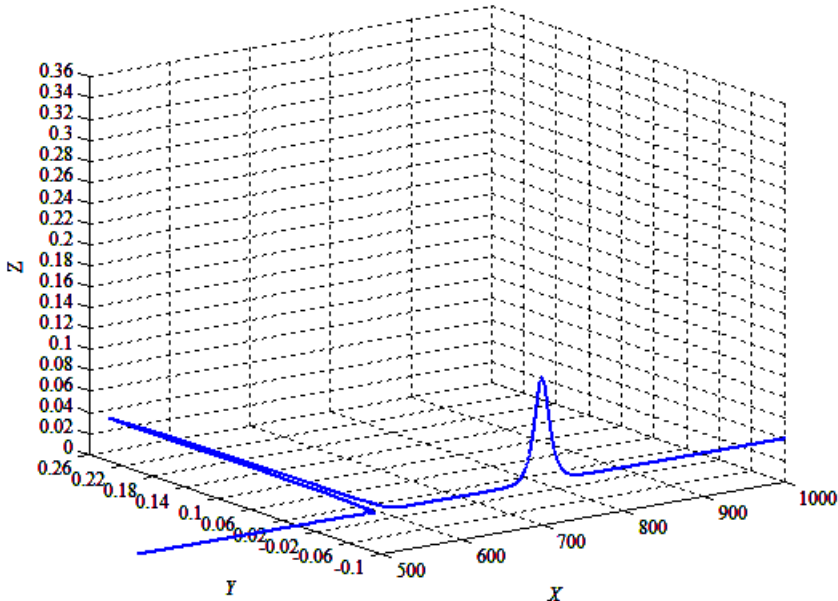
Figure 3.12: Two plane solitons initially at 90 degrees before interaction.
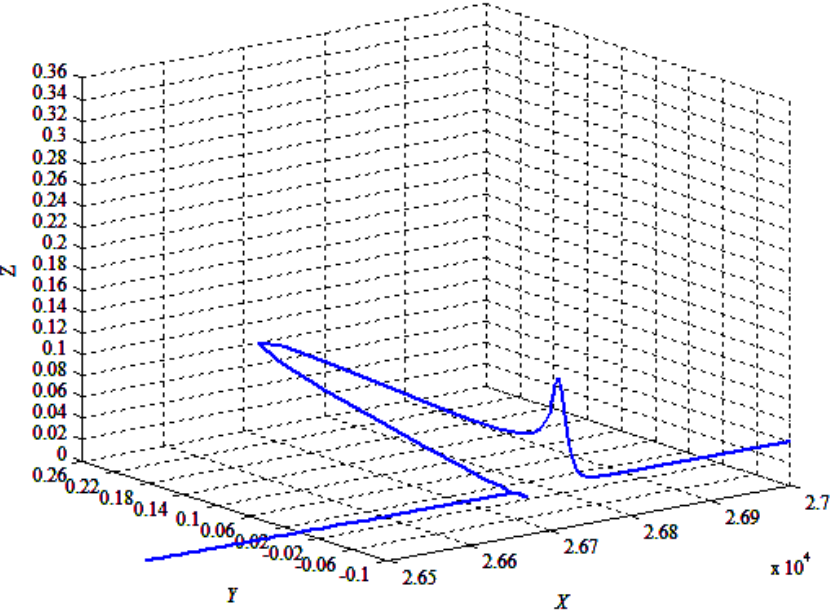
Figure 3.13: Two plane solitons initially at 90 degrees during interaction.
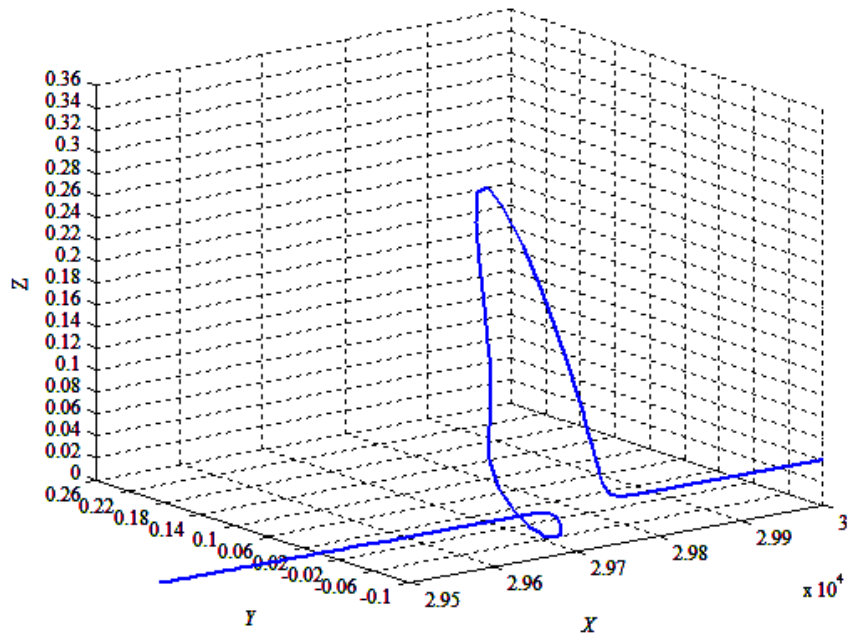
Figure 3.14: Two plane solitons initially at 90 degrees during interaction.
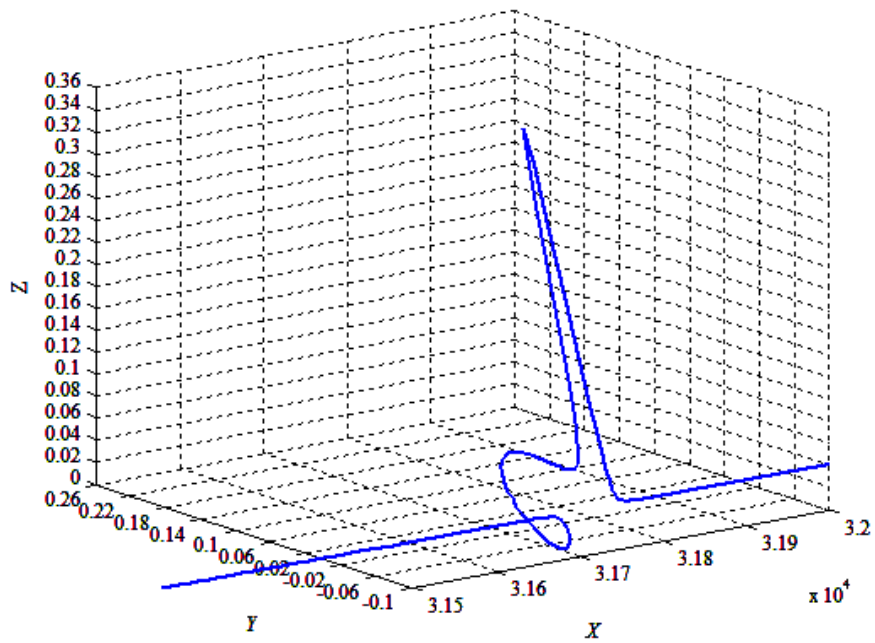
Figure 3.15: Two plane solitons initially at 90 degrees during interaction.

54
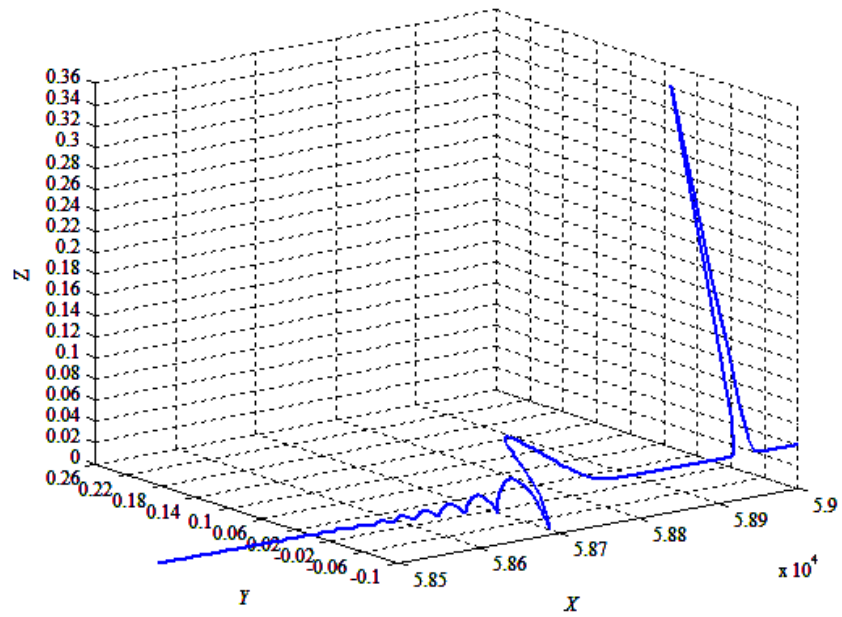
Figure 3.16: Two plane solitons initially at 90 degrees after interaction.

3.5.4 Interaction of Plane Solitons Initially at 120 degrees in the Non Integrable Case
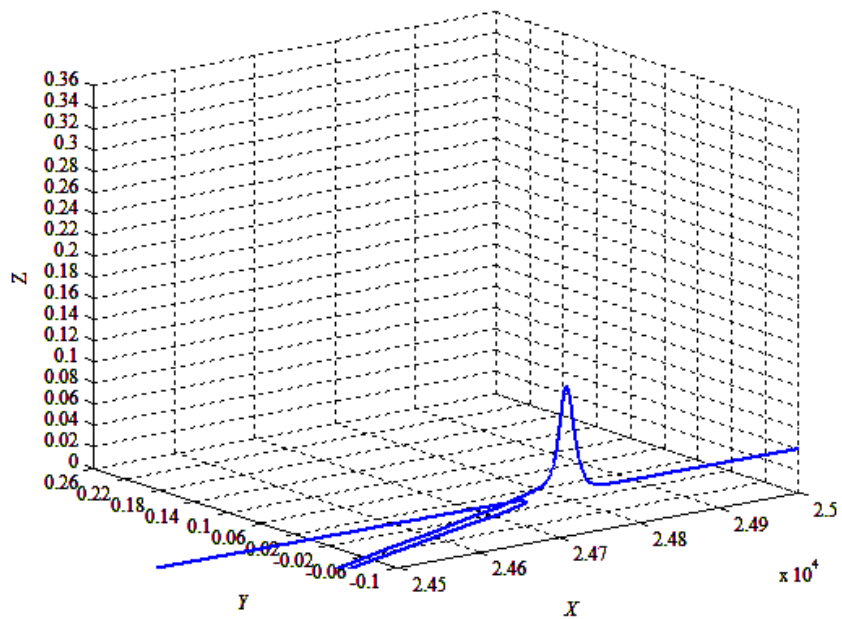
Figure 3.17: Two plane solitons initially at 120 degrees before interaction.
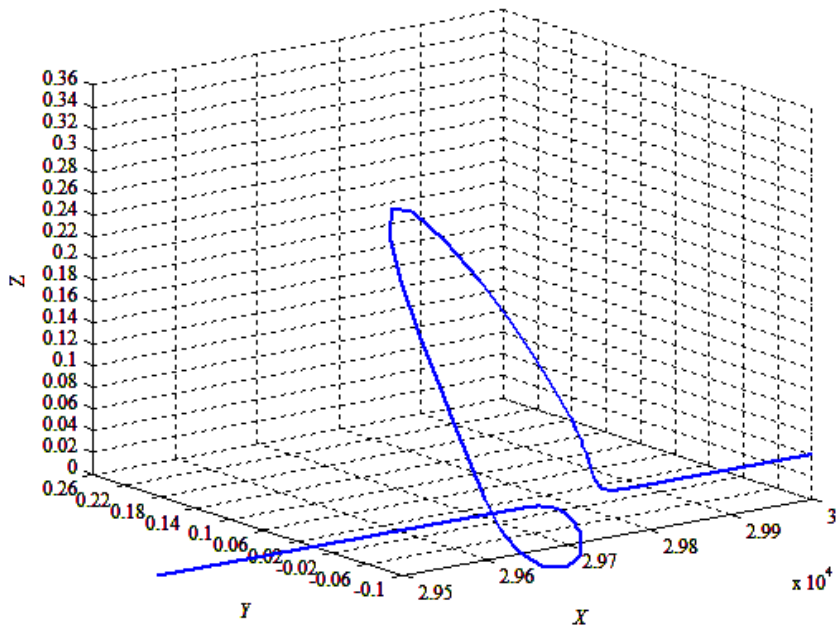
Figure 3.18: Two plane solitons initially at 120 degrees during interaction.
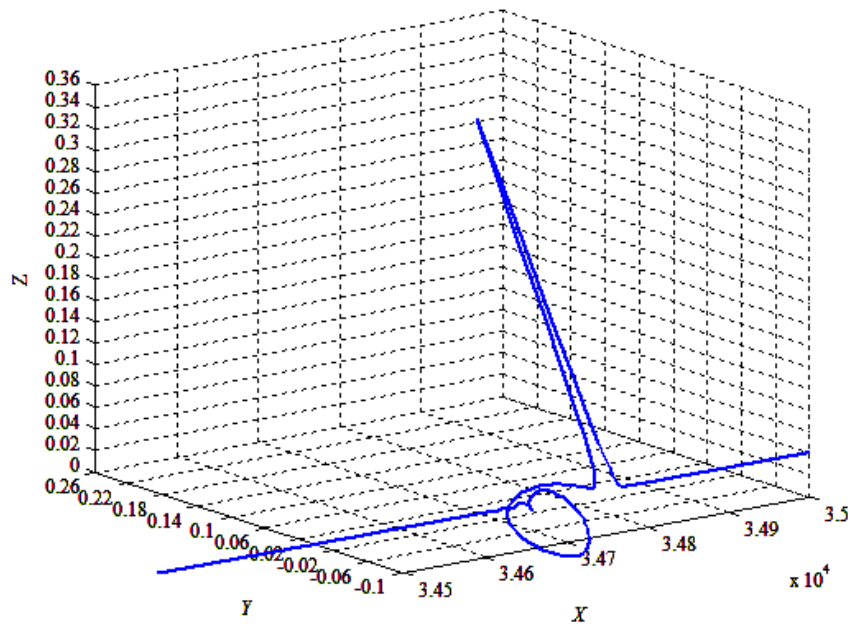
Figure 3.19: Two plane solitons initially at 120 degrees during interaction.

56
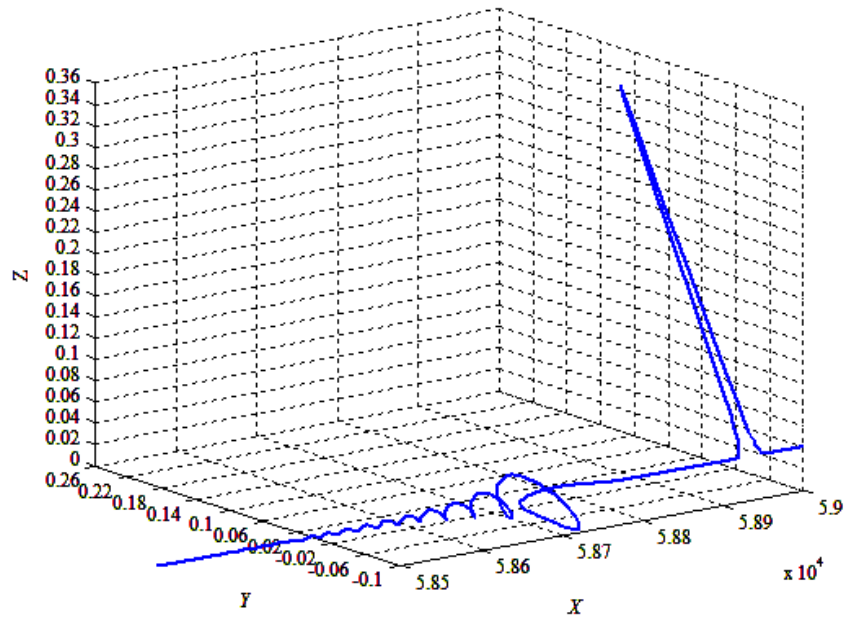
Figure 3.20: Two plane solitons initially at 120 degrees after interaction.

3.6 Interaction of Plane and Helical Solitons

This section shows how the plane and helical solitons behave in the process of collision. The interaction was studied numerically within the framework of vector mKDV equation (2.47). Two cases were studied – the integrable one, when the right-hand side of equation (2.47) is zero, and non-integrable, when the right-hand side is non-zero. The helical soliton approaches and passes through the plane soliton. The solitons return to their original form after the interaction in both the integrable and non-integrable case. The normal oscillations of the carrier waves are disturbed during this process as the helical solitons moves the through the profile of the plane soliton. The figures 3.21 – 3.32 show the interaction process between the plane and helical soliton.

57

3.6.1 Interaction of Plane and Helical Solitons in the Integrable Case
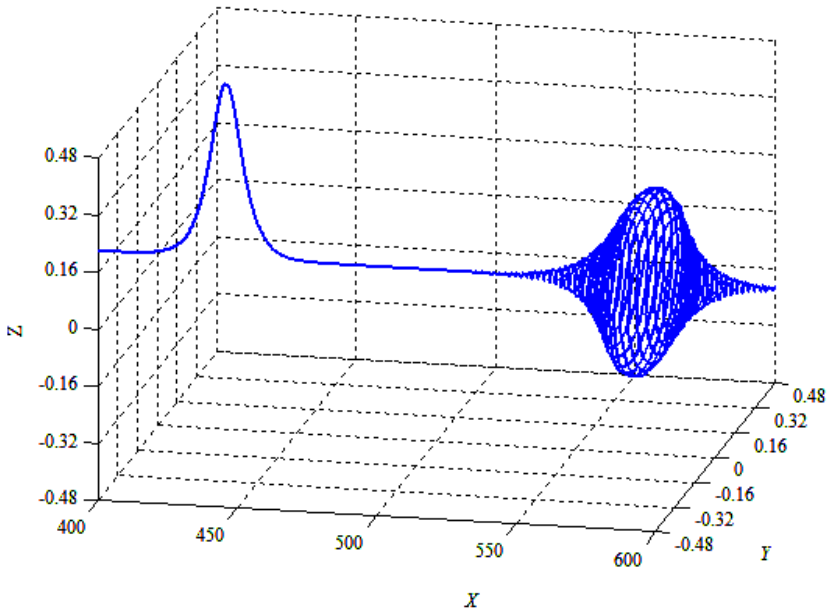
Figure 3.21: Plane and helical solitons moving closer in the integrable case of interaction.
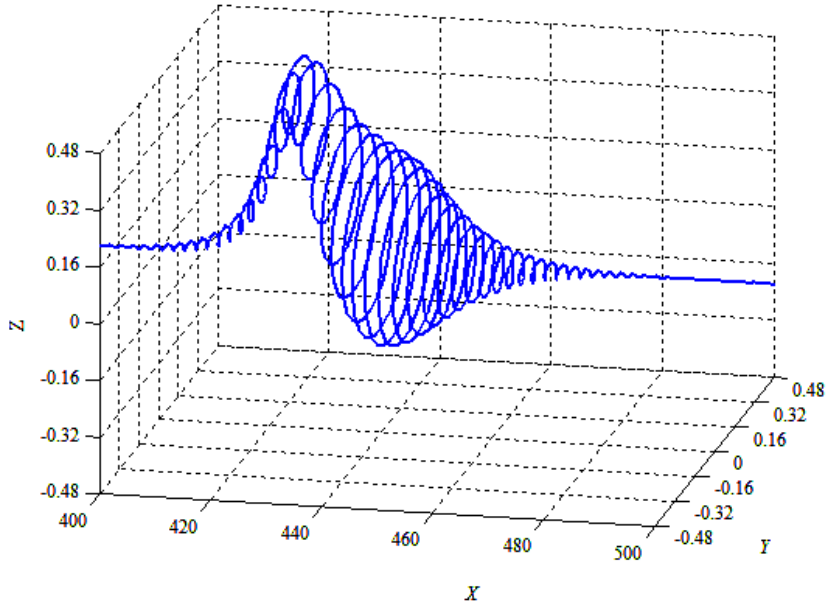
Figure 3.22: The helical soliton is passing through the plane soliton.
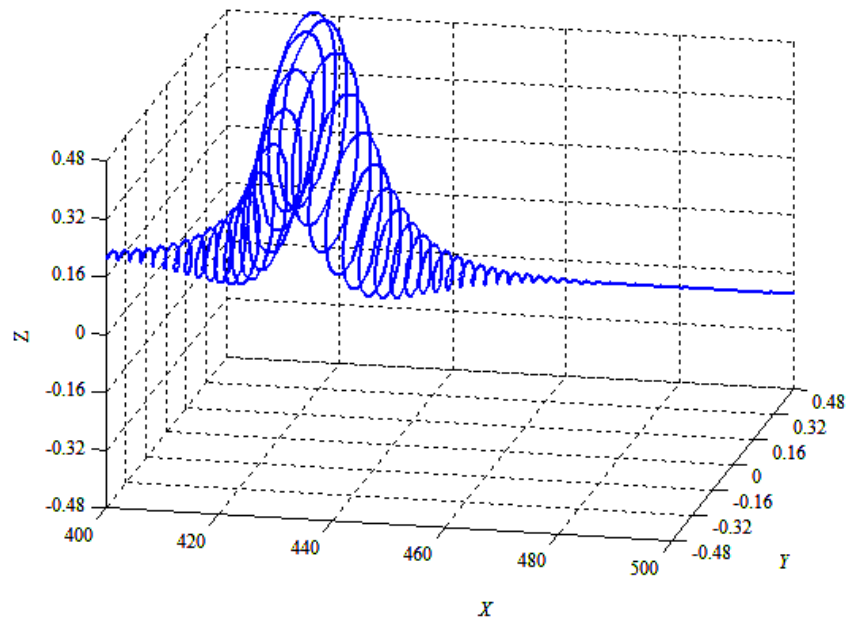
Figure 3.23: The helical and plane soliton in the process of interaction.
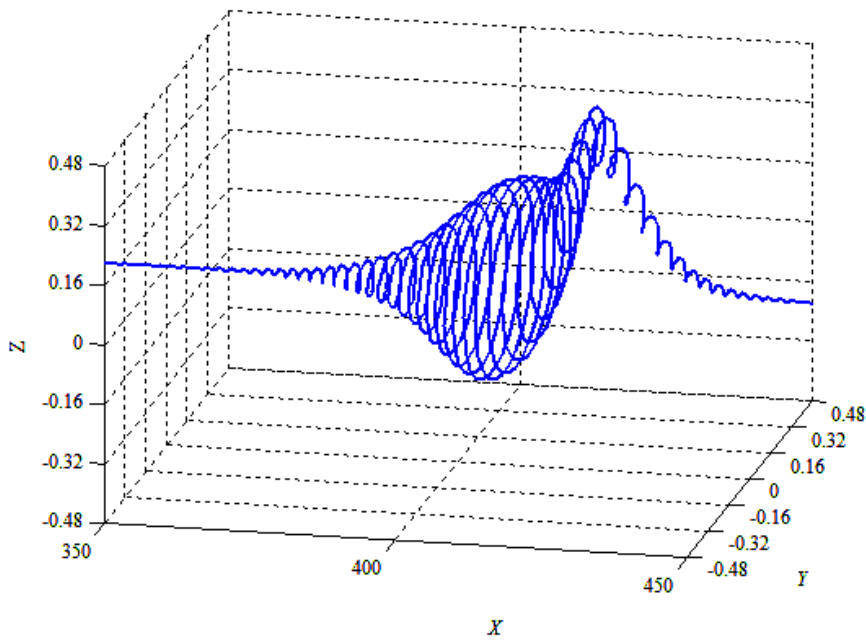
Figure 3.24: The helical soliton is in the process of moving away from the plane soliton.
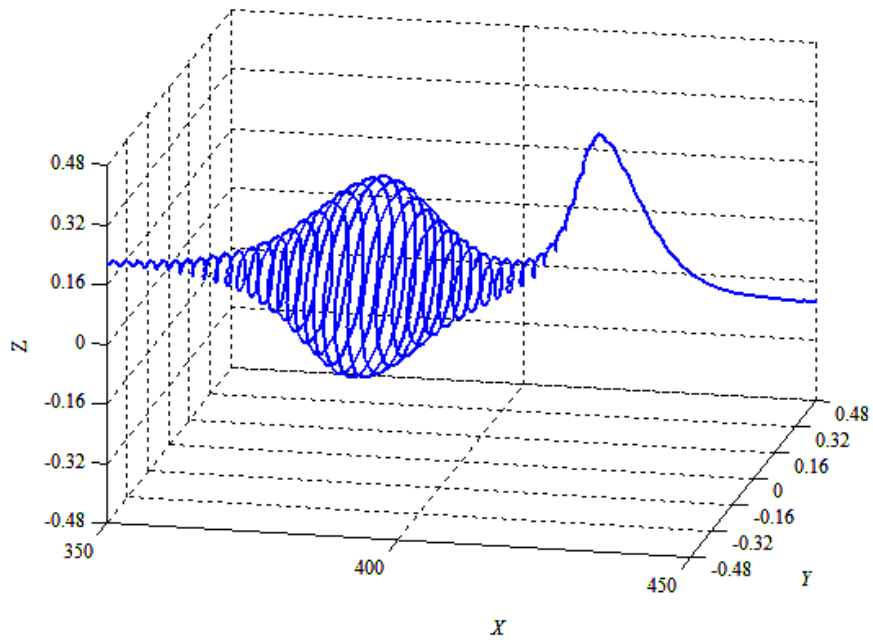
Figure 3.25: The solitons in the process of recovering their initial forms after the interaction.
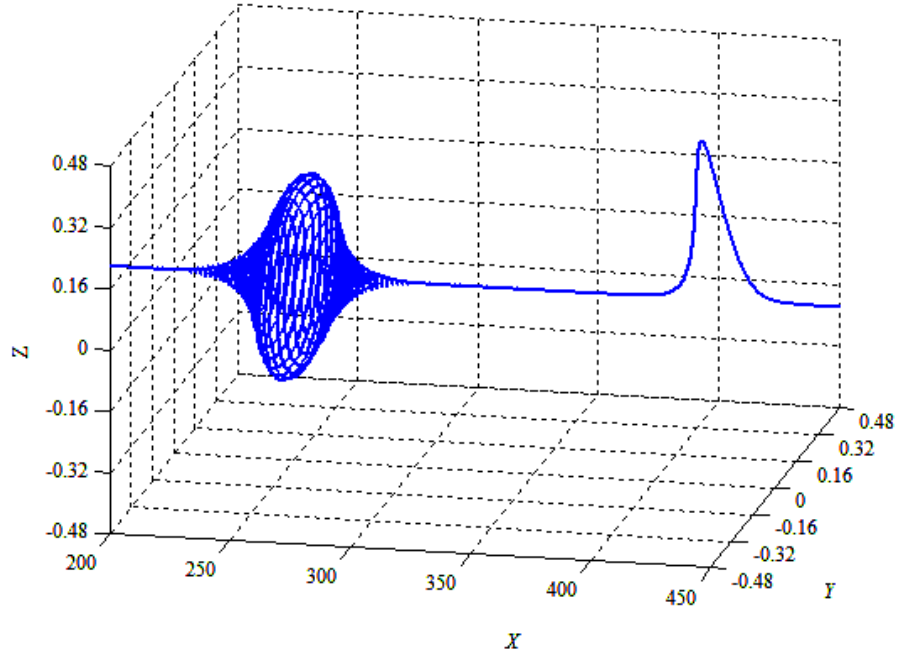
Figure 3.26: The helical and plane soliton move away after the interaction with their initial forms.

3.6.2   Interaction of Plane and Helical Solitons in the Non-Integrable Case
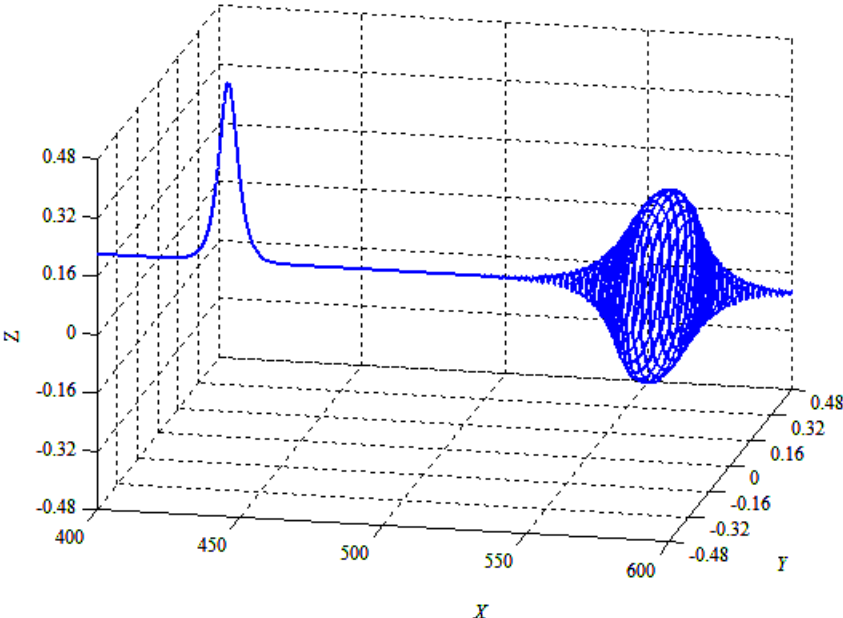
Figure 3.27: Plane and helical solitons moving closer before interaction.
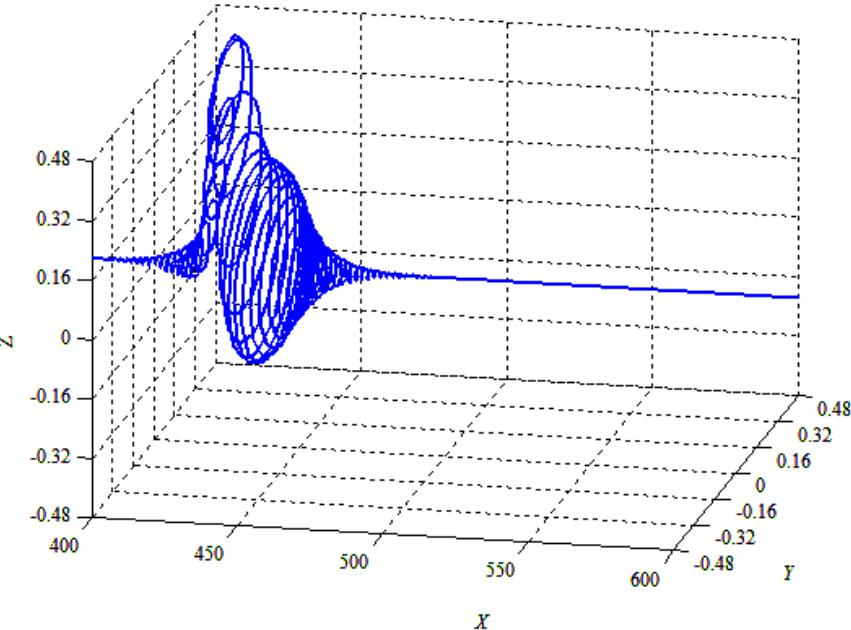
Figure 3.28: The helical soliton is passing through the plane soliton and causes the change of the form.
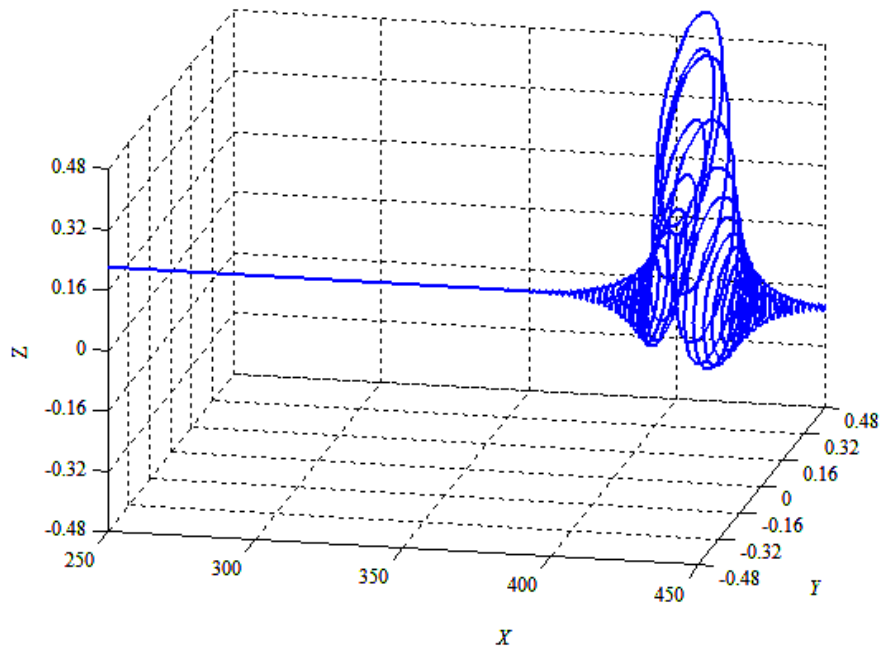
Figure 3.29: The helical and plane solitons are in the process of interaction with each other.
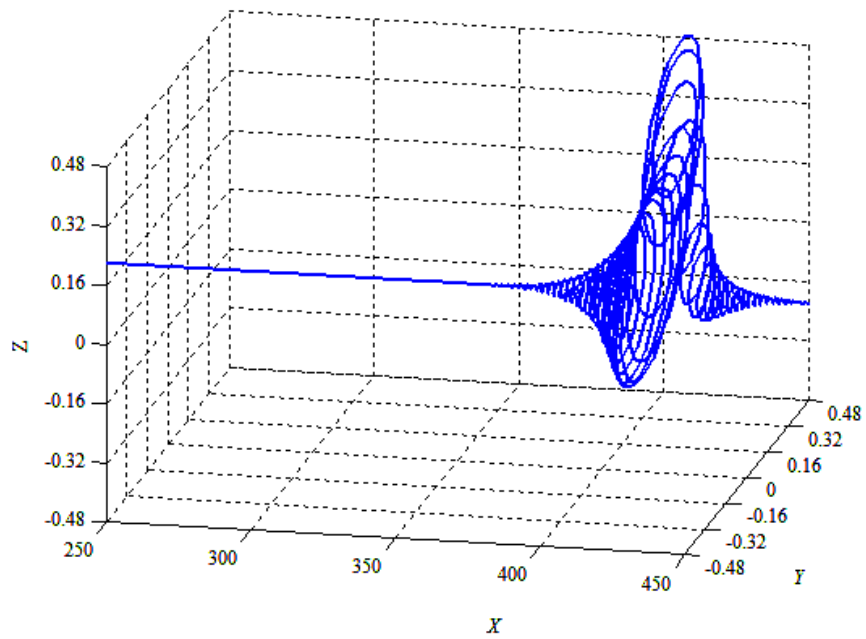
Figure 3.30: The solitons are in the process of recovering their initial forms after the interaction.

62
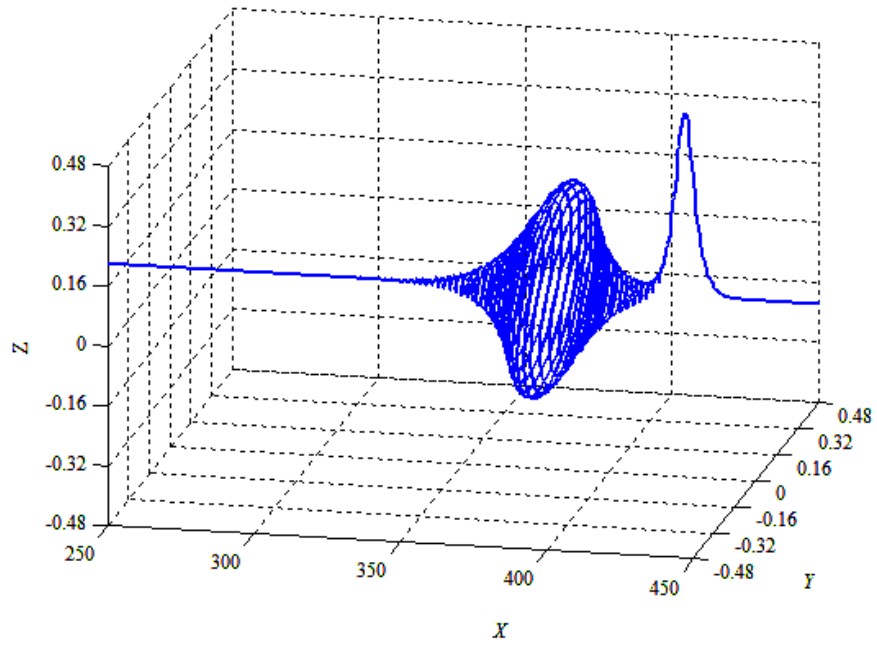
Figure 3.31: The solitons are in the process of recovering their initial forms.
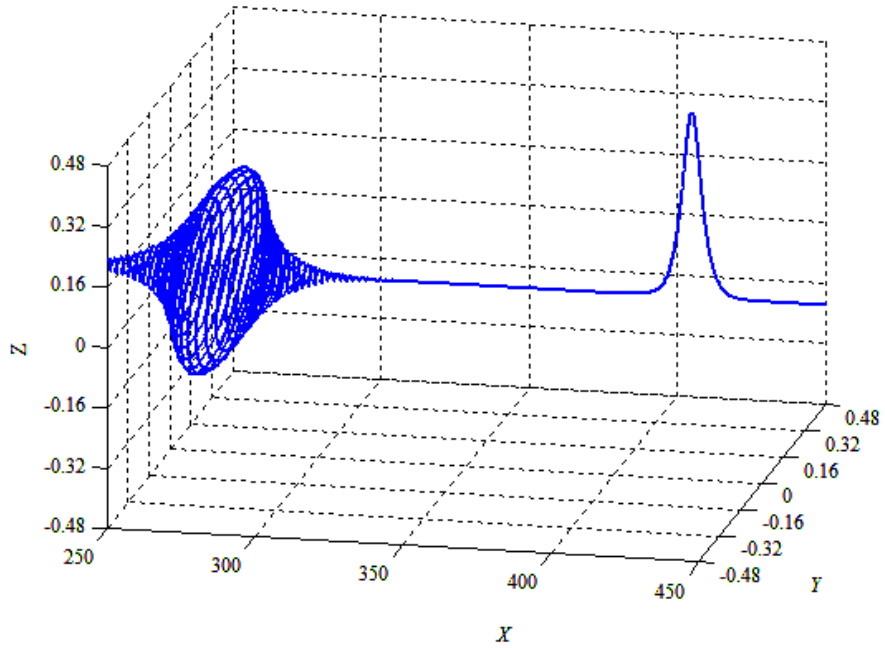
Figure 3.32: The helical and plane soliton move away after the interaction with their initial forms.

3.7 Interaction of Helical Solitons

3.7.1 Interaction of Helical Solitons of the Same Helicity in the Integrable Case

The interaction of helical solitons of the same helicity in the integrable case is very interesting and non-trivial – see figures 3.33 – 3.39. The helical soliton of a smaller amplitude moves faster than the larger soliton. In the process of collision the helical solitons form a compact state and the smaller soliton does move past the larger one. However, after passing the bigger soliton, it moves backwards and moves to the right of the larger soliton. It seems to remain at the vicinity of larger soliton and oscillate around it.
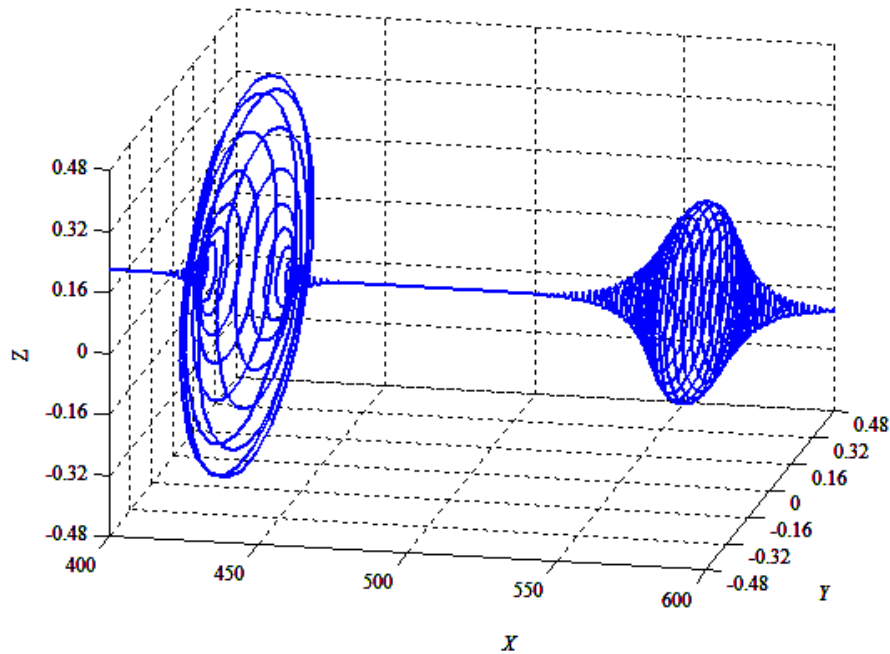
Figure 3.33: Helical solitons of the same helicity at a distance.
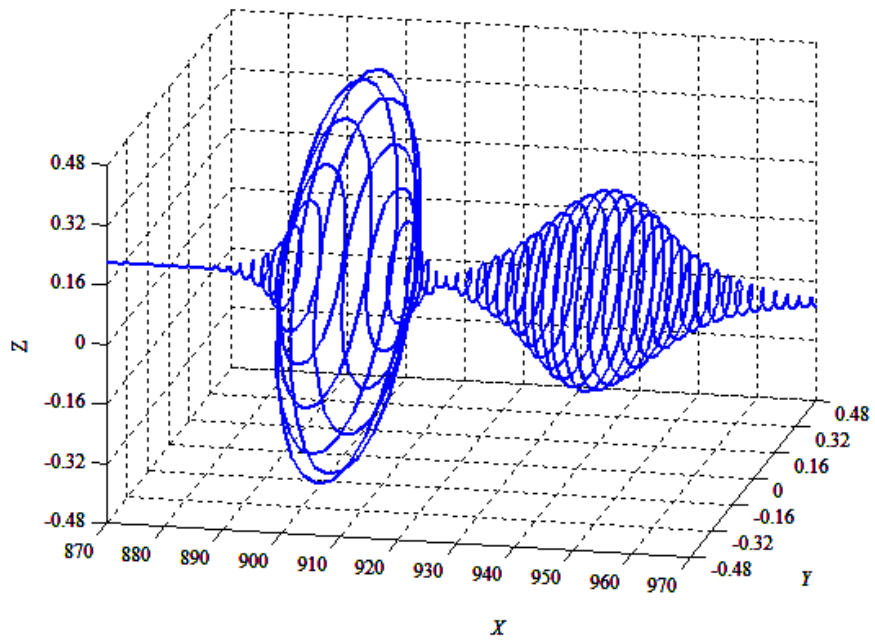
Figure 3.34: The helical solitons come close for interaction.
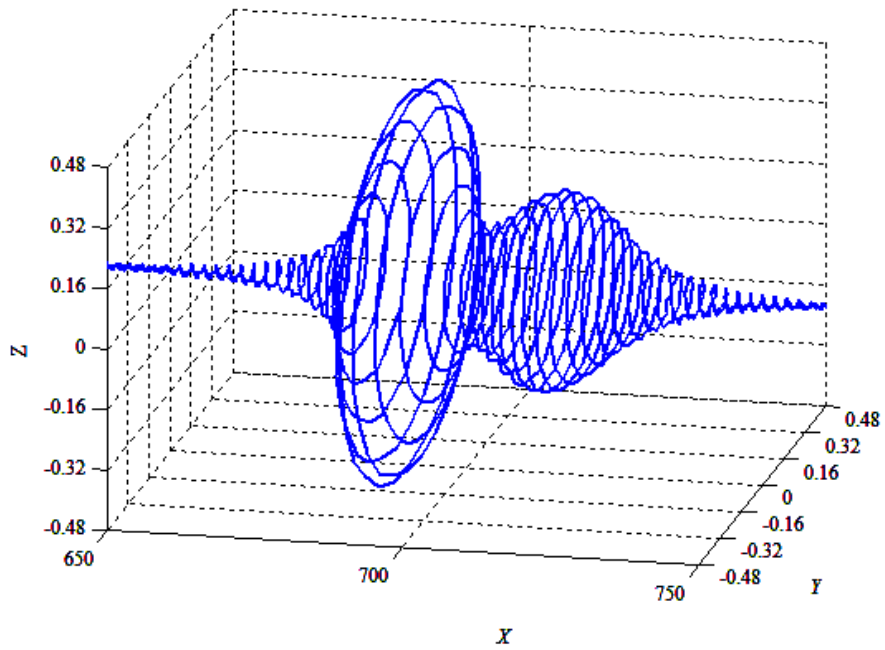
Figure 3.35: The helical solitons in the process of interaction.

65
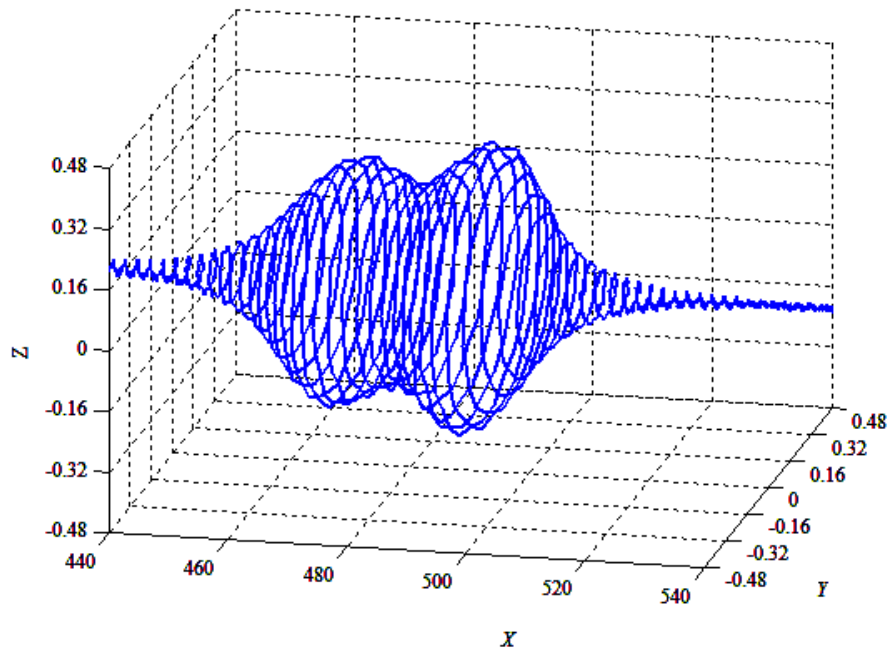
Figure 3.36: The helical solitons in a compact form in the interaction.
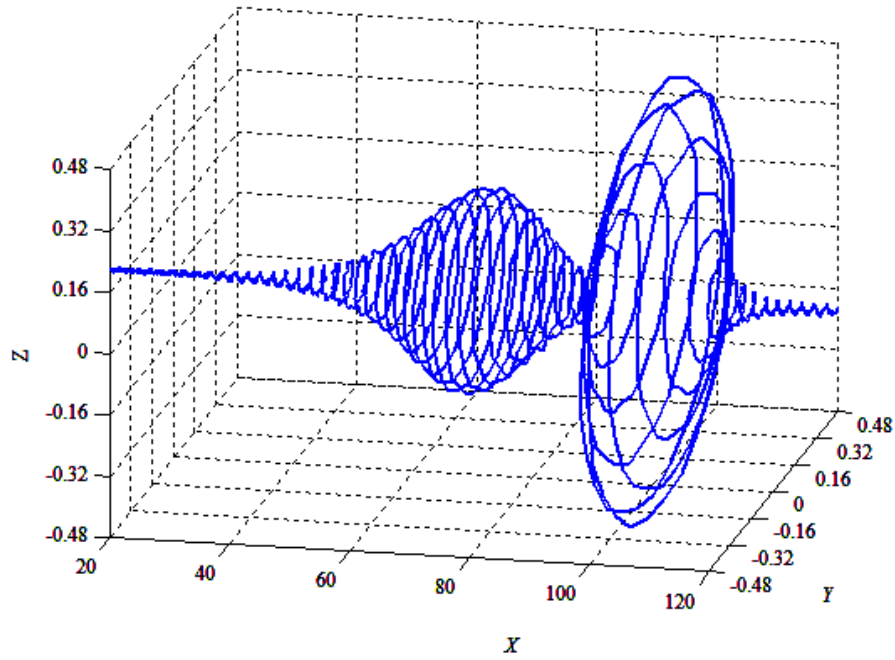
Figure 3.37: The small helical soliton has moved through the larger helical soliton.

66
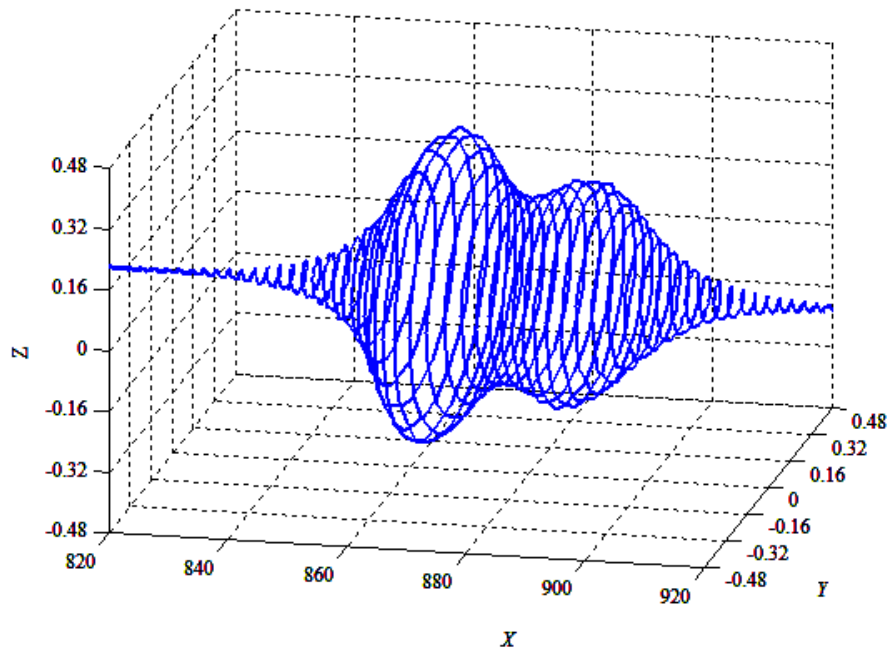
Figure 3.38: The smaller helical soliton has moved backwards on the right of the larger helical soliton.
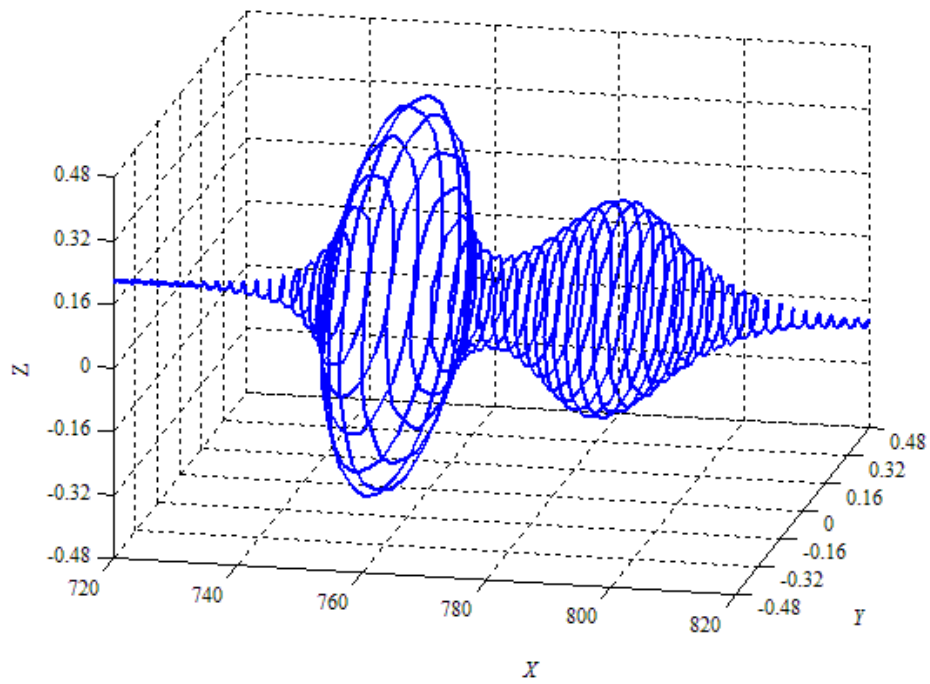
Figure 3.39: The smaller helical soliton has moved backwards further in the interaction process.

3.7.2 Interaction of Helical Solitons of the Same Helicity in the Non-Integrable Case

The interaction of solitons of the same helicity in the non-integrable case is different to the results obtained for the integrable case. The helical solitons move closer and form a compact state at some stage. On momentarily being in the compact state, the smaller soliton starts to move through the larger one. After the interaction, the solitons move in the same direction maintaining their initial forms without any residual ripples. Thus the interaction of helical solitons of the same helicity is elastic – see figures 3.40 – 3.45.
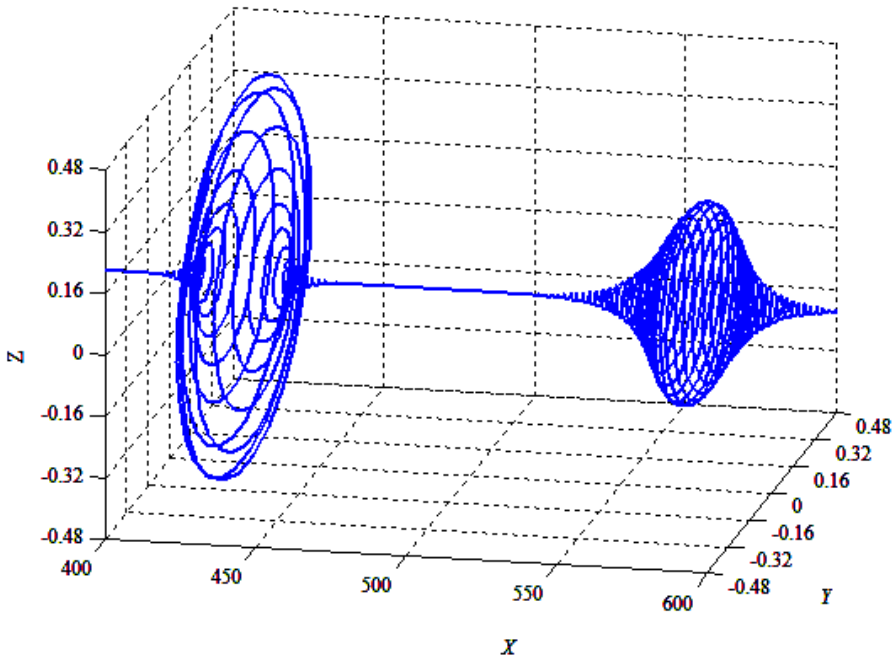
Figure 3.40: The helical solitons with same helicity at a distance.
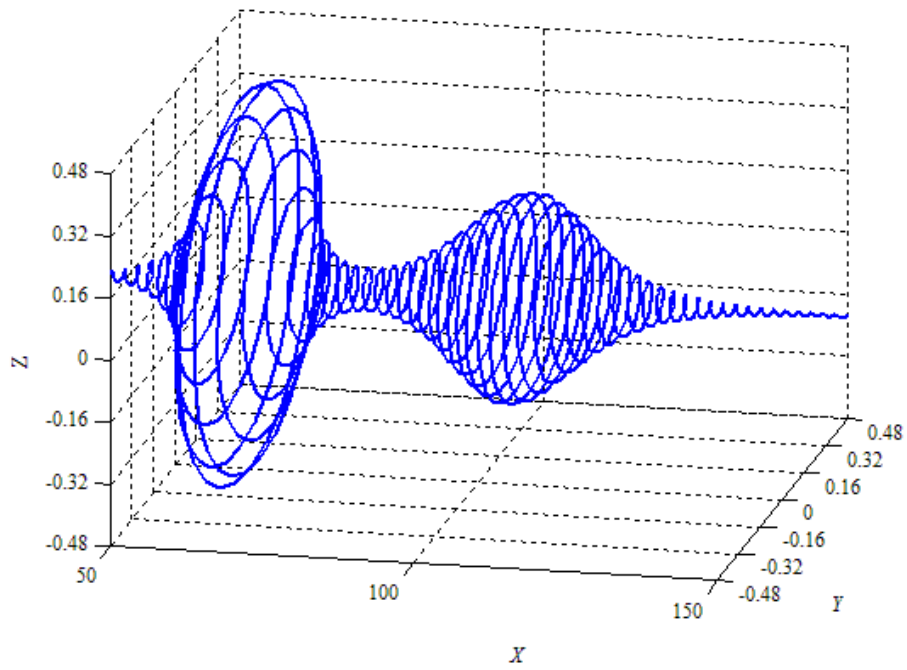
Figure 3.41: The helical solitons come close for the interaction.
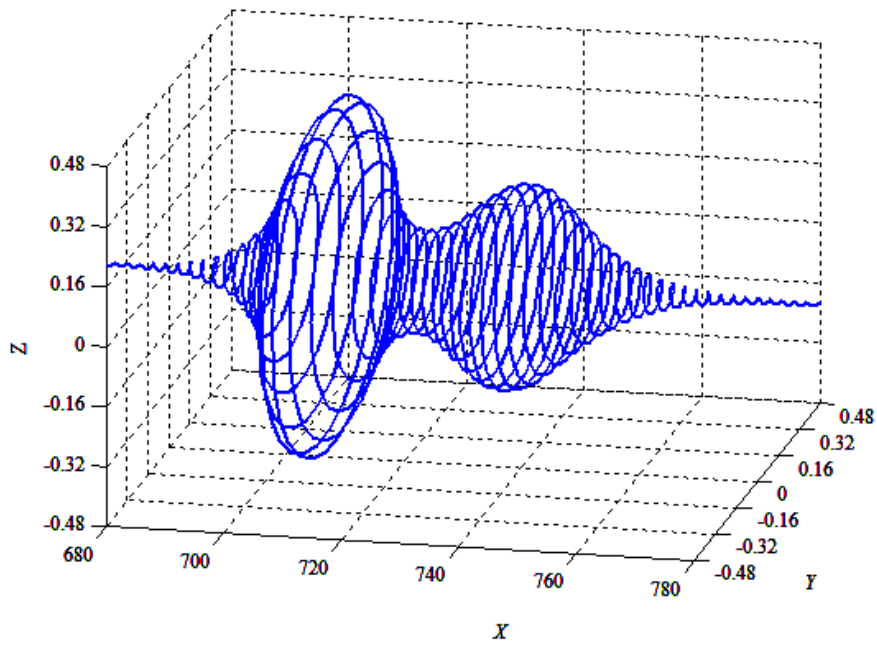
Figure 3.42: The helical solitons begin to form a compact state during the interaction.
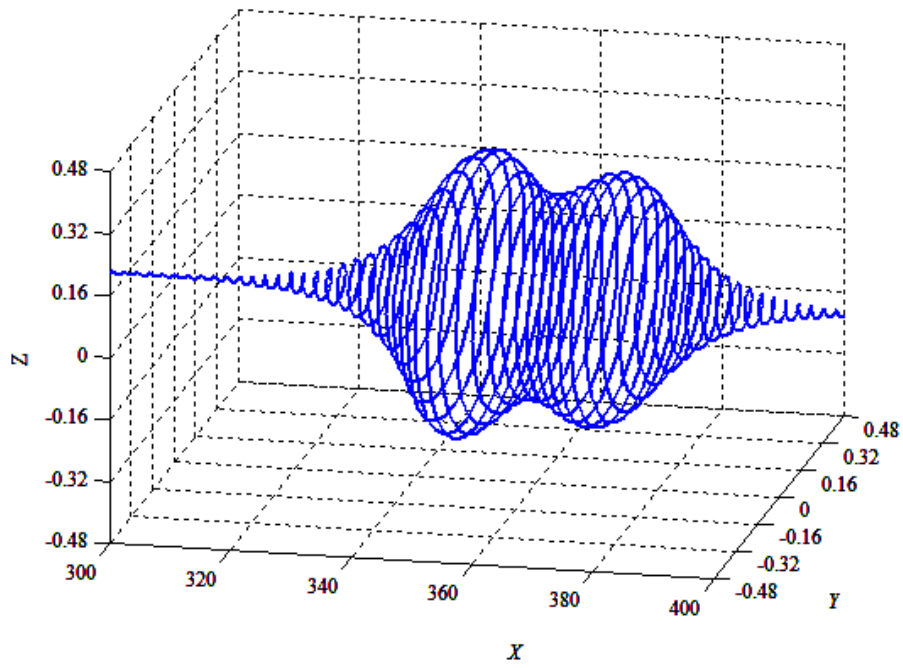
Figure 3.43: The helical solitons are in a compact state during the interaction.
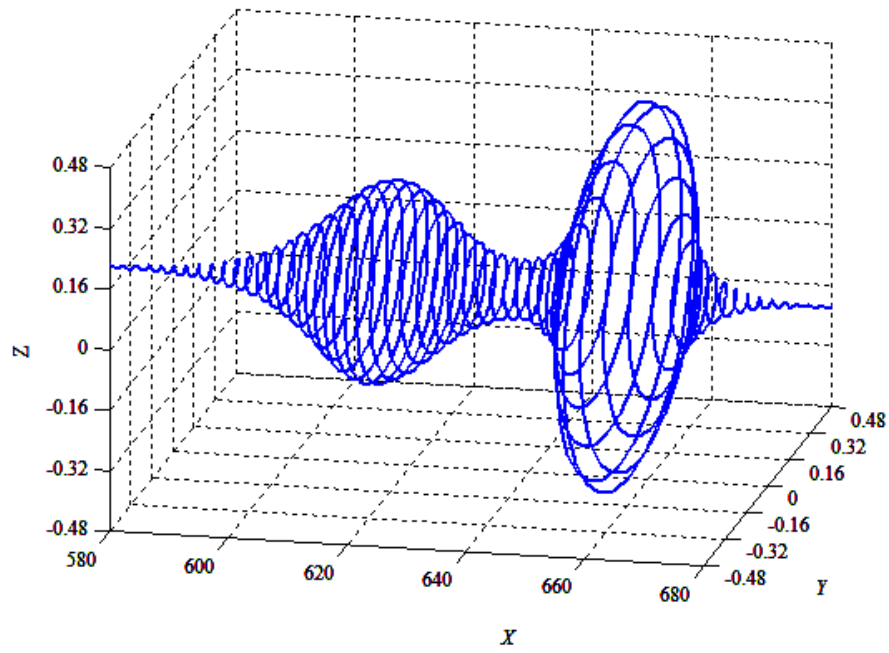
Figure 3.44: The smaller helical soliton has moved through the larger helical soliton.
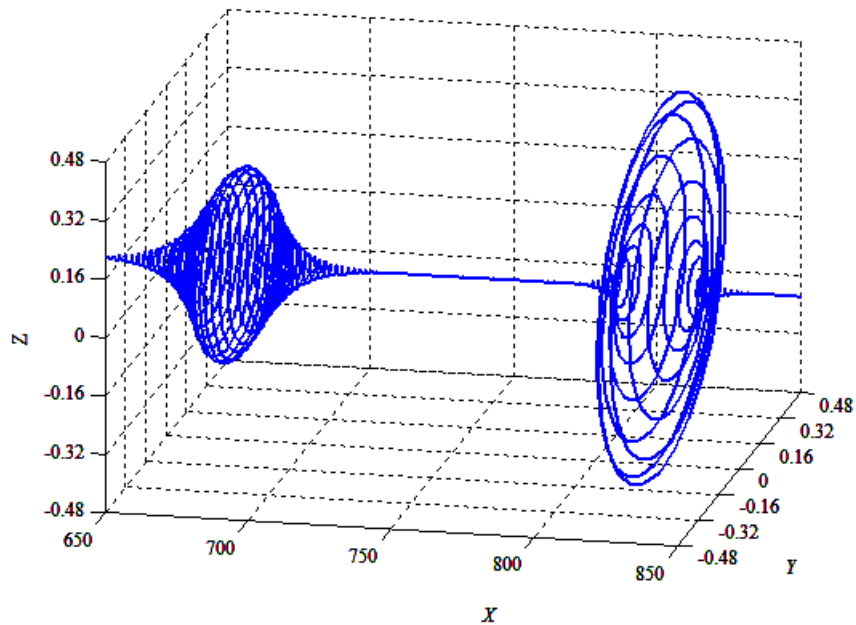
Figure 3.45: The helical solitons have moved away after the interaction with their initial forms.

3.7.3 Interaction of Helical Solitons of Opposite Helicity in the Integrable Case

Both helical solitons lose their forms and the disturbance is along the axis. The solitons then repel and start to move away from each other. The process of interaction is interesting and shows an unstable form during very close contact of the helical solitons in this. They slowly move away from each other keeping their initial forms, and oscillations of the carrier wave remain stable – see figures 3.46 – 3.51
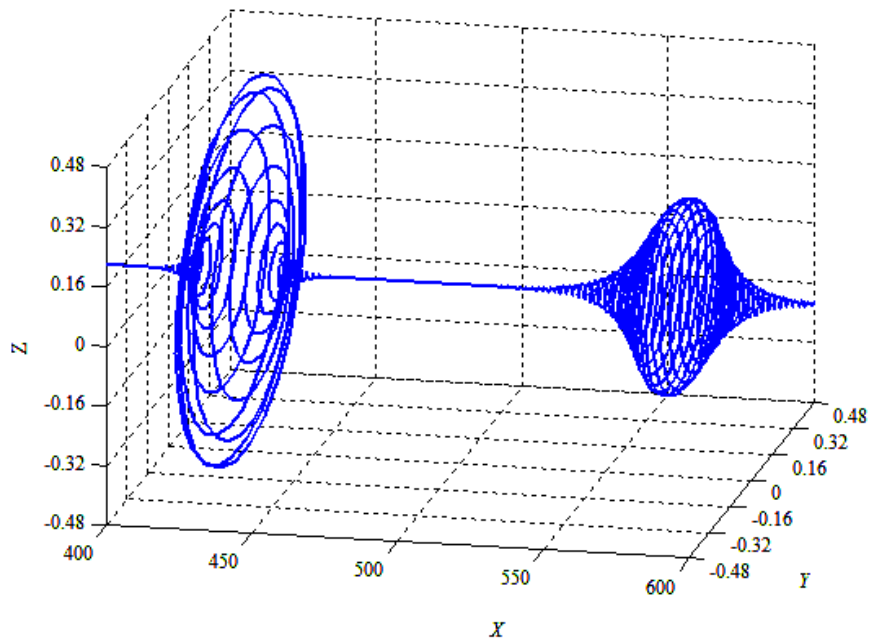
Figure 3.46: The two helical solitons with opposite helicity at a distance.
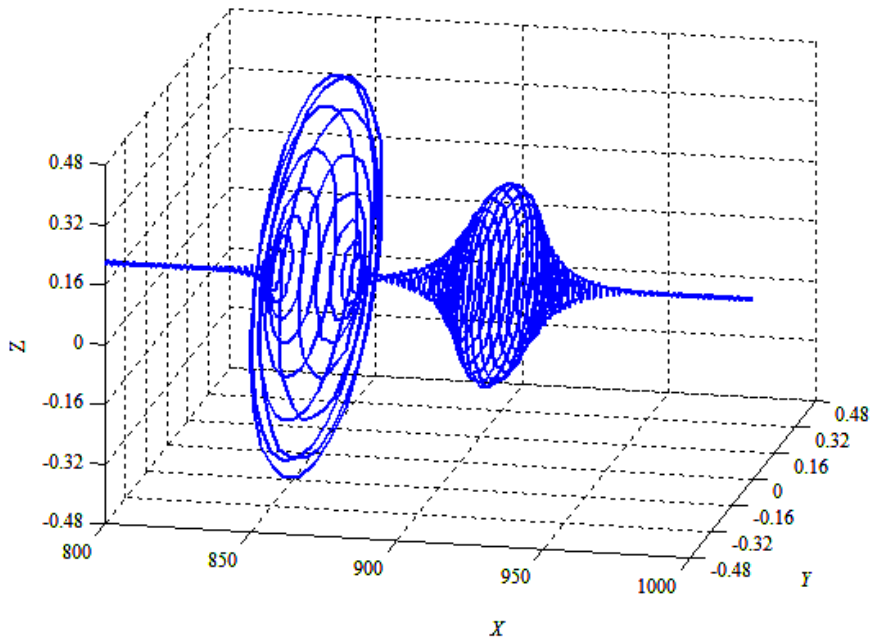
Figure 3.47: The helical solitons move closer and are about to interact.
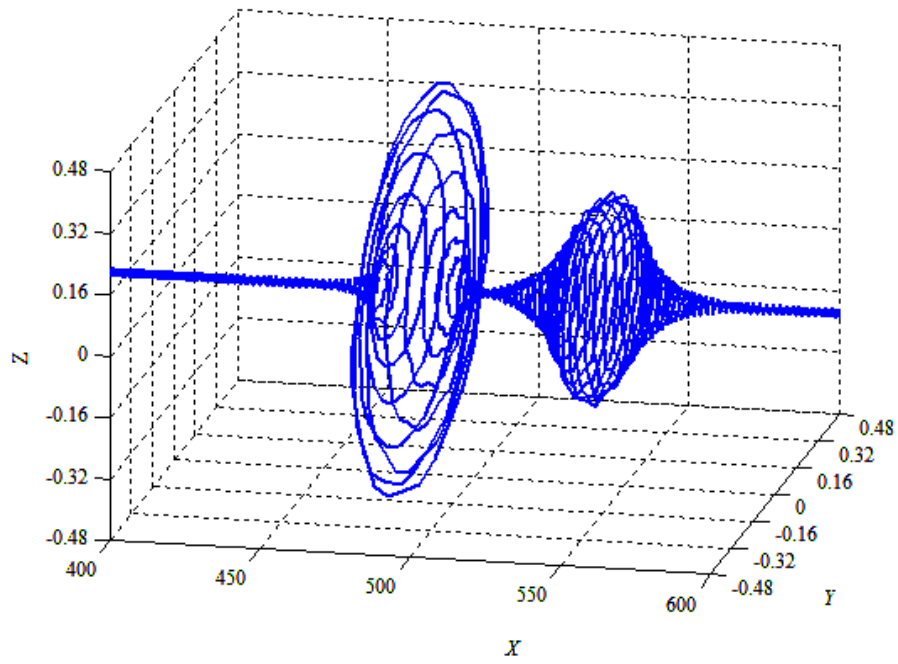
Figure 3.48: The helical solitons are in the process of interaction and cause a slight change of the forms.
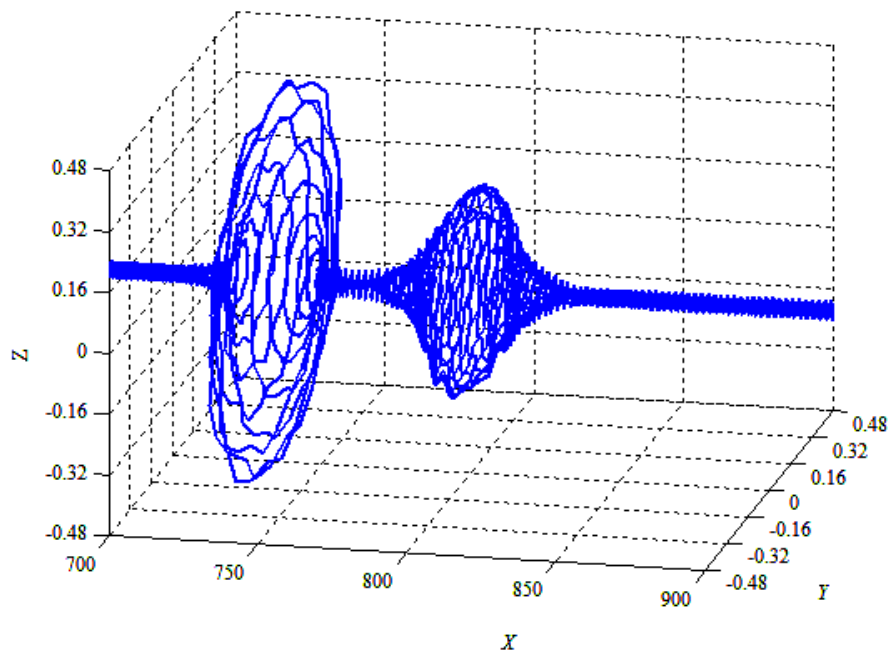
Figure 3.49: The helical solitons experiencing a repulsive effect and their forms are notably disturbed.

73
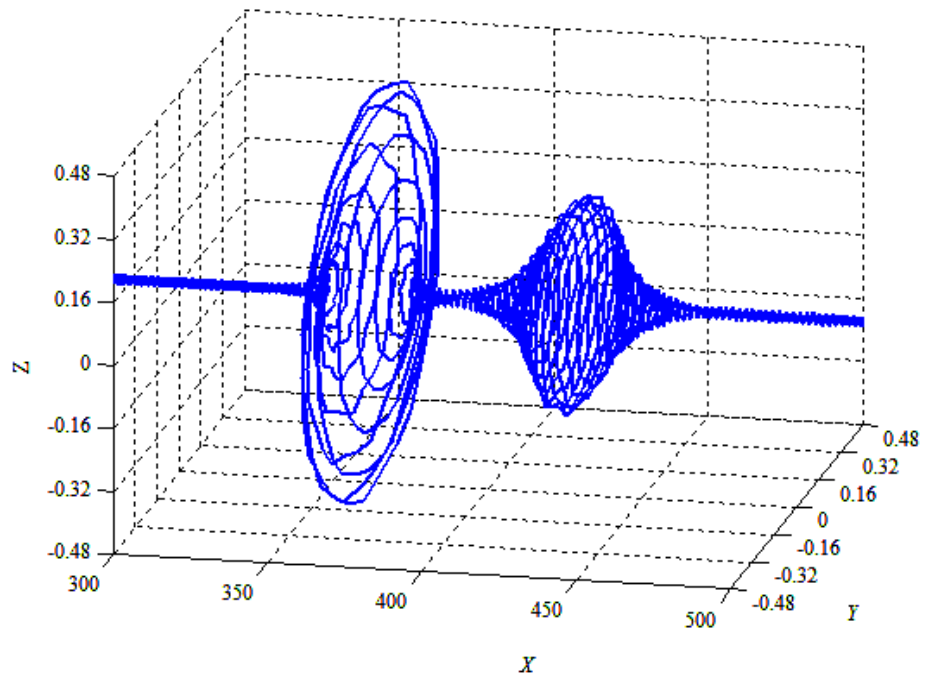
Figure 3.50: The helical solitons repel away as they regain their forms.
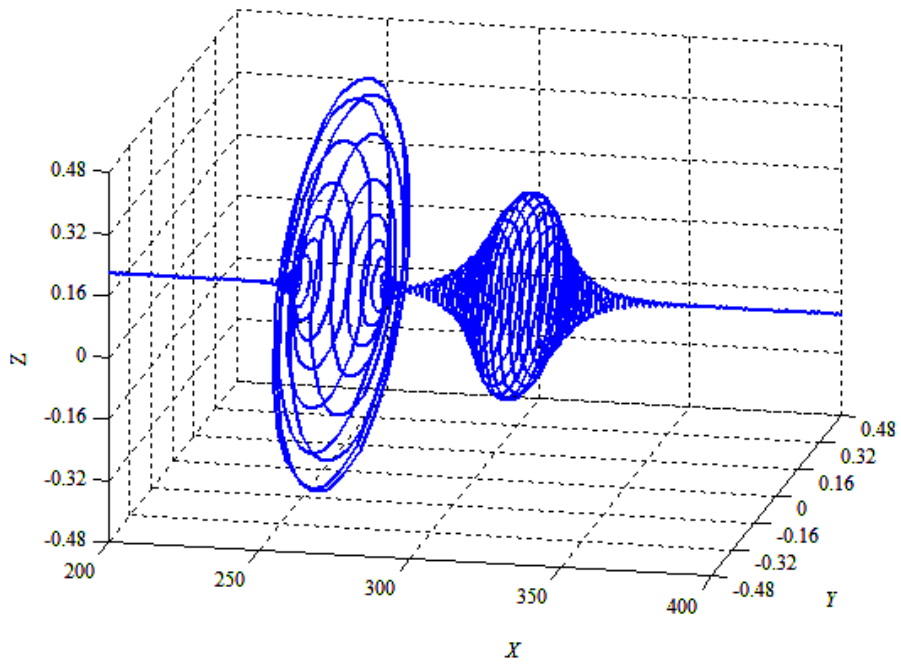
Figure 3.51: The helical solitons regain their initial forms.

74

3.7.4 Interaction of Helical Solitons of Opposite Helicity in the Non-Integrable Case

This non-integrable case shows that the solitons come close and enter into the interaction however there is no loss of their forms. There is not as much disturbance in the structure as in the previous case and the solitons start to repel. The solitons move away from each other with their initial forms, and oscillations of the carrier wave remains stable – see figures 3.52 – 3.57.
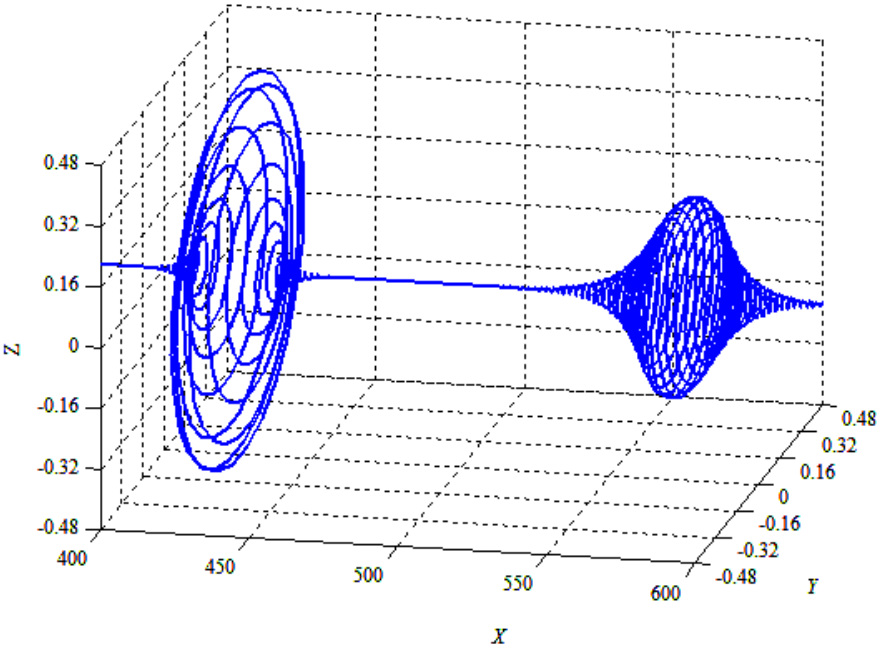
Figure 3.52: The two helical solitons with opposite helicity at a distance.
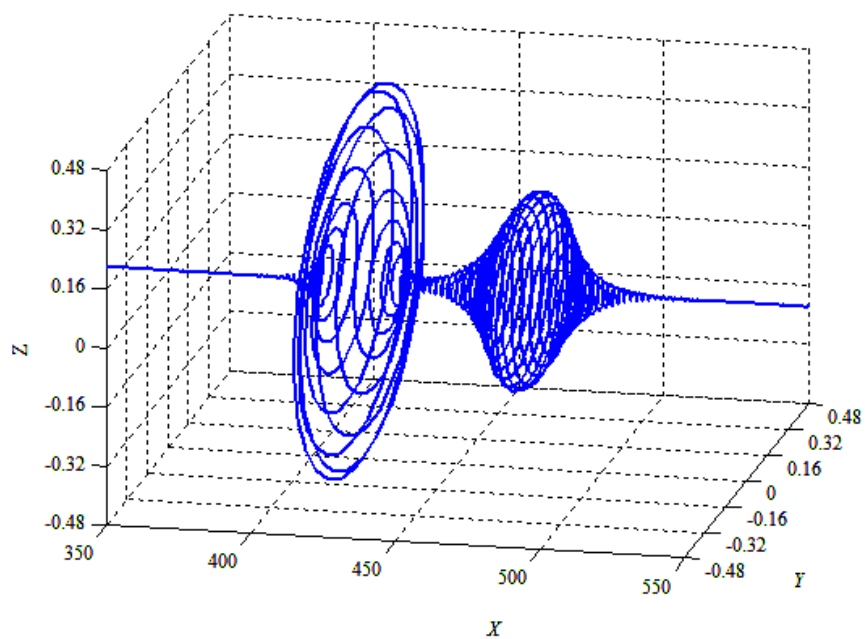
Figure 3.53: The helical solitons come closer and are in the interaction.
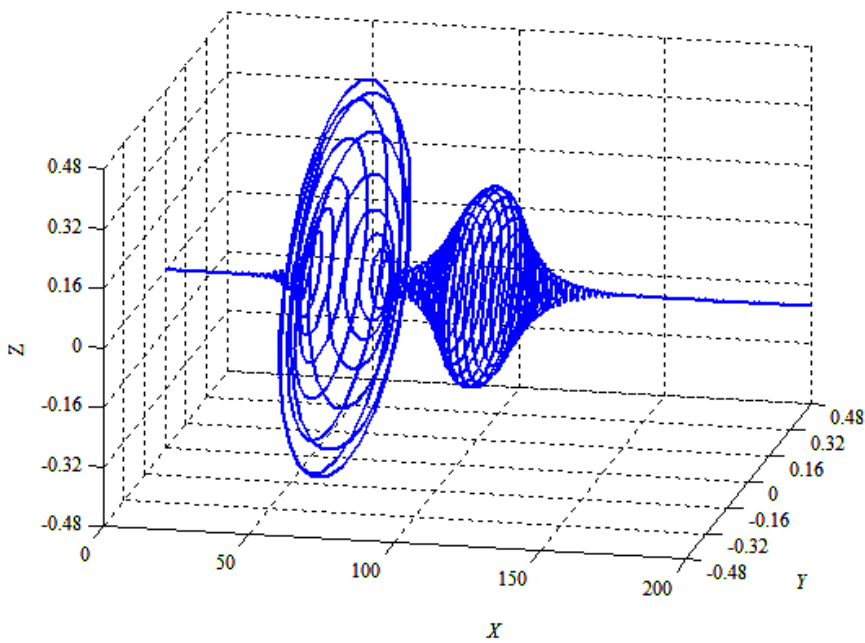
Figure 3.54: The helical solitons are in the interaction, but retain their initial forms.

76
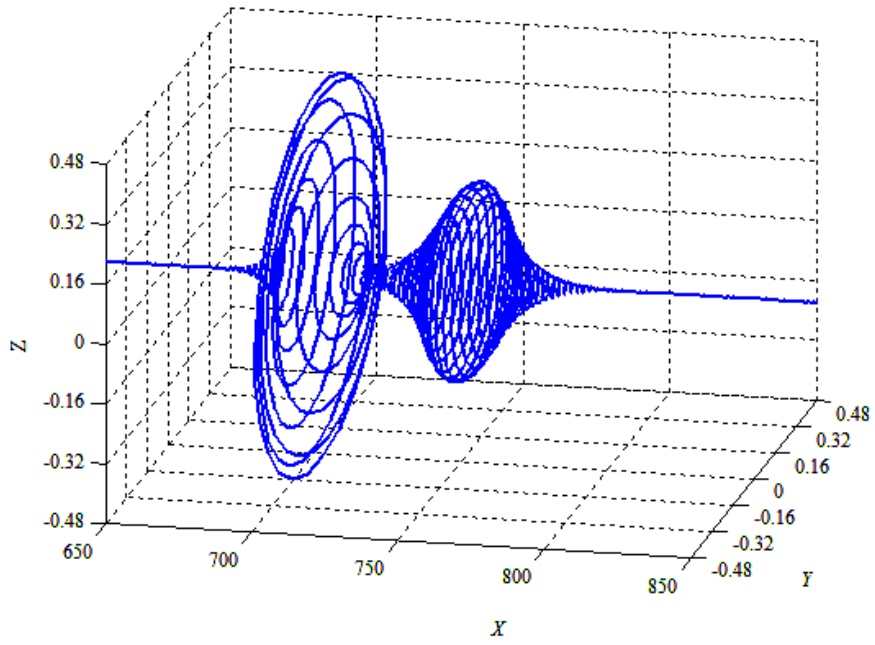
Figure 3.55: The helical solitons show repulsion as they have started to move away from each other.
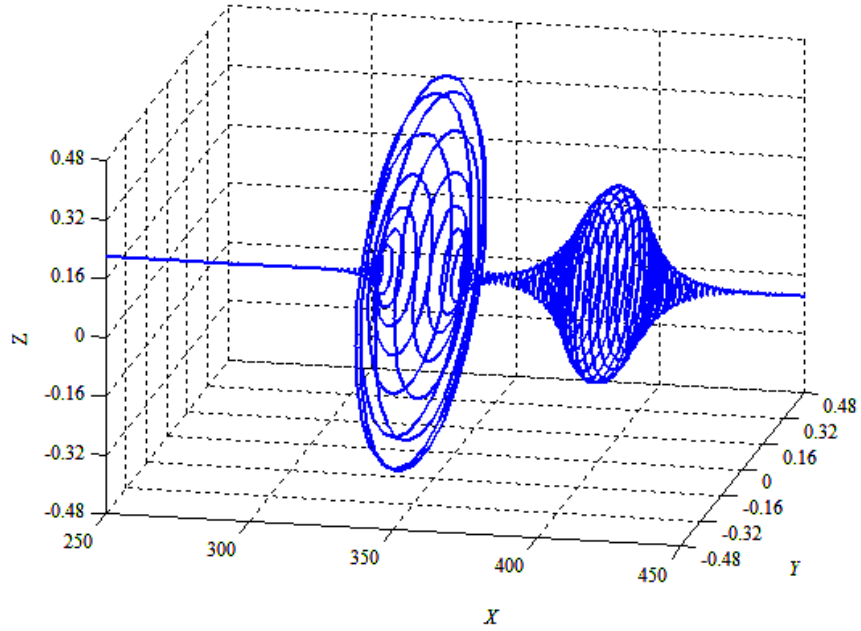
Figure 3.56: The helical solitons repel each other and move away after the interaction.
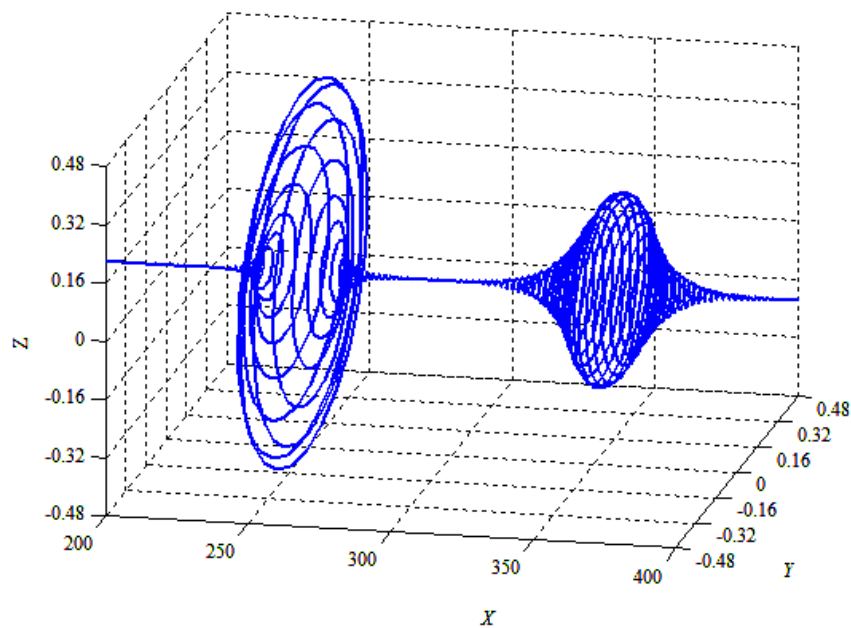
Figure 3.57: The helical solitons have moved further away.

3.8 Relevant Experiment to Helical Solitons

An experiment conducted by science presenter Steve Mould on self-siphoning beads is very relevant to the numerical study of helical solitons in this research. It shows the occurrence of helicity in the chain of beads as the chain falls from the beaker to the ground. The beads rise up in helical form as they leave the beaker (see figure 3.58). The presence of transverse vector waves as discussed (see figure 2.1) is clearly demonstrated in this amazing experiment. The behavior of the beads and the overall effect on the chain is seen in the slow motion part of this video.

Figure 3.58: Amazing bead chain experiment in slow motion (Steve Mould, YouTube, http://youtu.be/6ukMId5fIi0).

3.9 Conclusion

The simplest non stationary interactions of solitary waves of different polarisations have been investigated in this chapter. The evolution of civmKdV equation has been numerically studied within the integrable vmKdV (3.2) under the influence of small right hand side. The existences of helical solutions are confirmed. The chapter further shows the many scenarios of soliton interaction. The interaction of plane solitons under different polarisation revealed many important results. Similarly, graphical results obtained from numerical computation provided useful information on the interaction of helical solitons.

Chapter 4 Modelling of the Gardner–Ostrovsky Equation by Means of the Transmission Line

4.1 Introduction

Numerical modeling of complex physical phenomena plays an important role in the contemporary mathematical physics. In many cases when exact solutions of mathematical equations are unavailable, researchers are forced to use numerical simulations. There are various numerical approaches to simulate partial differential equations (PDEs) such as the finite-difference methods, spectral methods based on the Fourier transformation, finite element methods, and so on. However, a usage of these approaches is related with many problems appearing either explicitly or implicitly in the process of discretisation of PDEs.

Among them, the formation of a proper numerical scheme approximating the concrete PDE and investigation of the scheme for stability and convergence after the solution is obtained by numerical method. These problems are very nontrivial, especially the problem of the numerical scheme's stability and convergence. Only in the rare cases the scheme stability can be theoretically studied and the criterion of stability can be derived. In some cases the stability problem is considered empirically by undertaking calculations with different time and space steps. More frequently, especially when each run is very costly in terms of computational time and machine resources, researchers assess the results simply relying on the common sense or intuitive physical judgment.

One of the alternatives to the approaches described above is a usage of discrete chain models. Such models are described by sets of ODEs which can be readily solved with a high accuracy by existing well-developed solvers realized in many mathematical software.

The next section derives a one-dimensional chain model which possesses rather big universality and can be used for the modeling of various nonlinear wave processes in dispersive media. It can be shown that for some particular choice of nonlinear and dispersive terms, the chain model can be used for the effective simulation of internal waves in a rotating ocean as described by the Gardner–Ostrovsky (GO) equation (Holloway *et al*., 1999), (Grimshaw *et al*., 2006), (Obregon & Stepanyants, 2012). The model is also used to study numerically the terminal decay of KdV and Gardner solitons and the results are compared with theoretical predictions obtained within the framework of the adiabatic approximation.

Appendix A has the developed codes for particle chain model. The developed codes for the chain model used to obtain the solution for Toda chain are given in appendix C and D. Appendix E has the numerical codes for the chain model used in obtaining the solution of Gardner–Ostrovsky equation.

4.2 Generalised sine-Gordon–Toda Chain Model and the Ostrovsky Equation

The ladder type transmission line (figure 4.10) is used to derive the electric version of the sine-Gordon–Toda chain. A similar model leading to the discrete and continuous

versions of the sine-Gordon model has been studied in Parmentier (1978). A modified Toda chain with an additional linear term was considered in Yagi and Kawahara (2001). The analogy between the long-wave models of the same Toda chain with the Ostrovsky equation was discussed in Khusnutdinova and Moore (2011).

The transmission line contains the nonlinear elements, the capacitor whose charge nonlinearly depends on the voltage $Q(v)$ and inductance L_1 with a nonlinear dependence between the current J_n and electric flux $\Phi_n(J_n)$.
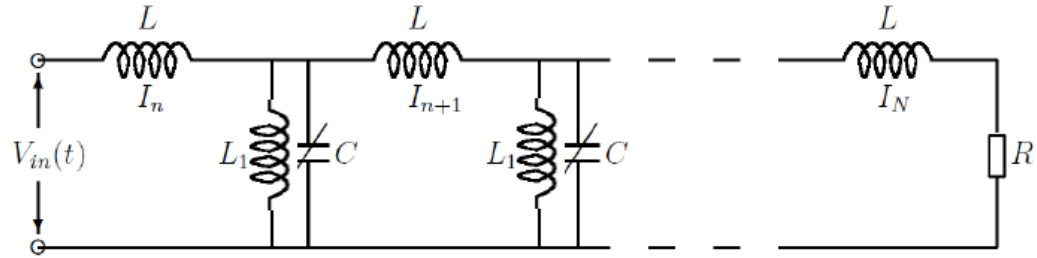
Figure 4.1: The ladder-type transmission line with the nonlinear capacitor and inductance L_1.

Applying the Kirchhoff's laws to two neighbor cells with the indices n and $n + 1$, the following set of equations are obtained:

$$I_n = I_{n+1} + \frac{dQ_n}{dt} + J_n; \quad v_n = v_{n+1} + L\frac{dI_{n+1}}{dt}; \quad v_n = \frac{d\Phi_n}{dt} = \frac{d\Phi_n}{dJ_n}\frac{dJ_n}{dt}. \tag{4.1}$$

After simple manipulations, this set of equations can be reduced to the set of second-order ODEs:

$$\frac{d^2 Q_n}{dt^2} = \frac{1}{L}\left(\upsilon_{n-1} - 2\upsilon_n + \upsilon_{n+1}\right) - \frac{dJ_n}{d\Phi_n}\upsilon_n \qquad \textbf{(4.2)}$$

where $J_n(\Phi_n)$ is the inverse function to $\Phi_n(J_n)$.

Equations (4.2) are rather general; making different assumptions regarding $Q_n(\upsilon_n)$ and $J_n(\Phi_n)$, various useful and interesting models are obtained which are reducible in the long wave approximation to different PDEs.

Consider, for example, the case when:

$$Q_n\left(\upsilon_n\right) = Q_0 \ln\left(1 + \upsilon_n/a\right) \quad \text{and} \quad dJ_n/d\Phi_n = \left(r/\upsilon_n\right)\sin\left(\upsilon_n/b\right). \qquad \textbf{(4.3)}$$

Note that in the case of the conventional linear inductive element, the flux Φ_n is simply proportional to the current J_n; this case follows from equation (4.3) when $\upsilon_n/b \ll 1$, and $\sin\left(\upsilon_n/b\right) \approx \upsilon_n/b$.

With such choice of the functions $Q_n(\upsilon_n)$ and $J_n(\Phi_n)$ as in equation (4.3), (4.4) is obtained from equation (4.2):

$$Q_0 \frac{d^2 \ln\left(1 + \upsilon_n/a\right)}{dt^2} = \frac{1}{L}\left(\upsilon_{n-1} - 2\upsilon_n + \upsilon_{n+1}\right) - r\sin\frac{\upsilon_n}{b}. \qquad \textbf{(4.4)}$$

In the normalized variables, $u_n = \upsilon_n/rL$ and $\tau = t\,(r/Q_0)^{1/2}$ equation (4.3) reads:

$$\frac{d^2 \ln\left(1 + \varepsilon u_n\right)}{d\tau^2} = u_{n-1} - 2u_n + u_{n+1} - \sin\left(\mu u_n\right) \qquad \textbf{(4.5)}$$

where $\varepsilon = rL/a$ and $\mu = rL/b$. Equation (4.5) readily reduces to the classical Toda chain (Toda, 1989a) when $\mu = 0$.

In another limiting case when $\mu \neq 0$ and $\varepsilon \ll 1$, one can replace $\ln(1 + \varepsilon u_n) \approx \varepsilon u_n$, then equation (4.5) reduces to the discrete sine-Gordon equation (Han *et al.,* 2008). For the perturbations of infinitely small amplitudes, $u_n \to 0$, equation (4.5) can be linearized:

$$\varepsilon \frac{d^2 u_n}{d\tau^2} = u_{n-1} - 2u_n + u_{n+1} - \mu u_n , \qquad (4.6)$$

then the dispersion relation can be derived for the sinusoidal perturbations

$u_n \sim \exp[i(\omega\tau - kn)]$:

$$\omega^2 = \frac{4}{\varepsilon} \sin^2 \frac{k}{2} + \frac{\mu}{\varepsilon} . \qquad (4.7)$$

This dispersion relation is shown in Figure 4.2 for $\varepsilon = 1$ and two values of μ: $\mu = 0$ and $\mu = 0.05$.
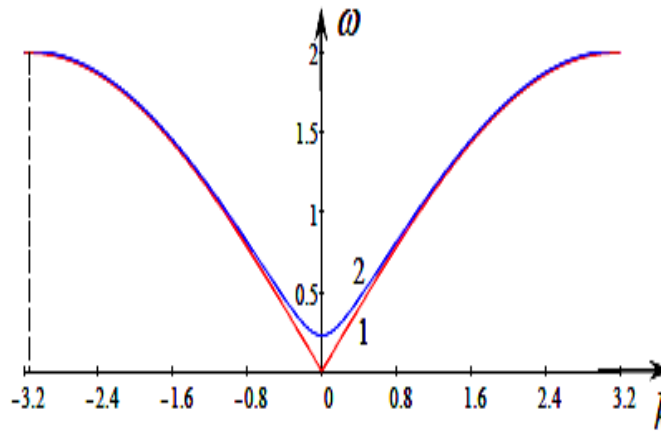
Figure 4.2: Dispersion relation (4.7) for $\mu = 0$ (line 1) and $\mu = 0.05$ (line 2); $\varepsilon = 1$ in both cases.

In the long-wave approximation when $k \ll 1$ and $\mu \ll k^2$ the dispersion relation (4.7) can be approximated as:

$$\omega \approx \frac{|k|}{\sqrt{\varepsilon}}\left(1 - \frac{k^2}{24} + \frac{\mu}{2k^2}\right). \tag{4.8}$$

This dispersion relation is similar to the dispersion relation describing water waves in rotating fluids (Grimshaw *et al.*, 1998b), and the corresponding nonlinear evolution equation, the Ostrovsky equation, can be derived from the discrete generalized Toda-chain model (4.5).

To demonstrate this, it is assumed that the parameter μ in equation (4.5) is so small that even for the largest possible value of u_n function $\sin(\mu u_n)$ can be replaced by μu_n with the appropriate accuracy. It can be assumed further that $\varepsilon \sim 1$ and small-amplitude perturbation can be considered such that $u_n \ll 1$ for any n. Then equation (4.5) reduces to the following:

$$\frac{d^2}{d\tau^2}\left(\varepsilon u_n - \frac{\varepsilon^2 u_n^2}{2}\right) = u_{n-1} - 2u_n + u_{n+1} - \mu u_n. \tag{4.9}$$

If a wave has the characteristic wavelength much greater than the spatial size of one cell of the chain (assumed that it is 1), $\Lambda \gg 1$. Then, $u_{n\pm1}$ can be presented through the Taylor series around the node n. Keeping only two non-vanishing leading terms of the Taylor series in the combination $u_{n-1} - 2u_n + u_{n+1}$, and after simple manipulations, equation (4.10) is derived:

$$\frac{\partial^2 u}{\partial \tau^2} - \frac{1}{\varepsilon}\frac{\partial^2 u}{\partial x^2} = \frac{\varepsilon}{2}\frac{\partial^2 u^2}{\partial \tau^2} + \frac{1}{12\varepsilon}\frac{\partial^4 u}{\partial x^4} - \frac{\mu}{\varepsilon}u \; . \tag{4.10}$$

(index n of the function $u_n(t)$ has been omitted)

In accordance with the assumptions, all terms in the right-hand side of equation (4.10) are small in comparison with the terms in the left-hand side. Therefore, in the zero approximation on small parameters, one can simply neglect the terms in the right-hand side and present the remaining wave equation in the factorized form:

$$\frac{\partial^2 u}{\partial \tau^2} - \frac{1}{\varepsilon}\frac{\partial^2 u}{\partial x^2} \equiv \left(\frac{\partial}{\partial \tau} - \frac{1}{\sqrt{\varepsilon}}\frac{\partial}{\partial x}\right)\left(\frac{\partial}{\partial \tau} + \frac{1}{\sqrt{\varepsilon}}\frac{\partial}{\partial x}\right)u \approx 0 \; . \tag{4.11}$$

Each bracket in this equation describes independent wave propagating either to the left or to the right.

Considering only a wave propagating to the right, the temporal and spatial derivatives in the zero-order approximation are linked by the formula: $\partial/\partial x \approx -\sqrt{\varepsilon}\,\partial/\partial \tau$, where $c_0 = 1/\sqrt{\varepsilon}$ is the phase velocity of long linear waves. This relationship between the derivatives can be used in the next approximation yielding after substitution into equation (4.10) and simple manipulations, the following equation:

$$\frac{\partial}{\partial \tau}\left(\frac{\partial u}{\partial x} + \sqrt{\varepsilon}\frac{\partial u}{\partial \tau} - \frac{\varepsilon\sqrt{\varepsilon}}{2}u\frac{\partial u}{\partial \tau} - \frac{\varepsilon\sqrt{\varepsilon}}{24}\frac{\partial^3 u}{\partial \tau^3}\right) = -\frac{\mu}{2\sqrt{\varepsilon}}u \; . \tag{4.12}$$

This is the well-known Ostrovsky equation which is very popular in the context of physical oceanography [see for details (Grimshaw *et al.*, 1998b), (Stepanyants, 2006)]. When $\mu = 0$, equation (4.12) reduces to the classical KdV equation which is completely

integrable and has a particular solution in the form of stationary solitary wave, alias soliton (Ablowitz & Segur, 1981):

$$u = A \operatorname{sech}^2 \frac{\tau - x/V}{T}, \quad \text{where} \quad T = \frac{1}{\sqrt{A}}, \quad V = \frac{1}{\sqrt{\varepsilon}\left(1 - \varepsilon A/6\right)}. \tag{4.13}$$

The next section considers adiabatic evolution of the KdV soliton under the influence of small perturbation in the right-hand side of equation (4.12) which models influence of Earth' rotation in the oceanographic context.

4.3   Adiabatic Evolution of KdV Soliton within the Ostrovsky Equation

Assuming that the term in the right-hand side of equation (4.12) is small enough, the approximate solution to the equation in the form of KdV soliton with gradually varying parameters in space (amplitude A, velocity V, and duration T) could be found. Applying the perturbation method described in (Grimshaw *et al.*, 1998a), one can derive the energy balance equation:

$$\frac{\partial}{\partial x} \int_{-\infty}^{+\infty} u^2 d\tau = -\frac{\mu}{\sqrt{\varepsilon}} \int_{-\infty}^{+\infty} \left[u(x,\tau) \int_{-\infty}^{\tau} u(x,\tau') d\tau' \right] d\tau. \tag{4.14}$$

Substituting soliton solution (4.13) in (4.14), the soliton amplitude is obtained:

$$\frac{dA}{dx} = -\mu \sqrt{\frac{A}{\varepsilon}}. \tag{4.15}$$

87

This equation can be readily integrated yielding [cf. (Grimshaw *et al.,* 1998a), (Grimshaw *et al*., 1998b)]:

$$A(x) = A_0 \left(1 - x/X_t\right)^2 \tag{4.16}$$

where A_0 is the amplitude of an input soliton entering into the chain at $x = 0$ and $X_t = 2(\varepsilon A_0)^{1/2}/\mu$ is the terminal length – the length at which the soliton vanishes as its amplitude formally turns to zero.

However, in reality the soliton dynamics is more complicated. Numerical calculations show that when the leading soliton decays, it produces an intense trailing perturbation which in turn evolves into another solitary wave of almost the same amplitude as the original soliton. This secondary soliton is also accompanied by trailing wave train. Then the process of secondary soliton decay repeats with a resurrection of a new soliton and more intense trailing perturbation (Grimshaw *et al*., 1998b). Such quasi-recurrence phenomenon may occur many times. Eventually, the soliton transfers into the stationary envelope soliton (which can be described by the generalized NLS equation) and dispersive wave train. This process has been investigated in details for the KdV soliton within the framework of Ostrovsky equation (Grimshaw & Helfrich, 2008).

Soliton amplitude decay (4.16) derived within the framework of the adiabatic approximation was compared against numerical solution of the primitive set of Kirchhoff's equations (4.1) with the Toda nonlinearity for the charge on the capacitor $Q_n(\upsilon_n) = Q_0 \ln(1 + \upsilon_n/a)$ and linear dependence of the flux $\Phi_n(J_n)$. Then in the normalized variables the generalized Toda chain model reduces to equation (4.5) with

the linear perturbative term $\mu\, u_n$ rather than the sinusoidal one. Without loss of generality, one can put in this case $\varepsilon = 1$, then equation (4.5) with $\mu = 0$ has the soliton solution (Toda soliton):

$$u_n(t) = A_T \operatorname{sech}^2 \frac{t - n/V_T}{T_T}, \qquad \text{where}$$

$$T_T = \frac{1}{\sqrt{A_T}}, \qquad V_T = \frac{1}{T_T\left[\ln\left(1+\sqrt{1+T_T^2}\right) - \ln T_T\right]} . \qquad \textbf{(4.17)}$$

The Toda soliton rapidly reduces to the KdV soliton when its amplitude becomes small $A_T \to 0$. The primitive set of Kirchhoff's equations (4.1) with the functions $Q_n(v_n)$ and $\Phi_n(J_n)$ indicated above was solved numerically for different values of the parameter μ. The standard FORTRAN code was elaborated on the basis of the fourth-order Runge–Kutta Solver RKGS with the modification due to Gill (see appendix). Results obtained are shown in Figure 4.3 in normalized variables $A(X)/A_0$ versus $X = x/X_t$.
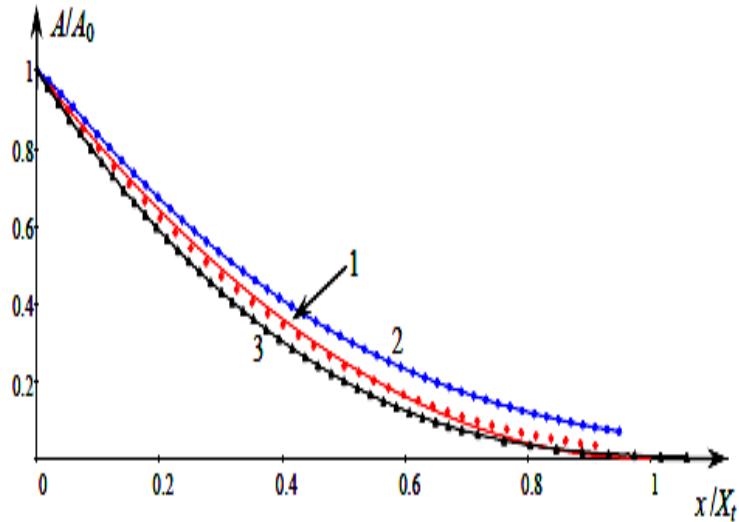
Figure 4.3: Terminal decay of Toda soliton (4.17) in the electric chain (4.5).

Red line 1 shows the theoretical dependence (4.6) derived in the adiabatic approximation. Dots on that line show the numerical data obtained with $A_0 = 0.25$ and characteristic time duration of the input Toda soliton $T_{T0} = 2$. Blue line 2 with small diamonds pertains to the numerical data with $A_0 = 0.1$ ($T_{T0} = \sqrt{10}$), and black line 3 with triangles pertains to numerical data with $A_0 = 0.5$ ($T_{T0} = \sqrt{2}$). The parameter $\mu = 10^{-4}$ in all these cases. As seen in the figure (4.3), the numerical data in lines 2 and 3 deviate from the theoretical dependence for the KdV soliton (line 1), although their behavior is qualitatively similar to what is shown by line 1.

The data deviation can be explained by inconsistency of the adiabatic theory in application to the numerical data on line 2. According to the main assumption of the adiabatic theory, the term in the right-hand side of equation (4.12) should be small in comparison to any term in the left-hand side of that equation.

A rough estimate of the magnitudes of the first term in the left-hand side of equation (4.12) and the right-hand side is as follows:

$$LHS \equiv \frac{\partial^2 u}{\partial \tau \partial x} \sim \frac{A_0}{T_{T0}\Delta_0} \sim \frac{A_0}{T_{T0}\left(T_{T0}/\sqrt{\varepsilon}\right)} \sim \frac{A_0\sqrt{\varepsilon}}{T_{T0}^2};$$

$$(4.18)$$

$$RHS \equiv \frac{\mu}{2\sqrt{\varepsilon}}u \sim \frac{\mu}{2\sqrt{\varepsilon}}A_0,$$

where $\Delta_0 = T_{T0} \cdot c_0 = T_{T0}/\sqrt{\varepsilon}$ is the half-width of the input Toda soliton. Thus, the ratio of the terms in the right-hand side and left-hand side is:

RHS/LHS $= \mu T_{T0}^2/2\varepsilon$.

90

As we have put $\varepsilon = 1$, then for line 1 we have RHS/LHS $= 2 \cdot 10^{-4} \ll 1$, whereas for lines 2 and 3 we have correspondingly:

RHS/LHS$_2$ $= 5 \cdot 10^{-4}$ and RHS/LHS$_3$ $= 10^{-4}$.

The former of these two values is, apparently, not small enough, whereas the latter one is quite small, but soliton amplitude ($A_0 = 0.5$) is too large which makes the difference between the KdV and Toda solitons (the adiabatic theory is developed for the KdV solitons only).

4.4 Modeling of the Gardner–Ostrovsky Equation

Another choice for the nonlinear dependence between the charge on the capacitor (see Figure 4.1) and a voltage $Q(\upsilon) = Q_0 \, [\upsilon/a - (\alpha/2) \cdot (\upsilon/a)^2 - (\alpha_1/3) \cdot (\upsilon/a)^3]$ leads to the chain model similar to that studied in the Fermi–Pasta–Ulam experiments (see, e.g., (Ablowitz & Segur, 1981), (Toda, 1989a)). Inclusion of the additional inductance L_1 with the nonlinear dependence between the current J_n and electric flux $\Phi_n(J_n)$ as in equation (4.3) results in the following set of second order ODEs.

In the normalised variables, $u_n = \upsilon_n/rL$, $\tau = t \, (r/Q_0)^{1/2}$ the set reads:

$$\frac{d^2}{d\tau^2} \left[\varepsilon u_n - \frac{\alpha}{2} \left(\varepsilon u_n \right)^2 - \frac{\alpha_1}{2} \left(\varepsilon u_n \right)^3 \right] = u_{n-1} - 2u_n + u_{n+1} - \sin \left(\mu u_n \right) \qquad \textbf{(4.19)}$$

where α and α_1 are some coefficients. Assuming $\mu u_n \ll 1$ (so that $\sin(\mu u_n) \approx \mu u_n$) and repeating the manipulations undertaken above in the derivation of the Ostrovsky

91

equation, one can reduce the set of ODEs (4.19) to the well-known Gardner–Ostrovsky equation (Holloway *et al.,* 1999), (Grimshaw *et al.,* 2006), (Obregon & Stepanyants, 2012):

$$\frac{\partial}{\partial \tau}\left(\frac{\partial u}{\partial x} + \sqrt{\varepsilon}\frac{\partial u}{\partial \tau} - \alpha \frac{\varepsilon\sqrt{\varepsilon}}{2}u\frac{\partial u}{\partial \tau} - \alpha_1 \frac{\varepsilon^2\sqrt{\varepsilon}}{2}u^2\frac{\partial u}{\partial \tau} - \frac{\varepsilon\sqrt{\varepsilon}}{24}\frac{\partial^3 u}{\partial \tau^3} \right) = -\frac{\mu}{2\sqrt{\varepsilon}}u. \qquad \textbf{(4.20)}$$

When $\mu = 0$ this equation reduces to the Gardner (or extended KdV) equation which is completely integrable and also has soliton solutions (see, e.g., (Apel *et al.,* 2007)). However, the structure of Gardner solitons is different from the structure of KdV solitons and essentially depends on the sign of the parameter α_1, whereas the parameter α controls only the polarity of the Gardner soliton. In particular, the Gardner soliton with $\alpha_1 < 0$ and $\alpha > 0$ has a positive polarity:

$$u = -\frac{v}{2\varepsilon}\frac{\alpha}{\alpha_1}\left[\tanh\left(\frac{\tau - x/V}{T_G} + \phi \right) - \tanh\left(\frac{\tau - x/V}{T_G} - \phi \right) \right] \qquad \textbf{(4.21)}$$

where soliton amplitude $A = -\alpha v/\varepsilon\alpha_1$, velocity $V = (1 + \alpha^2 v^2/12\alpha_1)^{-1}/\sqrt{\varepsilon}$, characteristic duration $T_G = (-2\varepsilon\alpha_1)^{1/2}/v|\alpha|$, as well as $\phi = 0.25\ln\left[(1+v)/(1-v) \right]$ are determined by the parameter $v \in (0, 1)$. Under small perturbation in the right-hand side of equation (4.20) when $\mu \neq 0$ the Gardner soliton gradually decays. From the energy balance equation (4.14) it follows the equation for the parameter v:

$$\frac{dv}{dx} = -\frac{\mu}{4}\frac{1-v^2}{v}\ln^2\frac{1-v}{1+v}. \qquad \textbf{(4.22)}$$

92

This equation is not solvable analytically in general, however it can be readily solved numerically or asymptotically for $v \to 0$ (KdV limit) and $v \to 1$ (table-top limit).

The results obtained are shown in figure 4.6. Line 1 in that figure pertains to the KdV limit which corresponds to equation (4.16), whereas line 2 pertains to the table-top limit (obtained numerically by solving equation (4.22)).
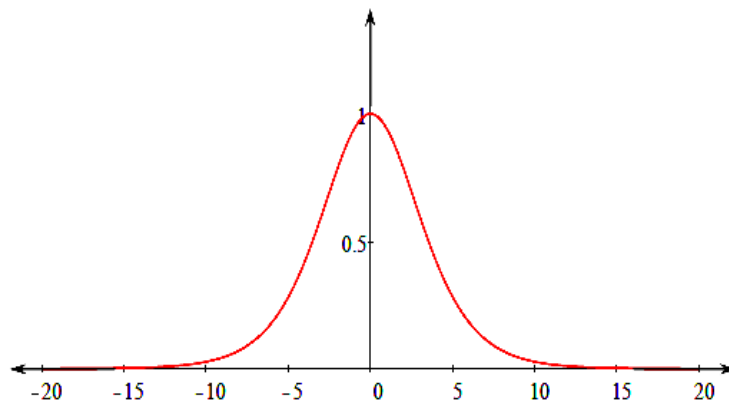
Figure 4.4: Bell-shaped pulse above corresponds to KdV soliton of unit amplitude.
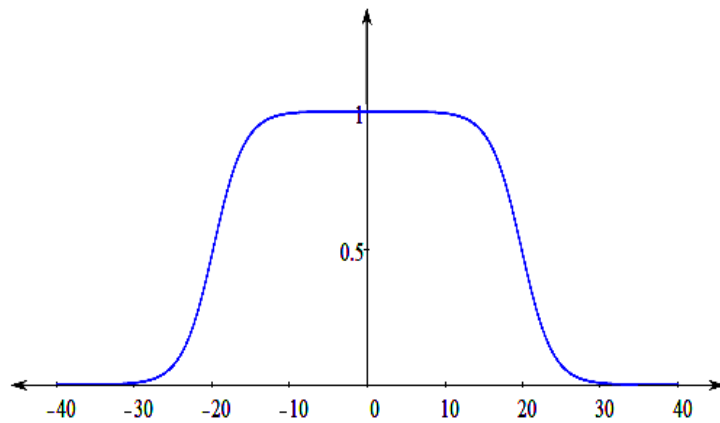
Figure 4.5: Wide pulse above illustrates the Table-Top soliton of unit amplitude.
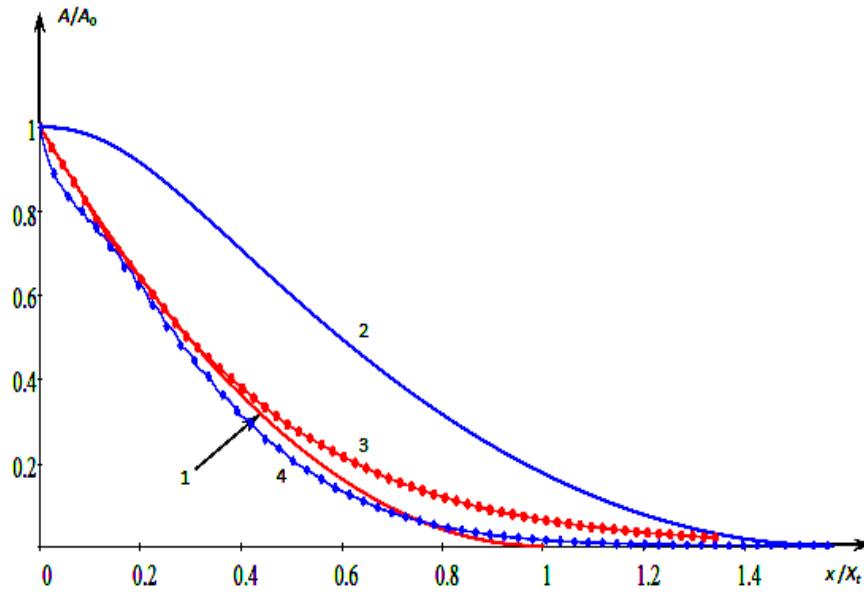
Figure 4.6: Terminal decay of the Gardner soliton (4.21) in the electric chain (4.19).

The theoretical results derived within the adiabatic approximation were compared against numerical data obtained from the direct solution of equation (4.19) with the Gardner soliton as the input signal. The following parameters of equation (4.19) were chosen:

$\alpha = -\alpha_1 = 0.1$, $\varepsilon = 1$, and $\mu = 10^{-4}$.

It was confirmed that for small and moderate soliton amplitudes, the decay law caused by small perturbative factor in the right-hand side of equation (4.19) agrees well with the theoretical prediction (see, e.g., line 3 in Figure 4.6 which is obtained for $v_0 = 0.5$). However, numerical data for large-amplitude table-top solitons are far from the theoretical prediction (see line 4 which pertain to the case of $v_0 = 10^{-7}$). The detailed inspection of soliton evolution shows that contrary to theoretical assumption, the table-

94

top soliton decays not preserving its shape even at very early stage of the evolution (see figure 4.7).
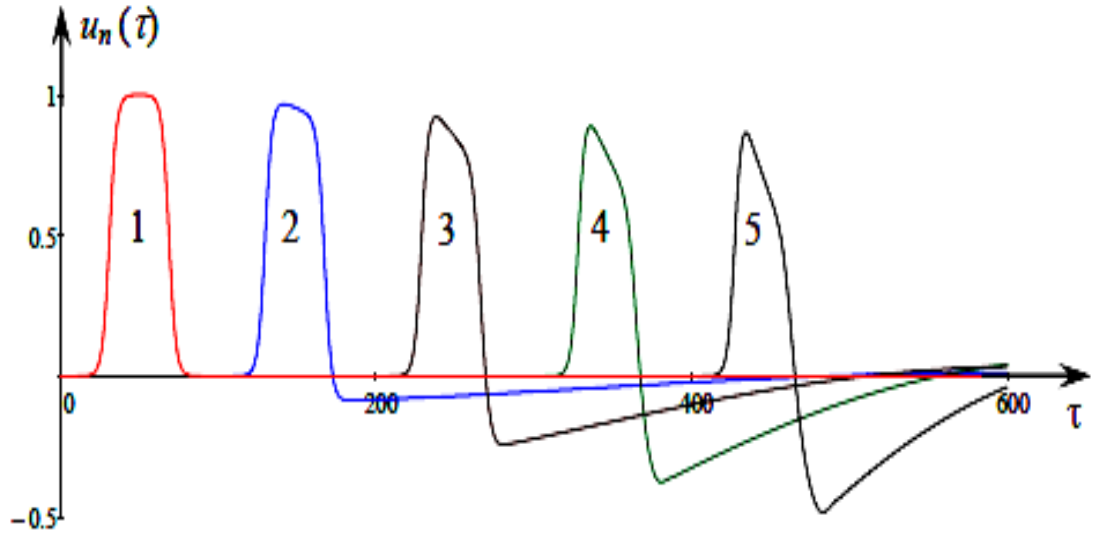
Figure 4.7: Time dependence of the signal generated by the Table-Top Gardner soliton (4.21) with $v_0 = 10^7$ in different cells of the electric lattice (4.19). Line 1 shows the input pulse, line 2 pertains to n = 100, line 3 to n = 200, line 4 to n = 300, line 5 – to n = 400.

4.5 Conclusion

It has been shown that chain models can be used for the effective modeling of partial differential equations describing nonlinear wave processes in continuous dispersive media. Dissipative terms can be also taken into account; this does not add any additional difficulty, whereas the numerical solution of PDEs containing both dispersive and dissipative terms is a more difficult problem. The results on KdV soliton decay within the framework of Ostrovsky equation (4.12) were obtained and it was demonstrated that within the range of applicability of the adiabatic theory, the numerical results agree fairly well with the theoretical predictions. It was also revealed

that the table-top Gardner soliton does not obey the adiabatic theory and decays much faster at the earlier stage due to transformation into bell-shaped pulse rather than preserving its own shape. This is in contrast to what was discovered for the adiabatic decay of Gardner soliton due to different dissipative perturbations (Grimshaw *et al.,* 2003).

Chapter 5 Conclusion and Future Work

5.1 Research Outcomes

The objective of this research was to study and investigate the dynamics of particle-like solitary waves. Various analytical and numerical methods were used to obtain interesting results describing the solitary waves under different conditions. Some derived model equations considered and studied in this research were obtained for the first time and provide valuable contribution to the existing literature. Numerical results obtained were of high accuracy at the advantage of less computational time using well developed numerical codes designed in FORTRAN and MATLAB.

Chapter 2 presented the case when transverse modes are considered as the equation of motion becomes vector equations in describing the particle displacements in two perpendicular directions transverse to the direction of wave propagation. The flexural transverse waves in an anharmonic chain of atoms were described by a general vector differential-difference equation which was reduced to the generalised "string equation" in the long-wave approximation. Various limiting cases were studied of the derived vector equation and their physical significance was studied in an anharmonic chain of atoms. This investigation considered the next two neighboring atoms in addition to the nearest neighbours. The variation of the studied parameter (β_2) realized in the long wave approximation ($\kappa \to 0$) provided different dispersion dependences observable in experiments. A new form of nonlinear 'pseudo-diffusion' vector equation was obtained which has not been derived before. The stationary waves were studied using a potential

form of equation derived which was interpreted as the energy integral for the point particle of unit mass moving in the potential field. Many cases are discussed depending upon the nature of the coefficients in the potential equation. It was found that breather solution and helical solutions also exist within the framework of the derived equation.

Chapter 3 presented the numerical results in the study of nonlinear non stationary waves in the flexural transverse waves in an anharmonic chain of atoms. The behavior and interaction of non stationary waves were also studied in detail. The results of numerical modeling of chain vibrations were computed and presented in graphical forms. This revealed the valuable information on the interactions of solitons on the same and perpendicular planes. The notable case is when there is a transfer of energy from one soliton to another while moving perpendicular to each other. More computations were carried out to study the interactions of helical solitons. The results were presented as snapshots of the interaction process which provided valuable information of their dynamics in integrable and non integrable case.

Chapter 4 provided an important and highly reliable alternative approach to describe a nonlinear wave model by the use of discrete chain models. Such models are described by sets of ODEs which can be solved with a very high accuracy. This one-dimensional chain model was effectively used for the modeling of various nonlinear wave processes in dispersive media. It was shown that at some particular choice of nonlinear and dispersive terms the chain model could simulate the internal waves in a rotating ocean as described by the Gardner–Ostrovsky (GO) equation revealing many properties of these interesting phenomena. An electric version of the sine-Gordon–Toda chain model

and Ostrovsky equation were derived using a ladder type transmission line with the nonlinear capacitors and inductors. The Ostrovsky equation studied is an important model as it considers the influence of Earth' rotation in the oceanographic context. The adiabatic evolutions of important solitons (KdV & Gardner) were studied within the framework of the derived Ostrovsky equation.

5.2   Future Directions

This research has investigated and presented many results on solitary wave dynamics. However, many aspects of solitary wave dynamics can still be studied within the framework of model equations. Surface and internal shallow-water waves and its generalization to the deep-water waves which are described by the NLS equation could also be an interesting and challenging problem.

Evidently, the non-dissipative perturbation considered in this research (see Chapter 3) and modeling the effect of Earth' rotation in physical oceanography acts differently on such solitons than the dissipative perturbations. Dissipative perturbations can also be considered within the framework of model equations derived in this research. The numerical solution of the equations containing both dispersive and dissipative terms can present more complexity in finding solution to the derived equations. This can also be a subject of further study.

Appendix A: Program Particle Chain

```fortran
Program ParticleChain

      IMPLICIT DOUBLE PRECISION (A-H,O-Z)

      EXTERNAL FCT, OUTP

      DIMENSION PRMT(5),Y(400000),DERY(400000),AUX(8,400000)

C MAXIMAL NUMBER OF CELLS IS NOW NN = 10000

      COMMON/PAR/NN,N2,N3,N4,T0,AMP1,AMP2,AMU,BETA2

      open(100,file='ParHel.dat')

      open(101,file='Data.dat')

      open(102,file='Chain.dat')

      open(1001,file='Work01.dat')

C PARAMETERS
******!********!********!********!********!********!*******!***************

      Ti = 0.D0

      read(100,*) Dt,T0,AMP1,AMP2,AMU,BETA2,NN,NTS

      write(101,100) Dt,T0,AMP1,AMP2,AMU,BETA2,NN,NTS

 100 Format(5X,'Dt',10X,'T0',10X,'AMP1',8X,'AMP2',8X,'AMU',
     &9X,'BETA2',8x,'NN',5x,'NTS'/1X,6E12.4,3X,2I6//)

      write(*,*) 'NN = ',NN, 'NTS = ',NTS

      write(*,*) 'T0 = ',T0, 'Dt = ',Dt

      write(*,*) 'AMP1 = ',AMP1, 'AMP2 = ',AMP2

      write(*,*) 'AMU = ',AMU, 'BETA2 = ',BETA2

      PRM = 1.D-1

      Accur = 1.D0
```

```
C*******!*******!*******!*******!*******!*******!*******!**
      NW=60 !NUMBER OF WORK FILES

          N2 = 2*NN

      N3 = 3*NN

      N4 = 4*NN ! N4 IS THE NUMBER OF EQUATIONS IN THE SYSTEM

      NT1 = NTS/NW

      PRMT(1) = Ti ! - THE LOWER BOUND OF THE INTEGRATION INTERVAL

      PRMT(2) = Dt ! - THE UPPER BOUND OF THE INTEGRATION INTERVAL

      PRMT(3) = Dt*PRM ! - THE INITIAL INCREMENT OF THE INDEPENDENT
VARIABLE

      PRMT(4) = ACCUR ! - THE UPPER ERROR BOUND

C ARRAY DERY BELOW IS THE INPUT VECTOR OF THE INITIAL ERROR
WEIGHTS

C THE SUM OF ITS COMPONENTS MUST BE EQUAL TO 1

      DO 1 I = 1,N4

        DERY(I) = 1.D0/FLOAT(N4)

    1 CONTINUE

C ARRAY Y BELOW IS A VECTOR OF INITIAL DATA

      DO 2 M = 1,N4

        Y(M) = 0.D0

    2  CONTINUE

C     NR = NN/100

C****************************************************************

C The initial perturbation:

      DO 5 J = 1,NN
```

```fortran
      WRITE(102,*) J,Y(J),Y(J+NN),Y(J+N2),Y(J+N3)

    5 CONTINUE
```

C***

```fortran
      DO 3 JW1 = 1,NW ! - the loop for NW times writing the results of integration

    DO 4 I = 1,NT1 ! integration of ODEs

      CALL RKGS(PRMT,Y,DERY,N4,IHLF,FCT,OUTP,AUX)

      PRMT(1) = PRMT(2)

      PRMT(2) = PRMT(2) + DT

    4 CONTINUE

    JW = 1000 + JW1

    DO 6 J = 1,NN

      WRITE(JW,*) J,Y(J),Y(J+NN),Y(J+N2),Y(J+N3)

    6 CONTINUE

    write(*,*) 'JW1 = ',JW1

    3    CONTINUE

    stop

    end
```

C***

```fortran
    SUBROUTINE FCT(T,Y,DERY)

    IMPLICIT DOUBLE PRECISION(A-H,O-Z)

    COMMON/PAR/NN,N2,N3,N4,T0,AMP1,AMP2,AMU,BETA2

    DIMENSION Y(1),DERY(1)
```

C***

C THE INPUT SIGNAL IS A HELICAL SOLITON

102

DELT1 = DSQRT((1.D0 + 8.D0*BETA2)/(3.D0*(AMU*(1.D0 + 4.D0*BETA2)

&- (1.D0 + 2.D0*BETA2))))/DABS(AMP1)

V1 = DSQRT(1.D0 + 2.D0*BETA2 + 2.5D-1*AMP1**2*(AMU*(1.D0 +

&4.D0*BETA2) - (1.D0 + 2.D0*BETA2)))

PI = 4.D0*DATAN(1.D0)

OMEGA = 1.0D0*PI/DELT1

F0 = AMP1*DSQRT(1.D0 - (DTANH(V1*(T-
T0)/DELT1))**2)*DCOS(OMEGA*T)

F1 = AMP1*DSQRT(1.D0 - (DTANH(V1*(T - T0 - 1.D0/V1)/DELT1))**2)

&*DCOS(OMEGA*(T - 1.D0/V1))

G0 = AMP1*DSQRT(1.D0 - (DTANH(V1*(T-
T0)/DELT1))**2)*DSIN(OMEGA*T)

G1 = AMP1*DSQRT(1.D0 - (DTANH(V1*(T - T0 - 1.D0/V1)/DELT1))**2)

&*DSIN(OMEGA*(T - 1.D0/V1))

C   DELT2 = DSQRT((1.D0 + 8.D0*BETA2)/(3.D0*(AMU*(1.D0 + 4.D0*BETA2)

C   &- (1.D0 + 2.D0*BETA2))))/DABS(AMP2)

C   V2 = DSQRT(1.D0 + 2.D0*BETA2 + 2.5D-1*AMP2**2*(AMU*(1.D0 +

C   &4.D0*BETA2) - (1.D0 + 2.D0*BETA2)))

C   THET = 90.D0

C   SHIFT = 2.D0*T0 ! - TIME SHIFT BETWEEN TWO SOLITONS

C   SFP = 4.D0*T0 ! - TIME SHIFT IN THE 'HEVISIDE' STEP-FUNCTION TO
SWITCH ON PERIODIC BOUNDARY CONDITIONS

C   G00 = AMP2*DSQRT(1.D0 - (DTANH(V2*(T - SHIFT)/DELT2))**2)

C   G11=AMP2*DSQRT(1.D0 - (DTANH(V2*(T - SHIFT - 1.D0/V2)/DELT2))**2)

C***

DO 1 I = 3,NN-2
103

```
     DERY(I) = Y(NN+I)

     DERY(NN+I) = Y(I-1) - 2.D0*Y(I) + Y(I+1) + 5.D-1*BETA2*(Y(I-2) -
    &2.D0*Y(I) + Y(I+2)) + 5.0D-1*(AMU - 1.D0)*((Y(I+1)**2 +
    &Y(N2+I+1)**2)*Y(I+1)-2.D0*(Y(I)**2+Y(N2+I)**2)*Y(I)+(Y(I-1)**2 +
    &Y(N2+I-1)**2)*Y(I-1)) + 6.25D-2*BETA2*(2.0D0*AMU - 1.D0)*
    &(((Y(I+2)+Y(I+1))**2 + (Y(N2+I+2)+Y(N2+I+1))**2)*(Y(I+2)+Y(I+1))-
    &((Y(I)+Y(I-1))**2 + (Y(N2+I)+Y(N2+I-1))**2)*(Y(I)+Y(I-1)) -
    &((Y(I+1)+Y(I))**2 + (Y(N2+I+1)+Y(N2+I))**2)*(Y(I+1)+Y(I)) +
    &((Y(I-1)+Y(I-2))**2 + (Y(N2+I-1)+Y(N2+I-2))**2)*(Y(I-1)+Y(I-2)))

     DERY(N2+I) = Y(N3+I)

     DERY(N3+I) = Y(N2+I-1) - 2.D0*Y(N2+I)+Y(N2+I+1) + 5.D-1*BETA2*
    &(Y(N2+I-2) - 2.D0*Y(N2+I) + Y(N2+I+2)) + 5.0D-1*(AMU-1.D0)*
    &((Y(I+1)**2 + Y(N2+I+1)**2)*Y(N2+I+1)-2.D0*(Y(I)**2 + Y(N2+I)**2)*
    &Y(N2+I) + (Y(I-1)**2 + Y(N2+I-1)**2)*Y(N2+I-1)) + 6.25D-2*BETA2*
    &(2.0D0*AMU-1.D0)*(((Y(I+2)+Y(I+1))**2 + (Y(N2+I+2)+Y(N2+I+1))**2)*
    &(Y(N2+I+2)+Y(N2+I+1))-((Y(I)+Y(I-1))**2 + (Y(N2+I)+Y(N2+I-1))**2)*
    &(Y(N2+I)+Y(N2+I-1)) - ((Y(I+1)+Y(I))**2 + (Y(N2+I+1)+Y(N2+I))**2)*
    &(Y(N2+I+1)+Y(N2+I))+((Y(I-1)+Y(I-2))**2+(Y(N2+I-1)+Y(N2+I-2))**2)*
    &(Y(N2+I-1)+Y(N2+I-2)))
   1 continue
C***************************************************************************
C LEFT BOUNDARY COND. FOR THE FIRST COMPONENT OF VECTOR r:
     DERY(1) = Y(NN+1)

     DERY(2) = Y(NN+2)
```

104

```
      DERY(NN+1) = F0 - 2.D0*Y(1) + Y(2) + 5.D-1*BETA2*(F1 -

     &2.D0*Y(1) + Y(3)) + 5.0D-1*(AMU - 1.D0)*((Y(2)**2 +

     &Y(N2+2)**2)*Y(2)-2.D0*(Y(1)**2+Y(N2+1)**2)*Y(1)+(F0**2 +

     &G0**2)*F0) + 6.25D-2*BETA2*(2.0D0*AMU - 1.D0)*

     &(((Y(3) + Y(2))**2 + (Y(N2+3)+Y(N2+2))**2)*(Y(3) + Y(2))-

     &((Y(1) + F0)**2 + (Y(N2+1) + G0)**2)*(Y(1) + F0) -

     &((Y(2) + Y(1))**2 + (Y(N2+2) + Y(N2+1))**2)*(Y(2) + Y(1)) +

     &((F0 + F1)**2 + (G0 + G1)**2)*(F0 + F1))

      DERY(NN+2) = Y(1) - 2.D0*Y(2) + Y(3) + 5.D-1*BETA2*(F0 -

     &2.D0*Y(2) + Y(4)) + 5.0D-1*(AMU - 1.D0)*((Y(3)**2 +

     &Y(N2+3)**2)*Y(3)-2.D0*(Y(2)**2+Y(N2+2)**2)*Y(2)+(Y(1)**2 +

     &Y(N2+1)**2)*Y(1)) + 6.25D-2*BETA2*(2.0D0*AMU - 1.D0)*

     &(((Y(4) + Y(3))**2 + (Y(N2+4)+Y(N2+3))**2)*(Y(4) + Y(3))-

     &((Y(2) + Y(1))**2 + (Y(N2+2) + Y(N2+1))**2)*(Y(2) + Y(1)) -

     &((Y(3) + Y(2))**2 + (Y(N2+3) + Y(N2+2))**2)*(Y(3) + Y(2)) +

     &((Y(1) + F0)**2 + (Y(N2+1)+ G0)**2)*(Y(1) + F0))

C RIGHT BOUNDARY COND. FOR THE FIRST COMPONENT OF VECTOR r:

      DERY(NN-1) = Y(N2-1)

      DERY(NN) = Y(N2)

      DERY(N2-1) = 0.D0

      DERY(N2)= 0.D0

C*************************************************************************

C LEFT BOUNDARY CONDITION FOR THE 2-nd COMPONENT OF VECTOR r:

      DERY(N2+1) = Y(N3+1)
```

105

```
      DERY(N2+2) = Y(N3+2)

      DERY(N3+1) = G0 - 2.D0*Y(N2+1) + Y(N2+2) + 5.D-1*BETA2*(F1 -
     &2.D0*Y(N2+1) + Y(N2+3)) + 5.0D-1*(AMU - 1.D0)*((Y(2)**2 +
     &Y(N2+2)**2)*Y(N2+2)-2.D0*(Y(1)**2+Y(N2+1)**2)*Y(N2+1)+(F0**2 +
     &G0**2)*G0) + 6.25D-2*BETA2*(2.0D0*AMU - 1.D0)*
     &(((Y(3) + Y(2))**2 + (Y(N2+3)+Y(N2+2))**2)*(Y(N2+3) + Y(N2+2))-
     &((Y(1) + F0)**2 + (Y(N2+1) + G0)**2)*(Y(N2+1) + G0) -
     &((Y(2) + Y(1))**2 + (Y(N2+2) + Y(N2+1))**2)*(Y(N2+2) + Y(N2+1))+
     &((F0 + F1)**2 + (G0 + G1)**2)*(G0 + G1))

      DERY(N3+2) = Y(N2+1) - 2.D0*Y(N2+2) + Y(N2+3) + 5.D-1*BETA2*(G0 -
     &2.D0*Y(N2+2) + Y(N2+4)) + 5.0D-1*(AMU - 1.D0)*((Y(3)**2 +
     &Y(N2+3)**2)*Y(N2+3)-2.D0*(Y(2)**2+Y(N2+2)**2)*Y(N2+2)+(Y(1)**2 +
     &Y(N2+1)**2)*Y(N2+1)) + 6.25D-2*BETA2*(2.0D0*AMU - 1.D0)*
     &(((Y(4) + Y(3))**2 + (Y(N2+4)+Y(N2+3))**2)*(Y(N2+4) + Y(N2+3))-
     &((Y(2) + Y(1))**2 + (Y(N2+2) + Y(N2+1))**2)*(Y(N2+2) + Y(N2+1)) -
     &((Y(3) + Y(2))**2 + (Y(N2+3) + Y(N2+2))**2)*(Y(N2+3) + Y(N2+2)) +
     &((Y(1) + F0)**2 + (Y(N2+1)+ G0)**2)*(Y(N2+1) + G0))
C RIGHT BOUNDARY CONDITION FOR THE 2-nd COMPONENT OF VECTOR r:
      DERY(N3-1) = Y(N4-1)

      DERY(N3) = Y(N4)

      DERY(N4-1) = 0.D0

      DERY(N4)= 0.D0

      RETURN

      END
```

106

```
C*********************************************************************
      SUBROUTINE OUTP(X,Y,DERY,IHLF,NDIM,PRMT)
      IMPLICIT DOUBLE PRECISION (A-H,O-Z)
      DIMENSION PRMT(1),Y(1),DERY(1)
      RETURN
      END
```

Appendix B: Program Vector MKDV equation

Program Vector mKdV

C Spatial step H = RL/N, temporal step TAU

C Step for data presentation: DT = NB*TAU

C NWAY = 1: for analitically given initial conditions

C NWAY = 2: for numerical initial conditions

C Criterion of stability of the numerical scheme: TAU <, = 0.384*H**3/B

C Used markers: 1-21

C*******!*******!*******!*******!*******!*******!*******!**

   IMPLICIT DOUBLE PRECISION (A-H,O-Z)

   DIMENSION P(100004),U(100004),V(100000),S(100001),

  *P1(100004),U1(100004),V1(100000),S1(100001),X(100000)

   EQUIVALENCE (V(1),U(3)),(V1(1),U1(3))

   COMMON/SLT/A,A1,B,RL

  OPEN(10,FILE='VMKDV10.DAT')

  OPEN(101,FILE='VMKDV01.DAT') ! DATA FILE FOR RUN CONTINUATION

  WHEN NWAY=2

  OPEN(102,FILE='VMKDV02.DAT') ! INTEGRAL QUANTITIES

   OPEN(103,FILE='VMKDV03.DAT') ! MAXIMA AND MINIMA

   OPEN(104,FILE='VMKDV04.DAT') ! DATA STORED FOR THE NEXT RUN

C*******!*******!*******!*******!*******!*******!*******!**

C Parameters

  A=1.D0

  A1=1.D0 ! For the non-integrable case A1=1 and A1=0 for the integrable case

```fortran
      B=1.D0
      RL=1.D3
      N=12500
      H=RL/N
      TAUcr=3.84D-1*H**3/B
      TAU=1.8D-4
      DT=1.8D0
      NP=10
        print 8
 8    format(/1x,'NWAY = ?'/
     *  '  1 - for analyticaly given initial condition;'/
     *  '  2 - for numericaly given initial condition   ')
      READ(*,*) NWAY
      write(*,*) 'A = ',A, 'A1 = ',A1
      write(*,*) 'B = ',B, 'Rl = ',RL
      write(*,*) 'TAU = ',TAU, 'TAUcr = ',TAUcr
      write(*,*) 'H = ',H, 'DT = ',DT
      write(*,*) 'N = ',N, '    NP = ',NP
C********!********!********!********!********!********!********!**
      NB=DT/TAU+0.00001
      write(*,*) 'NB = ',NB, '   NWAY = ',NWAY
      N1=N+1
      N2=N+2
      N3=N+3
```

```
      N4=N+4

      DO 11 IR=1,N

  11  X(IR)=RL*(IR-1)/N

C********!********!********!********!********!********!********!**

C Initial conditions and first step

      GO TO (1,2), NWAY

  1  CALL STEP1(N,U,P,U1,P1,S,S1,A,A1,B,TAU,H,N1,N2,N3,N4)

      T=0.D0

      M=0

      NB1=NB-1

C********!********!********!********!********!********!********!**

C Momentum and energy

      DO 34 L=1,N

      S(L)=P(L)**2

      S1(L)=P1(L)**2

  34   CONTINUE

      SI1=0.D0

      SI2=0.D0

      SE1=0.D0

      SE2=0.D0

      DO 81 IJ=1,N

      SE1=SE1+S(IJ)

      SI1=SI1+P(IJ)

      SI2=SI2+P1(IJ)
```

```fortran
      SE2=SE2+S1(IJ)
81    CONTINUE
      QI1=SI1/N
      QI2=SI2/N
      QES=5.D-1*(SE1+SE2)/N
      UMA=P(1)
      UMA1=P1(1)
      UMI=P(1)
      UMI1=P1(1)
      DO 334 I=2,N
      IF (P(I).LE.UMA) GO TO 333
      UMA=P(I)
      LVMAX=I
333   IF(P(I).GE.UMI) GO TO 334
      UMI=P(I)
      LVMIN=I
334   CONTINUE
      DO 335 IM=2,N
      IF(P1(IM).LE.UMA1) GO TO 336
      UMA1=P1(IM)
      LU1MA=IM
336   IF (P1(IM).GE.UMI1) GO TO 335
      UMI1=P1(IM)
      LU1MI=IM
```

```
  335  CONTINUE

     XMA=(LVMAX-1)*H

     XMI=(LVMIN-1)*H

     X1MA=(LU1MA-1)*H

     X1MI=(LU1MI-1)*H

     PRINT 9,T,M,QI1,QI2,QES,UMA,XMA,UMI,XMI,UMA1,X1MA,UMI1,X1MI

     DO 10 J=1,N

     S(J)=DSQRT(P(J+2)**2+P1(J+2)**2)

  10  CONTINUE

C     DO 15 J=1,N

C     S1(J)=0.

C     IF(H*J.LT.35.) GO TO 15

C     S1(J)=ATAN2(P1(J+2),P(J+2))

C     IF(H*J.GT.130.) S1(J)=PI/2.

C  15  CONTINUE

     DO 337 IX=1,N

     WRITE(10,*) X(IX),P(IX+2),P1(IX+2),S(IX)

 337  CONTINUE

     GO TO 314

C*******!*******!*******!*******!*******!*******!*******!**

  2  DO 300 LN=1,N4

     READ(101,*) P(LN),U(LN),P1(LN),U1(LN)

 300  CONTINUE

     NB1=NB
```

```
      PRINT 9,T

C********!********!********!********!********!********!********!**

 314  CONTINUE

      WRITE(102,9)
T,M,QI1,QI2,QES,UMA,XMA,UMI,XMI,UMA1,X1MA,UMI1,X1MI

      DO 4 I=1,NP

      WRITE(*,*) 'NSTEP = ',I, 'T = ', T

      DO 5 IA=1,NB1

      UB1=U(1)

      UV1=U1(1)

      YU=U(2)

      YU1=U1(2)

      UF1=U(3)

      UFE1=U1(3)

      UF2=U(4)

      UFE2=U1(4)

      DO 6 J=3,N2

      UB2=UB1

      UB1=YU

      YU=UF1

      UF1=UF2

      UF2=U(J+2)

      UV2=UV1

      UV1=YU1

      YU1=UFE1
```

113

```
      UFE1=UFE2

      UFE2=U1(J+2)

C********!********!********!********!********!********!********!**

      P(J)=P(J)-(TAU/H)*((B/H**2)*(UF2-2.D0*UF1+2.D0*UB1-UB2)

     &+A*(YU**2+YU1**2+2.D0*A1*A*YU**2)*(UF1-
UB1)+2.D0*A1*A*YU1*YU*

     &(UFE1-UV1))

      P1(J)=P1(J)-(TAU/H)*((B/H**2)*(UFE2-2.D0*UFE1+2.D0*UV1-UV2)

     &+A*(YU1**2+YU**2+2.D0*A1*A*YU1**2)*(UFE1-
UV1)+2.D0*A1*A*YU1*YU*

     &(UF1-UB1))

   6  CONTINUE

      DO 7 K=3,N2

      W=P(K)

      P(K)=U(K)

      W1=P1(K)

      P1(K)=U1(K)

      U1(K)=W1

   7  U(K)=W

      U(1)=U(N1)

      U(2)=U(N2)

      U(N3)=U(3)

      U(N4)=U(4)

      U1(1)=U1(N1)

      U1(2)=U1(N2)
```

114

```
      U1(N3)=U1(3)

      U1(N4)=U1(4)

  5  CONTINUE

      NB1=NB

C********!********!********!********!********!********!********!**

      DO 234 L=1,N

      S(L)=U(L+2)**2

      S1(L)=U1(L+2)**2

 234  CONTINUE

      SI1=0.

      SI2=0.

      SE1=0.

      SE2=0.

      DO 281 IJ=1,N

      SE1=SE1+S(IJ)

      SI1=SI1+V(IJ)

      SI2=SI2+V1(IJ)

      SE2=SE2+S1(IJ)

 281  CONTINUE

      QI1=SI1/N

      QI2=SI2/N

      QES=5.D-1*(SE1+SE2)/N

      UMA=V(1)

      UMA1=V1(1)
```

```
          UMI=V(1)

          UMI1=V1(1)

          DO 134 I0=2,N

          IF (V(I0).LE.UMA) GO TO 133

          UMA=V(I0)

          LVMAX=I0

133  IF(V(I0).GE.UMI) GO TO 134

          UMI=V(I0)

          LVMIN=I0

134  CONTINUE

          DO 135 IM=2,N

          IF (V1(IM).LE.UMA1) GO TO 136

          UMA1=V1(IM)

          LU1MA=IM

136  IF(V1(IM).GE.UMI1) GO TO 135

          UMI1=V1(IM)

          LU1MI=IM

135  CONTINUE

          XMA=(LVMAX-1)*H

          XMI=(LVMIN-1)*H

          X1MA=(LU1MA-1)*H

          X1MI=(LU1MI-1)*H

          M=M+NB

          T=T+DT
```

```fortran
C     PRINT 9,T,M,QI1,QI2,QES,UMA,XMA,UMI,XMI,UMA1,X1MA,UMI1,X1MI
      WRITE(102,22) T,QI1,QI2,QES
      WRITE(103,23) T,UMA,XMA,UMI,XMI,UMA1,X1MA,UMI1,X1MI
      DO 110 J=1,N
      S(J)=DSQRT(V(J)**2+V1(J)**2)
  110 CONTINUE
C     DO 115 J=1,N
C     S1(J)=0.
C     IF(H*J.LT.35.) GO TO 115
C     S1(J)=ATAN2(V1(J),V(J))
C     IF(H*J.GT.130.) S1(J)=PI/2.
C 115 CONTINUE
      DO 237 IX=1,N
      WRITE(10+I,*) X(IX),P(IX+2),P1(IX+2),S(IX)
  237 CONTINUE
    4 CONTINUE
      DO 200 LN=1,N4
      WRITE(104,*) P(LN),U(LN),P1(LN),U1(LN)
  200 CONTINUE
      CLOSE(104)
C********!********!********!********!********!********!********!**
      STOP
    9 FORMAT(/1X,2HT=,G10.4,3X,2HM=,I7,3X,'QI1=',G10.4,3X,'QI2=',G10.4,
     &3X,'QES=',G16.10,1X,'UMA= ',G10.4,3X,'XMA= ',G10.4,'UMI= ',G10.4,
```

117

```
    &3X,'XMI=',G10.4,1X,'U1MA=',G10.4,3X,'X1MA=',G10.4,'U1MI=',G10.4,
    &3X,'X1MI=',G10.4)
22  FORMAT(4E12.4)
23  FORMAT(9E12.4)
    END
```

Appendix C: The Toda Chain Program

```
Program Tchain

    IMPLICIT DOUBLE PRECISION (A-H,O-Z)

    EXTERNAL FCT, OUTP

    DIMENSION PRMT(5),Y(1000),DERY(1000),AUX(8,1000)

    COMMON/PAR/NN, N2, T0, R, Del

    open(0,file='Param.dat')

    open(1,file='Work1.dat')

    open(2,file='Work2.dat')

    open(3,file='Work3.dat')

    open(10,file='Data.dat')

    open(11,file='Chain.dat')

C PARAMETERS
******!*********!*********!*********!*********!*********!***************

    Ti = 0.D0

    read(0,*) Dt,T0,R,Del,NN,NTS

    write(10,100) Dt,T0,R,Del,NN,NTS

100 Format(7X,2HDt,14X,2HT0,15X,1HR,18X,3HDel,13x,2HNN,5x,3HNTS/
   &1X,4E12.4,3X,2I5//)

    PRM = 1.D-2

    Accur = 1.D0

C********!*********!*********!*********!*********!*********!*********!**

!    NN = 500

    N2 = 2*NN ! N2 IS THE NUMBER OF EQUATIONS IN THE SYSTEM

!    NTS = 500 ! - NUMBER OF TIME STEPS FROM Ti

!    Dt = 5.D-1 ! - STEP OF INTEGRATION
```

PRMT(1) = Ti ! - THE LOWER BOUND OF THE INTEGRATION INTERVAL

PRMT(2) = Dt ! - THE UPPER BOUND OF THE INTEGRATION INTERVAL

PRMT(3) = Dt*PRM ! - THE INITIAL INCREMENT OF THE INDEPENDENT VARIABLE

PRMT(4) = ACCUR ! - THE UPPER ERROR BOUND

C ARRAY DERY BELOW IS THE INPUT VECTOR OF THE INITIAL ERROR WEIGHTS

C THE SUM OF ITS COMPONENTS MUST BE EQUAL TO 1

DO 1 I = 1,N2

DERY(I) = 1.D0/FLOAT(N2)

1 CONTINUE

C ARRAY Y BELOW IS A VECTOR OF INITIAL DATA

DO 2 M = 1,N2

Y(M) = 0.D0

2 CONTINUE

C   DO 4 M = 1,NN ! - SMALL INITIAL PERTURBATION

C   Y(M) = 2.D-2*DEXP(-(M - NN/4)**2/5.D0)

C 4 CONTINUE

NR = NN/10

write(1,*) Ti, Y(NR), Y(NN+NR)

write(2,*) Ti, Y(2*NR), Y(NN+2*NR)

write(3,*) Ti, Y(3*NR), Y(NN+3*NR)

C**

DO 3 I = 1,NTS ! integration of ODEs

CALL RKGS(PRMT,Y,DERY,N2,IHLF,FCT,OUTP,AUX)

write(1,*) PRMT(2), Y(NR), Y(NN+NR)

write(2,*) PRMT(2), Y(2*NR), Y(NN+2*NR)

```fortran
      write(3,*) PRMT(2), Y(3*NR), Y(NN+3*NR)

      PRMT(1) = PRMT(2)

      PRMT(2) = PRMT(2) + DT

    3 continue

      DO 5 J = 1,NN

         WRITE(11,*) J,Y(J)

    5 CONTINUE

      stop

      end
```

C***

```fortran
      SUBROUTINE FCT1(T,Y,DERY)
```

C INPUT SIGNAL - A KINK

```fortran
      IMPLICIT DOUBLE PRECISION(A-H,O-Z)

      COMMON/PAR/NN, N2, T0, R, Del

      DIMENSION Y(1),DERY(1)

      A = 1.D0

      DO 1 I = 2,NN-1

         DERY(I) = (Y(NN+I) - Y(NN+I+1))*(1.D0 + Y(I))

         DERY(NN+I) = Y(I-1) - Y(I)

    1  continue

      Y(1) = 5.D-1*A*(1.D0 + DTANH((T - T0)/Del)) ! Y(1) = u(1)

      Y(NN+1) = 0.D0
```

C MATHCHED LOAD BOUNDARY CONDITION

```fortran
      Y(NN) = R*Y(N2)

      DERY(N2) = (1.D0 + Y(NN))*(Y(N2-1) - Y(N2))/R

      RETURN
```

```fortran
      END
C*********************************************************************
      SUBROUTINE FCT(T,Y,DERY)
C INPUT SIGNAL - SOLITON TODA
      IMPLICIT DOUBLE PRECISION(A-H,O-Z)
      COMMON/PAR/NN, N2, T0, R, Del
      DIMENSION Y(1),DERY(1)
      A = 2.D0*(DSINH(1.D0/Del))**2
      V = Del*DSINH(1.D0/Del)
      DO 1 I = 2,NN-1
        DERY(I) = (Y(NN+I) - Y(NN+I+1))*(1.D0 + Y(I))
        DERY(NN+I) = Y(I-1) - Y(I)
    1 continue
      Y(1) = A*(1.D0 - (DTANH((T - T0)*V/Del))**2) ! Y(1) = u(1)
c     Y(NN+1) = 0.D0
      Y(NN+1) = (A*Del/V)*(DTANH((T - T0)*V/Del) -
     &DTANH(((T - T0)*V - 1)/Del)) ! Y(NN + M)) = i(M)
C MATHCHED LOAD BOUNDARY CONDITION
      Y(NN) = R*Y(N2)
      DERY(N2) = (1.D0 + Y(NN))*(Y(N2-1) - Y(N2))/R
      RETURN
      END
C*********************************************************************
      SUBROUTINE OUTP(X,Y,DERY,IHLF,NDIM,PRMT)
      IMPLICIT DOUBLE PRECISION (A-H,O-Z)
      DIMENSION PRMT(1),Y(1),DERY(1)
```

122

```
RETURN

END
```

Appendix D: Rotational Toda Chain Program

Program RotationalTodaChain

```
    IMPLICIT DOUBLE PRECISION (A-H,O-Z)

    EXTERNAL FCT, OUTP

    DIMENSION PRMT(5),Y(1500),DERY(1500),AUX(8,1500)

C MAXIMAL NUMBER OF CELLS IS NOW NN = 500

    COMMON/PAR/NN, N2, N3, T0, R, Del, F

    open(0,file='Rparam.dat')

    open(1,file='Work1.dat')

    open(2,file='Work2.dat')

    open(3,file='Work3.dat')

    open(10,file='Data.dat')

    open(11,file='Chain.dat')

C PARAMETERS
******!*********!*********!*********!*********!*********!**************

    Ti = 0.D0

    read(0,*) Dt,T0,R,Del,F,NN,NTS

    write(10,100) Dt,T0,R,Del,F,NN,NTS

 100 Format(7X,'Dt',14X,'T0',15X,'HR',18X,'Del',18X,'F',11x,'NN',5x,
    &'NTS'/1X,5E12.4,3X,2I5//)

    PRM = 1.D-2

    Accur = 1.D0

C*******!*********!*********!*********!*********!*********!*********!**

    N2 = 2*NN
```

```fortran
      N3 = 3*NN ! N3 IS THE NUMBER OF EQUATIONS IN THE SYSTEM

      PRMT(1) = Ti ! - THE LOWER BOUND OF THE INTEGRATION INTERVAL

      PRMT(2) = Dt ! - THE UPPER BOUND OF THE INTEGRATION INTERVAL

      PRMT(3) = Dt*PRM ! - THE INITIAL INCREMENT OF THE INDEPENDENT
VARIABLE

      PRMT(4) = ACCUR ! - THE UPPER ERROR BOUND
C ARRAY DERY BELOW IS THE INPUT VECTOR OF THE INITIAL ERROR
WEIGHTS
C THE SUM OF ITS COMPONENTS MUST BE EQUAL TO 1
      DO 1 I = 1,N3

         DERY(I) = 1.D0/FLOAT(N3)

    1 CONTINUE
C ARRAY Y BELOW IS A VECTOR OF INITIAL DATA
      DO 2 M = 1,N3

         Y(M) = 0.D0

    2  CONTINUE

      NR = NN/100

      write(1,*) Ti, Y(4*NR), Y(NN+NR)

      write(2,*) Ti, Y(5*NR), Y(NN+2*NR)

      write(3,*) Ti, Y(6*NR), Y(NN+3*NR)
C****************************************************************
      DO 3 I = 1,NTS ! integration of ODEs

         CALL RKGS(PRMT,Y,DERY,N3,IHLF,FCT,OUTP,AUX)

         write(1,*) PRMT(2), Y(4*NR), Y(NN+NR)

         write(2,*) PRMT(2), Y(5*NR), Y(NN+2*NR)
```

```fortran
      write(3,*) PRMT(2), Y(6*NR), Y(NN+3*NR)

      PRMT(1) = PRMT(2)

      PRMT(2) = PRMT(2) + DT

    3 continue

      DO 5 J = 1,NN

         WRITE(11,*) J,Y(J)

    5 CONTINUE

      stop

      end
```

```fortran
C******************************************************************

      SUBROUTINE FCT(T,Y,DERY)

C INPUT SIGNAL - SOLITON TODA

      IMPLICIT DOUBLE PRECISION(A-H,O-Z)

      COMMON/PAR/NN, N2, N3, T0, R, Del, F

      DIMENSION Y(1),DERY(1)

      A = 2.D0*(DSINH(1.D0/Del))**2

      V = Del*DSINH(1.D0/Del)

      DO 1 I = 2,NN-1

         DERY(I) = (Y(NN+I) - Y(NN+I+1) - Y(N2+I))*(1.D0 + Y(I))

         DERY(NN+I) = Y(I-1) - Y(I)

         DERY(N2+I) = Y(I)/F

    1 continue

      Y(1) = A*(1.D0 - (DTANH((T - T0)*V/Del))**2) ! Y(1) = u(1)

      Y(NN+1) = 0.D0
```

```fortran
      Y(N2+1) = 0.D0
C     Y(NN+1) = Y(NN+2) + (A*Del/V*F)*(DTANH((T - T0)*V/Del) -
C    &DTANH(((T - T0)*V - 1)/Del)) ! - this is current j
C MATHCHED LOAD BOUNDARY CONDITION
      Y(NN) = R*Y(N2)
      DERY(N2) = (1.D0 + Y(NN))*(Y(N2-1) - Y(N2))/R
      Y(N3) = 0.D0
      RETURN
      END
C******************************************************************
      SUBROUTINE OUTP(X,Y,DERY,IHLF,NDIM,PRMT)
      IMPLICIT DOUBLE PRECISION (A-H,O-Z)
      DIMENSION PRMT(1),Y(1),DERY(1)
      RETURN
      END
```

Appendix E: Program Chain Model for the Gardner–Ostrovsky Equation

ParticleChainGO

```
    IMPLICIT DOUBLE PRECISION (A-H,O-Z)

    EXTERNAL FCT, OUTP

    DIMENSION PRMT(5),Y(30000),DERY(30000),AUX(8,30000)

C MAXIMAL NUMBER OF CELLS IS NOW NN = 10000

    COMMON/PAR/NN,N2,N3,T0,R,F,ALPHA,ALPHA1,ANU,PHI,TG

    open(100,file='Rparam.dat')

    open(101,file='Data.dat')

    open(102,file='Chain.dat')

    open(1001,file='Work1.dat')

    open(1002,file='Work50.dat')

    open(1003,file='Work100.dat')

    open(1004,file='Work150.dat')

    open(1005,file='Work200.dat')


C PARAMETERS
******!*********!*********!*********!*********!*********!**************

    Ti = 0.D0

    read(100,*) Dt,T0,R,F,ALPHA,ALPHA1,ANU,NN,NTS

    write(101,100) Dt,T0,R,F,ALPHA,ALPHA1,ANU,NN,NTS

100 Format(7X,'Dt',14X,'T0',15X,'HR',18X,'F',15X,'ALPHA',10X,'ALPHA1',
   &10X,'ANU',13x,'NN',5x,'NTS'/1X,7E12.4,3X,2I6//)
```

PHI = 2.5D-1*DLOG((1.D0 + ANU)/(1.D0 - ANU))

TG = DSQRT(-2.D0*ALPHA1)/(ANU*DABS(ALPHA))

write(*,*) Dt,T0,R

write(*,*) F,ALPHA,ALPHA1

write(*,*) ANU,NN,NTS

write(*,*) PHI,TG

PRM = 1.D-2

Accur = 1.D0

C********!********!********!********!********!********!********!**

N2 = 2*NN

N3 = 3*NN ! N3 IS THE NUMBER OF EQUATIONS IN THE SYSTEM

PRMT(1) = Ti ! - THE LOWER BOUND OF THE INTEGRATION INTERVAL

PRMT(2) = Dt ! - THE UPPER BOUND OF THE INTEGRATION INTERVAL

PRMT(3) = Dt*PRM ! - THE INITIAL INCREMENT OF THE INDEPENDENT VARIABLE

PRMT(4) = ACCUR ! - THE UPPER ERROR BOUND

C ARRAY DERY BELOW IS THE INPUT VECTOR OF THE INITIAL ERROR WEIGHTS

C THE SUM OF ITS COMPONENTS MUST BE EQUAL TO 1

DO 1 I = 1,N3

   DERY(I) = 1.D0/FLOAT(N3)

 1 CONTINUE

C ARRAY Y BELOW IS A VECTOR OF INITIAL DATA

DO 2 M = 1,N3

   Y(M) = 0.D0

129

```fortran
    2  CONTINUE
C      NR = NN/100
      write(1001,*) Ti, Y(1)
      write(1002,*) Ti, Y(50)
      write(1003,*) Ti,Y(100)
      write(1004,*) Ti,Y(150)
      write(1005,*) Ti,Y(200)
C****************************************************************
      DO 3 I = 1,NTS ! integration of ODEs
        CALL RKGS(PRMT,Y,DERY,N3,IHLF,FCT,OUTP,AUX)
      write(1001,*) PRMT(2), Y(1)
      write(1002,*) PRMT(2), Y(50)
      write(1003,*) PRMT(2), Y(100)
      write(1004,*) PRMT(2), Y(150)
      write(1005,*) PRMT(2), Y(200)
        PRMT(1) = PRMT(2)
        PRMT(2) = PRMT(2) + DT
    3 continue
      DO 5 J = 1,NN
        WRITE(102,*) J,Y(J)
    5 CONTINUE
      stop
      end
C****************************************************************
```

```fortran
      SUBROUTINE FCT(T,Y,DERY)
C THE INPUT SIGNAL IS TODA SOLITON
      IMPLICIT DOUBLE PRECISION(A-H,O-Z)
      COMMON/PAR/NN,N2,N3,T0,R,F,ALPHA,ALPHA1,ANU,PHI,TG
      DIMENSION Y(1),DERY(1)
      DO 1 I = 2,NN-1
        DERY(I) = (Y(NN+I) - Y(NN+I+1) - Y(N2+I))
     &/(1.D0 - ALPHA*Y(I) - ALPHA1*Y(I)**2)
        DERY(NN+I) = Y(I-1) - Y(I)
        DERY(N2+I) = Y(I)/F
    1 continue
      Y(1) = -(5.D-1*ANU*ALPHA/ALPHA1)*(DTANH((T - T0)/TG + PHI) -
     &DTANH((T - T0)/TG - PHI)) ! Y(1) = u(1)
      Y(NN+1) = 0.D0
      Y(N2+1) = 0.D0
C MATHCHED LOAD BOUNDARY CONDITION
      Y(NN) = R*Y(N2)
      DERY(N2) = (1.D0 + Y(NN))*(Y(N2-1) - Y(N2))/R
      Y(N3) = 0.D0
      RETURN
      END
C****************************************************************
      SUBROUTINE OUTP(X,Y,DERY,IHLF,NDIM,PRMT)
      IMPLICIT DOUBLE PRECISION (A-H,O-Z)
```

```
DIMENSION PRMT(1),Y(1),DERY(1)

RETURN

END
```

Bibliography

Ablowitz, M. J., & Segur, H. (1981). *Solitons and the Inverse Scattering Transform.* Philadelphia: SIAM.

Ablowitz, M. J., Kaup, D. J., Newell, A. C., & Segur, H. (1973, July). Nonlinear Evolution Equations of Physical Significance. *Phys. Rev. Lett., 31*(2), 125-127.

Ablowitz, M., & Ladik, J. F. (1976). Non Linear Differential- Difference Equations and Fourier Analysis. *J. Math. Phys., 17*, 1011-1018.

Apel, J., Ostrovsky, L. A., Stepanyants, Y. A., & Lynch, J. F. (2007). Internal Solitons in the Ocean and their Effect on Underwater Sound. *J. Accoust. Soc. Am., 121*(2), 695-722.

Belenkii, G. L., Salaev, E. Y., & Suleimanov, R. A. (1988). Deformation Effects in Layer Crystals. *Sov. Phys. Uspekhi, 31*, 433-455.

Bespalov, V. I., & Talanov, V. I. (1966). Filamentary Structures of Light Beams in Nonlinear Liquids. *Zh. Eksp. Teor. Fiz. Pis'ma, 3*, 471-476.

Bishop, A. R., Krumhansl, J. A., & Trullinger, S. E. (1980). Solitons in Condensed Matter. *Physica D: Nonlinear Phenomena, 1*(1), 1-44.

Boussinesq, J. (1871). Theorie de l'intumescence liquide appelee onde solitaire ou de translation, se propageant dans un canal rectangulaire. *C. R. Acad. Sci., 72*, 755-759.

Brandt, N. B., & Kulbachinsky, B. A. (2007). *Quasiparticles in the Physics of Condensed State.* Moscow: Fizmatlit.

Calogero, F. (1971). Solution of the One-Dimensional N-body Problems with Quadratic and/or Inversely Quadratic Pair potentials. *J. Math. Phys., 12*, 419-436.

Christiansen, P. L., Zolotaryuk, A. V., & Savin, A. V. (1997). Solitons in an Isolated Helix Chain. *Phys. Rev. E, 56*(1), 877-889.

Davydov, A. S. (1985). *Solitons in Molecular Systems.* Norwell, MA: Dordrecht. See also Kluwer Academic Publications, 1991, USA.

Destrade, M., & Saccomandi, G. (2008). Nonlinear Transverse Waves in Deformed Dispersive Solids. *Wave Motion, 45*, 325-336.

Dodd, R. K., Eilbeck, J. C., Gibbon, J. D., & Morris, H. C. (1982). *Solitons and Nonlinear Wave Equations.* London: Academic Press.

Erbay, H. A. (1998). Nonlinear Transverse Waves in a Generalised Elastic Solid and the Complex Modified Korteweg-de Vries Equation. *Physica Scripta, 58*, 9-14.

Farokhi, B., Kourakis, I., & Shukla, P. K. (2006). Nonlinear Modulated Dust Lattice Wave Packets in Two Dimensional Hexagonal Dust Crystals. *Phys. Plasma, 13*(122304), 10.

Fermi, E., Pasta, J., & Ulam, S. (1955). Studies of nonlinear Problems. *Los Alamos Report LA-1940. See also in : E. Segre (ed.), Collected Papers of Enrico Fermi, v. 2, University of Chicago Press, Chicago, 1965.*

Fortov, V. E., Khrapak, A. G., Khrapak, S. A., Molotkov, V. I., & Petrov, O. F. (2004). Dusty Plasmas. *Phys.- Uspekhi, 47*(5), 447-492.

Frenkel, J., & Kontrova, T. (1939). On the theory of Plastic Deformation and Twinning. *J. Phys. USSR, 1*, 137-149.

Gardner, C. S., Green, J. M., Kruskal, M. D., & Miura, R. M. (1967). Method for Solving the Korteweg De Vries Equation. *Phys. Rev. Lett., 19*, 1095-1097.

Gorbacheva, O. B., & Ostrovsky, L. A. (1983). Nonlinear Vector Waves in a Mechanical Model of a Molecular Chain. *Physica D., 8*, 223-228.

Grimshaw, R. H., He, J.-M., & Ostrovsky, L. A. (1998a). Terminal Damping of a Solitary Wave due to Radiation in Rotational Systems. *Stud. Appl. Math, 101*, 197-210.

Grimshaw, R., & Helfrich, K. (2008). Long-Time Solutions of the Ostrovsky Equation. *Stud. Appl. Math., 121*, 71-88.

Grimshaw, R., Ostrovsky, L. A., Shrira, V. I., & Stepanyants, Y. A. (1998b). Long Nonlinear Surface and Internal Gravity Waves in a Rotating Ocean . *Surveys in Geophys., 19*, 289-338.

Grimshaw, R., Pelinovsky, E. N., & Talipova, T. G. (2003). Damping of Large-Amplitude Solitary Waves. *Wave Motion, 37*, 351-364.

Grimshaw, R., Pelinovsky, E., Stepanyants, Y., & Talipova, T. (2006). Modeling Internal Solitary Waves on the Australian North West Shelf. *Marine and Freshwater Research, 57*, 265-272.

Grimshaw, R., Slunyaev, A., & Pelinovsky, E. (2010, January). Generation of solitons and breathers in the extended Korteweg–de Vries equation with positive cubic nonlinearity . *Chaos, 20*(1).

Grundland, A. M., & Infeld, E. (1992). A family of non-linear Klein-Gordon Equations and their Solutions. *J.Math.Phys., 33*(7).

Han, H., Zhang , J., & Brunner, H. (2008). Numerical Soliton Solutions for a Discrete sine-Gordon System. 16.

Hasegawa, A., & Tappert, F. (1973). Transmission of Stationary Nonlinear Optical Pulses in Dispersive Dielectric Fibres. *Appl. Phys. Lett., 23*, 142-144.

Hereman, W., Banerjee, P. P., Korpel, A., Assanto, G., Van, I. A., & Meerpole, A. (1986). Exact Solitary Wave Solutions of Nonlinear Evolution and Wave Equations Using a Direct Algebraic Method. *J. Phys. A. Math. Gen., 19*(5), 607-628.

Hirota, R., & Suzuki, K. (1973, October). Theoretical and Experimental Studies of Lattice Solitons in Nonlinear Lumped Networks. *Proceedings of the IEEE, 61*(10), 1483-1491.

Holloway, P., Pelinovsky, E., & Talipova, T. (1999). A Generalised Korteweg-de Vries Model of Internal Tide Transformation in the Coastal Zone. *Geophys Research, 104*(18), 333-350.

Ismail, M. S. (2008). Numerical Solution of Complex Modified Korteweg-de Vries Equation by Petrov-Galerkin Method. *Appl. Math. Comput., 202*, 520-531.

Ismail, M. S. (2009). Numerical Solution of Complex Modified Korteweg-de Vries Equation by Collocation Method. *Commun. Nonlinear Sci. Numer. Simul., 14*, 749-759.

Kalinikos, B. A., Kovshikov, N. G., & Slavin, A. N. (1983). Nonlinear Envelope Spin waves in Ferromagnets. *JETTP Lett., 38*, 413-420.

Karney, C. F., Sen, A., & Chu, F. Y. (1979, May). Nonlinear Evolution of Lower Hybrid Waves. *Phy. Fluids, 22*(5), 940-952.

Karpman, V. I. (1967). Self-Modulation of Nonlinear Plane Waves in Dispersive Media. *Zh. Eksp. Teor. Fiz. Pis'ma, 6*, 829-932.

Karpman, V. I. (1975). *Nonlinear Waves in Dispersive Media.* Oxford: Pergamon Press.

Kevrekidis, P. G. (2011). Non-Linear Waves in Lattices:Past, Present, Future. *IMA Journal of Applied Mathematics, 3*(76), 389-423.

Khusnutdinova, K. R., & Moore, K. R. (2011). Initial-value problem for coupled Boussinesq equations and a hierachy of Ostrovsky equations. *Wave Motion, 48*, 738-752.

Kolmogorov, A. N., Petrovsky, I. G., & Piskunov, N. S. (1937). Etude de l'éqution de la diffusion avec croissance de la quantité de malière et son application à un problème biologique. *Bulletin Universite d'Etat à Moscou (Bulleten Moskowskogo Gos. Univ.), Série Internationale, Section A, 1*, 1-26.

Korteweg, D. J., & De Vries, G. (1895). On the Change of Form of long Waves Advancing in a Rectangular Channel and on a New type of Long Stationary Waves. *Phil. Mag., 39*(5), 442-443.

Lamb, G. L. (1980). *Elements of Soliton Theory.* New York: John Wiley & Sons.

Lifshitz, I. M. (1952). On Heat Properties of Chain and Layered Structures at Low Temperatures. *Zh. Eksp. Teor. Fiz., 22*, 475-486.

Lonngren, K. E. (1978). Observation of Solitons on a Nonlinear Transmission Lines. In K. E. Lonngren, K. Lonngren, & A. C. Scott (Eds.), *Solitons in Action.* New York: Academic Press.

Malomed, B. A., & Stepanyants, Y. A. (2010). Localised nonlinear optical modes and the corresponding support structures: Exact solutions to the nonlinear Schrödinger equation with external potentials. *Proc. International Conference on Electromagnetics in Adavanced Applications, ICEA'10.* Sydney.

Maugin, G. A. (1999). *Nonlinear Waves in Elastic Crystals.* Oxford: University Press.

Mollenauer, L. F., Stolen, R. H., & Gordon, J. P. (1980). Experimental Observation of Picosecond Pulse Narrowing and Solitons in Optical Fibers. *Phys. Rev. Lett., 45*, 1095-1098.

Moser, J. (1975). Three Integrable Hamiltonian Systems Connected with Isospectral Deformations. *Adv. Math, 16*, 197-220.

Mould, S. (2013, June 27). *Amazing bead chain experiment in slow motion, Earth Unplugged [Video File].* Retrieved from http://youtu.be/6ukMId5fIi0.

Muslu, G. M., & Erbay, H. A. (2003). A Split-Step Fourier Method for the Complex Modified Korteweg-de Vries Equation. *Comput. Math Appl., 45*, 503-514.

Nagovitsyn, A. P., Pelinovsky, E. N., & Stepanyants, Y. A. (1991). Observation and Analysis of Solitary Internal Waves in the Coastal Zone of Sea of Okhotsk. *Sov. J. Phys. Oceanography, 2*(1), 65-70.

Najafi, M. (2012). Multiple SolitonSolutions of Second Order Benjamin-Ono Equation. *TWMS J. App. Eng. Math., 2*(1), 94-100.

Nicklow, R., Wakabayashi, N., & Smith, H. G. (1972). Lattice Dynamics of Pyrolytic Graphite. *Phys. Rev. B, 5*, 4951–4962.

Nikitenkova, S. P., Raj, N., & Stepanyants, Y. A. (2014a). Nonlinear Vector Waves of a Flexural Mode in a Chain Model of Atomic Particles. *Communications in Nonlinear Science and Numerical Simulation (in press)*.

Nikitenkova, S. P., Raj, N., & Stepanyants, Y. A. (2015). Interactions of Vector Solitons within the framework of vector mKdV equation. *Submitted to the Journal Communications in Nonlinear Science and Numerical Simulation*.

Obregon, M., & Stepanyants, Y. (2012). On Numerical Solution of the Gardner-Ostrovsky Equation. *Mathematical Modeling of Natural Phenomena, 7*(2), 113-130.

Osborne, A. R. (1995). Solitons in the Periodic Korteweg-de Vries Equation, the FTHETA-function Representation, and the Analysis of Nonlinear, Stochastic Wave Trains. *Phys. Rev. E., 52*(1), 1105-1122.

Osborne, A. R. (1995). The Inverse Scattering Transform: Tools for the Nonlinear Fourier Analysis and Filtering of Ocean Surface Waves. *Chaos, Solitons and Fractals, 5*(12), 2623-2637.

Osborne, A. R., Segre, E., Boffetta, G., & Cavaleri, L. (1991). Soliton Basis States in Shallow Water Ocean Surface Waves. *Phys. Rev. Lett., 67*(5), 592-595.

Ostrovskii, L. A. (1963). Electromagnetics Waves in Nonlinear Media with Dispersion. *Zh. Tek. Fiz., 33*, 905-908.

Ostrovsky, L. (1978). Nonlinear Internal Waves in a Rotating Ocean. *Oceanogology, 18*(2), 119-125.

Parmentier, R. D. (1978). Fluxons in Long Josephson Junctions. In R. D. Parmentier, K. Lonngren, & A. C. Scott (Eds.), *Solitons in Action.* New York: Academic Press.

Perring, J. K., & Skyrme, T. H. (1962). A Model Unified Field Equation. *Nucl. Phys., 31*, 550-555.

Potapov, A. I., Pavlov, I. S., Gorshkov, K. A., & Maugin, G. A. (2001). Nonlinear Interactions of Solitary Waves in a 2D Lattice. *Wave Motion, 34*, 83–95.

Rabinovich, M. I., & Trubetskov, D. I. (1989). *Oscillations and Waves in Linear and Nonlinear Systems.* Dordrecht: Kluwer Academic.

Rebbi, C. (1979). Solitons. *Scientific American, 240*(2), 92-99.

Remoissenet, M. (2002). *Waves Called Solitons:Concepts and Experiments* (3rd ed.). Germany: Springer-Verlag.

Rudenko, O. V., & Solodov, E. V. (2011). Strongly Nonlinear Shear Perturbations in Discrete and Continuous Cubic Nonlinear Systems. *Acoust. Phys., 57*(1), 51–58.

Russell, J. S. (1844). Report on Waves. *Rep. 14th Meet. British Assoc. Adv. Sci.*

Scott, A. (1970). *Active and Nonlinear Wave Propagation in Electronics.* New York: Wiley-Interscience.

Scott, A. C. (Ed.). (2005). *Encyclopedia of Nonlinear Science.* New York and London: Routledge.

Scott, A. C. (2005). *Encyclopedia of Nonlinear Science.* New York: Taylor and Francis Group.

Scott, A. C. (2007). *The Nonlinear Universe.* Berlin: Springer-Verlag.

Seegar, A., Donth, H., & Kochendorfer, A. (1953). Theorie der versetzungen in eindimensionalen Atomreihen. *Z. f. Physik, 134*, 173-193.

Segre, E., Boffetta, G., Osborne, A. R., & Petti, M. (1995). Analysis of Laboratory Surface Wave Data Using the Scattering Transform for the Periodic Korteweg-de Vries. *Chaos, Solitons and Fractals, 8*(10), 1935-1943.

Stepanyants, Y. (2006). On Stationary Solutions of the Reduced Ostrovsky Equation: Periodic Waves, Compactons and Compound Solitons. *Chaos, Solitons and Fractals, 28*(1), 193-204.

Stepanyants, Y. A. (1981). Experimental Investigation of Cylindrically Diverging Solitons in an Electric Lattice. *Wave Motion 3*(4), 335-341.

Stepanyants, Y. A. (1983, July). Experimental Study of "Cerenkov" Radiation from Solitons in Two-Dimensional LC-Lattices. *Radiophysics and Quantum Electronics, 26*(7), 601-607.

Stepanyants, Y. A. (1991). On the Theory of Internal Surges in Shallow Basins. *Sov. J. Phys. Oceanogr., 2*, 99-104.

Stepanyants, Y. A., & Malomed, B. A. (2010). The Inverse Problem for the Gross-Pitaevskii Equation. *Chaos, 20*, 14.

Syrkin, E. S., Feodosyev, S. B., Kravchenko, K. V., Yeremenko, A. V., Kantor, B. Y., & Kosevich, Y. A. (2009). Flexural Rigidity of Layers and its Effect on Vibrational Characteristics of Highly Anisotropic Layered Crystals . *Low Temp. Phys., 35*, 158–165.

Taghizadeh, N., Mirzazadeh, M., & Farahrooz, F. (2011). Exact Soliton Solutions for Second-Order Benjamin–Ono Equation. *Applications and Applied Mathematics: An international Journal (AAM), 6*(1), 384–395.

Toda, M. (1989a). *Theory of Nonlinear Lattices* (2nd ed.). Berlin: Springer.

Toda, M. (1989b). *Non-Linear Waves and Solitons.* Tokyo: KTK Scientific Publishers.

Triki , H., & Ismail, M. S. (2010). Solitary Wave Solutions for a Coupled Pair of mKdV Equations. *Appl. Math. and Comp., 217*, 1540-1548.

Uddin, M., & Jan, R. A. (2013). RBF-PS Scheme for the Numerical Solution of the Complex Modified Korteweg–de Vries Equation. *Appl. math. Inf. Sci. Lett., 1*(1), 9-17.

Uddin, M., Haq, S., & Islam, S. U. (2009). Numerical Solution of Complex Modified Kortewege–de Vries Equation by Mesh-Free Collocation Method . *Comput. Math. Appl., 58*, 566–578.

Wadati, M. (2001). Introduction to Solitons. *Pramana-J. Phys., 57*, 841-847.

Whitham, G. B. (1974). *Linear and Nonlinear Waves.* New York: Wiley-Interscience.

Yagi, D., & Kawahara, T. (2001). Strongly nonlinear envelope soliton in a lattice model for periodic structure. *Wave Motion, 34*, 97-107.

Yu., B. (1987). *Modelling Nonlinear Wave Processes.* VNU Science Press.

Yuen, H. C., & Lake, B. C. (1975). Nonlinear Deep Water Waves: Theory and Experiments. *Phys. Fluids, 18*, 956-960.

Zabusky, N. J., & Kruskal, M. D. (1965, August). Interaction of Solitons in a Collisionless Plasma and the Recurrence of Initial States. *Phys. Rev. Lett., 15*(6), 240-243.

Zakharov, V. E. (1968). Stability of Periodic Waves of Finite Amplitude on the Surface of a Deep Fluid. *Journal of Applied Mechanics and Technical Physics, 9*(2), 190-194.

Zakharov, V. E., & Shabat, A. B. (1972). Exact Theory of Two Dimensional Self-Focussing and One-Dimensional Self Modulationof Waves in Nonlinear Media. *Sov. Phys. JETP, 37*, 62-69.

Zolotaryuk, Y., Savin , A. V., & Christiansen, P. L. (1988). Solitary Plane Waves in an Isotropic Hexagonal Lattice. *Phys. Rev. B., 57*(22), 14213-14227.

Zvezdin, A. K., & Popkov. (1983). On the Nonlinear Theory of Magnetostatic Spin Waves. *Sov. Phys. JETP, 57*, 350-362.